The Synthesis of Fischer carbene complexes with metal-containing substituents

by

Elisia van der Watt

Submitted in partial fulfilment of the degree

Magister Scientiae
In Chemistry

In the Faculty of Natural- and Agricultural Sciences

University of Pretoria
Pretoria

Supervisor: Professor S. Lotz

January 2006

Declaration

I, the undersigned, hereby declare that the work contained in this dissertation is my own original work and that I have not previously in its entirety or in part submitted it at any university for a degree.

Signature:.................................

Date:..

Acknowledgements

I would like to express my sincere gratitude to

my Creator.

Prof Simon Lotz, my supervisor, for his guidance and support.

Mr Eric Palmer and Mr Dave Liles for providing me with data on my complexes.

my colleagues, Daniela Bezuidenhout and Werner Barnard, for their friendship

my parents and Thys Swart for his love and understanding.

the NRF for financial support.

Elisia

Table of Contents

Chapter 1
Introduction

Chapter 2

Monometallic Benzo[*b*]thienylcarbene Complexes

Chapter 3

Bimetallic Titanoxycarbene Complexes

Chapter 4

Bimetallic π-bonded Benzo[*b*]thienylcarbene Complexes

Chapter 5

Trimetallic Titanoxy-Benzo[*b*]thienylcarbene Complexes

Chapter 6
Conclusion

Chapter 7
Experimental

Summary

Fischer carbene complexes with metal-containing substituents were synthesized, fully characterized and systematically investigated with respect to their steric and electronic properties. Chromium and tungsten carbene complexes with benzo[*b*]thiophene, (η^6-benzo[*b*]thiophene)tricarbonylchromium(0), ethyl and titanocene dichloride as substituents were prepared. The (η^6- benzo[*b*]thiophene)tricarbonylchromium(0) was prepared by the displacement of the ammine ligands in the complex $[Cr(NH)_3(CO)_3]$ by the heteroarene in the presence of boron trifluoride diethyl etherate in boiling dibutyl ether. The carbene complexes were prepared *via* the classical Fischer method, in which the precursor heteroaromatic derivative is lithiated, reacted with a metal hexacarbonyl and quenched with an alkylating or metallating reagent, triethyl oxonium tetrafluoroborate or titanocene dichloride. The yield of the carbene complexes was further improved by washing the metal acylate with hexane before alkylation or metallation.

Carbene complexes with an ethoxy and a benzo[*b*]thienyl substituent of chromium- or tungsten pentacarbonyl were prepared and served as reference-complexes. Dimetallic Fischer carbene complexes were prepared by metallating the metal acylate with titanocene dichloride, thus yielding chromium and tungsten carbene complexes containing benzo[*b*]thiophene as heteroarene and a titanoxy-fragment as oxy substituent. Another type of dimetallic Fischer carbene complexes were obtained on reacting lithiated (η^6-benzo[*b*]thiophene)tricarbonylchromium(0) with chromium and tungsten hexacarbonyl and alkylating with triethyl oxonium tetrafluoroborate, thus yielding carbene complexes containing a metal-fragment π-bonded to the heteroarene substituent. Trimetallic Fischer carbene complexes were synthesized for the first time by lithiation of (η^6-benzo[*b*]-thiophene)tricarbonylchromium(0) and metallation with titanocene dichloride. These unique complexes displayed a carbene carbon atom surrounded by three metal-fragments and were studied in solution and in the solid state. The titanoxy substituent showed large electronic and steric effects in the structures of the trimetallic carbene complexes. By contrast, the chromium tricarbonyl fragment as part of the benzo[*b*]thienyl substituent has important electronic consequences, but does not affect the trimetallic carbene complexes sterically in any way.

List of Complexes

1:

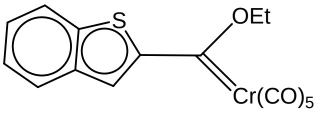

2:

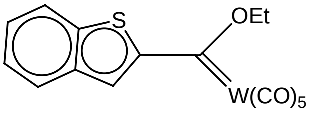

3:

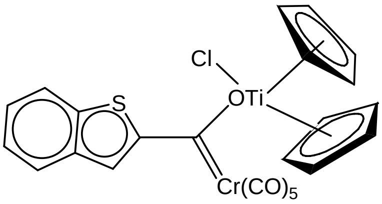

4:

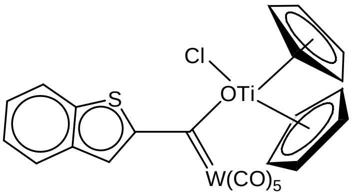

5:

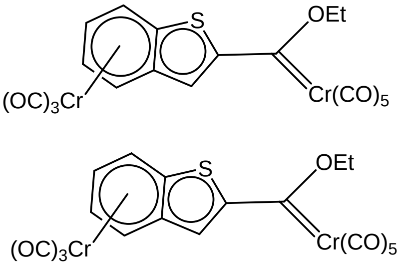
S
OEt
(OC)$_3$Cr
Cr(CO)$_5$
S
OEt
(OC)$_3$Cr
Cr(CO)$_5$

6:

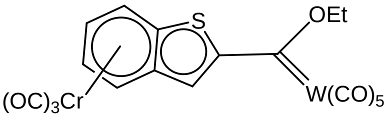
S
OEt
(OC)$_3$Cr
W(CO)$_5$

7:

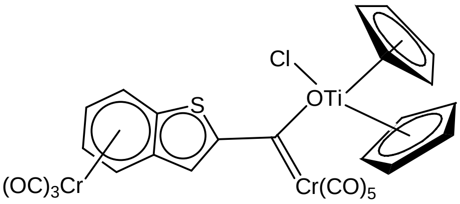
Cl
OTi
S
(OC)$_3$Cr
Cr(CO)$_5$

8:

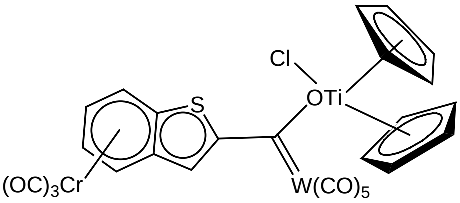
Cl
OTi
S
(OC)$_3$Cr
W(CO)$_5$

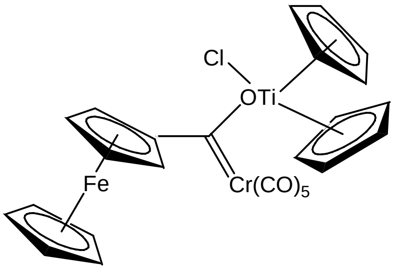
Cl
OTi
Fe
Cr(CO)$_5$

9.

List of Abbreviations

ar	:	aryl substituent
av	:	average
BT	:	benzo[*b*]thiophene
π-BTCr(CO)$_3$	:	(η^6-benzo[*b*]thiopene)tricarbonylchromium(0)
Bu	:	butyl
Cp	:	η^5-C_5H_5
d	:	doublet
dd	:	doublet of doublets
ddd	:	doublet of doublets of doublets
dddd	:	doublet of doublets of doublets of doublets
Et	:	ethyl
HETCOR	:	Heteronuclear Correlation Spectroscopy
IR	:	Infrared Spectroscopy
J	:	coupling constant
m	:	multiplet (NMR)
m	:	medium (IR)
m-s	:	medium to strong (IR)
Me	:	methyl
NMR	:	Nuclear Magnetic Resonance Spectroscopy
Ph	:	Phenyl
RT	:	room temperature
s	:	singlet (NMR)
s	:	strong (IR)

THF	:	tetrahydrofuran
TMEDA	:	N,N,N',N'-tetramethylethylenediamine
UV	:	ultraviolet
vs	:	very strong (IR)
vw	:	very weak (IR)
w	:	weak (IR)
Å	:	angstrom
δ	:	chemical shift
η^n	:	number, n, of ring atoms bonded to the metal in a π-ring fashion

1 Introduction

Organometallic chemistry deals with metal-carbon bonds and after the discovery of ferrocene, has become one of the most active areas of chemistry to be studied. Carbon can attach itself to metals in different ways of which the metal-carbon single (metal-alkyl), double (metal-carbene) and triple (metal-carbyne) bonds are examples. In addition, metals can coordinate to unsaturated carbon-carbon or carbon-heteroatom bonds in a "side-on" fashion, to give π-complexes.

1. π-complexes

1.1. Complexes with sandwich structures

The only true sandwich compounds with parallel rings are those of the types $(\eta^n\text{-}C_nH_n)_2M$ and $(\eta^n\text{-}C_nH_n)_2M^+$ (n represents the number of carbon atoms bonded to the metal). A large number of these complexes are known and ferrocene is the classical example.

Figure 1.1 Sandwich structures of (a) arene and (b) heteroarene complexes

1.2. Complexes with tilted sandwich structures

Three types of tilted sandwich compounds exist and they have one, two or three additional ligands. Titancene dichloride [Ti(η^5-C_5H_5)$_2$$Cl_2$] is an example of a bent or open shell sandwich compound with two terminal ligands.

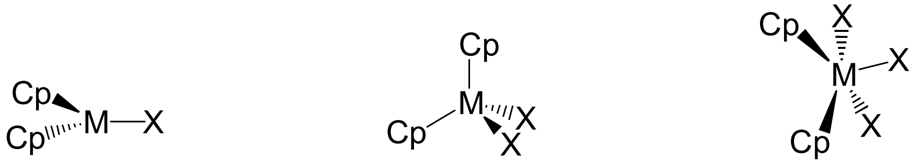

(a) (b) (c)

Figure 1.2 Bent sandwich complexes with (a) one (b) two and (c) three additional ligands

1.3. Complexes with half-sandwich structures

In π-arene complexes some of these structures exhibit a "piano stool" structure with the arene ring posing as the "seat" and the ligands as the "legs" of the stool. Also known are structures in the "milk stool" shape such as [Ni(η^5-C_5H_5)NO]. Although plenty of different structural examples exist, for this study the focus will be on the "piano stool" type. Complexes in discussion are of the type that contains arene or heteroarene moities and only one arene ring is π-bonded to a transition metal. The remaining coordination sites on the metal are occupied by ligands, e.g. Cl, CN, CO etc.

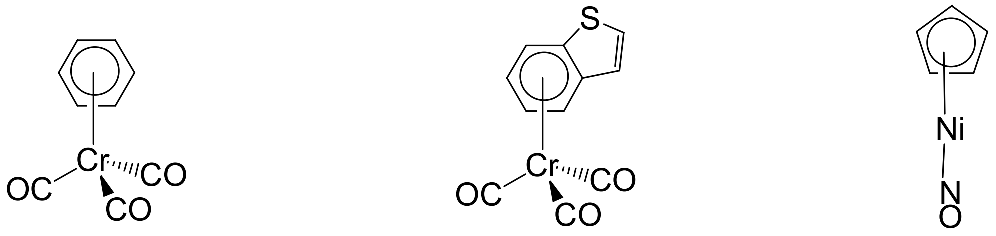

(a) (b) (c)

Figure 1.3 Examples of half-sandwich complexes: (a) arene and (b) heteroarene complexes in the "piano stool" and (c) an arene complex in the "milk stool" conformations

2. Carbene complexes

The term "carbene" refers to a divalent carbon species, that is, one in which a carbon atom forms two 2-electron bonds to adjacent atoms. The two remaining carbon electrons are then localized on the carbon atom, thus giving a sextet valence-electron configuration. This pair of carbon electrons may give rise to either a singlet or triplet spin ground state.[1] Complexes containing metal-carbon double bonds are generally referred to as metal-carbene complexes.

Even though carbenes are highly reactive species, some are stable and can be isolated.[2,3] Fischer and Maasböl were the first to synthesize and characterize a stable transition metal carbene complex[4] followed by the first nucleophilic carbene complexes that were prepared by Schrock in an effort to prepare a homoleptic tantalum(V) alkyl.[5] Thus, carbene complexes of two different types can be distinguished and they are named after their discoverers, i.e. Schrock and Fischer.

2.1. Fischer carbene complexes

In 1973 E.O. Fischer was awarded the Nobel Prize in Chemistry, not for discovering the first Fischer carbene complexes, but for solving the structure of ferrocene and other metallocenes.

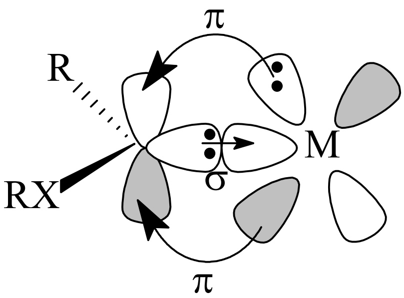

Figure 1.4 Important metal-orbital interactions in an electrophilic (Fischer) carbene complex (XR = heteroatom substituent)

Fischer carbene complexes have an electrophillic metal-coordinated *sp^2*-carbon atom and it can be considered as a neutral 2-electron ligand (L-type) derived from a singlet carbene carbon atom. These complexes are generally afforded by the reaction of metal carbonyls of transition metals in low oxidation states like ruthenium, rhenium, iron, manganese, molybdenum, chromium and tungsten with an organolithium reagent (Figure 1.5).

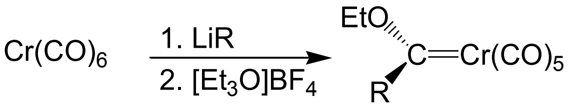

Figure 1.5 Synthesis of a Fischer carbene complex

2.1.1 Application of Fischer carbene complexes

Note also, that due to the strong electron-withdrawing pentacarbonyl metal fragment, that decreases the metal to carbene carbon π-backbonding, it is clear that the carbene carbon possesses a positive charge. Fischer carbene complexes can undergo reactions at several sites, outlined in Figure 1.6. Much of the reactivity of Fischer carbene complexes is directly analogous to the reactivity of carboxylic acid derivatives. Both have electrophilic carbon centers with leaving groups.

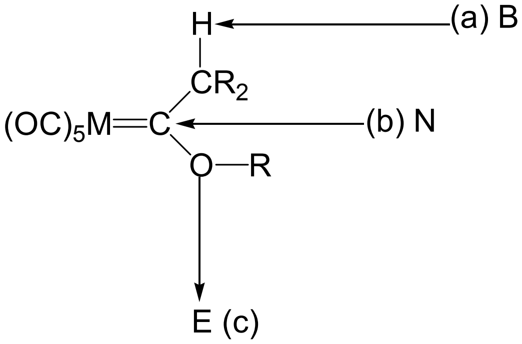

Figure 1.6 Reactivity of Fischer carbene complexes with bases (B), nucleophiles (N) and electrophiles (E)

Fischer carbene complexes with alkyl substituents can be deprotonated by bases (B) due to the acidity of the α-CH groups, to form metal carbene anions (route a), while nucleophilic (N) attack occurs at the elctrophilic carbene carbon atom (route b) e.g. aminolysis. Electrophiles (E), for instance Lewis acids, can coordinate to the alkoxy substituent (route c), leading to the formation of metal-coordinated carbyne complexes after C-O bond breakage. In the past few years interest in Fischer carbene complexes with respect to their ability to act as templates for the synthesis of organic compounds has grown immensely. Several review articles and books have addressed this topic.[6-11]

Fischer carbene ligands exhibit a wide range of reactivity and can be readily modified. Some of the more common reaction pathways serve as examples.

The heteroatom of a Fischer carbene complex can often be exhanged by simple nucleophilic displacement (see Figure 1.6 route b); this is referred to as heteroatom substitution.[12]

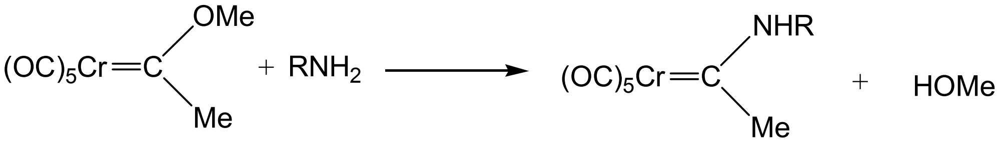

Figure 1.7 Heteroatom substitution[12]

The Dötz Reaction is another example. A carbene ligand containing a α-olefinic unit, an alkyne and carbon monoxide are converted into a benzannulated product.

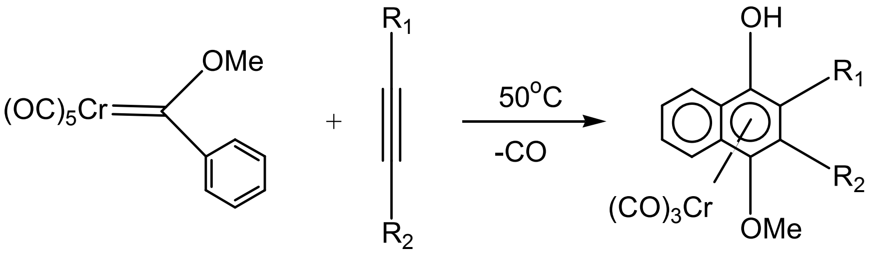

Figure 1.8 The Dötz reaction affording substituted naphthols

Dötz-type chemistry is well developed and has been used to prepare Vitamin E as well as some antibiotics. Fischer carbene complexes undergo many other kinds of annulation reactions where the Diels-Alder reaction is just another example.

2.2. Schrock carbene complexes

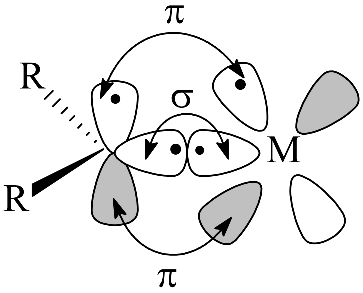

Figure 1.9 Important metal-orbital interactions in a nucleophilic (Schrock) carbene complex (R = alkyl substituents)

These complexes are afforded by using early transition metals in high oxidation states with strong donor and weak π-acceptor ligands.

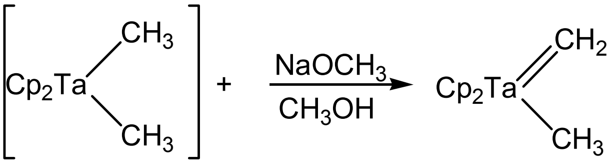

Figure 1.10 Example of a Schrock carbene complex

Schrock carbene complexes act as nucleophiles due to the partial negative charge that resides on the carbene carbon atom (Figure 1.10), as a result of polarization of shared electrons between an electropositive metal and a more electronegative carbene carbon atom. The carbene ligand is formally considered as a X_2-type ligand derived from a triplet carbene carbon atom, resulting in electron sharing in a metal-carbon σ- and π-bond.

2.2.1 Application of Schrock carbene complexes

Due to the nucleophilic character of Schrock carbene complexes, many reactions can take place for example by adding Lewis acid adducts (Figure 1.11) or addition to carbonyls, reactions similar to Figure 1.12 can be accomplished.

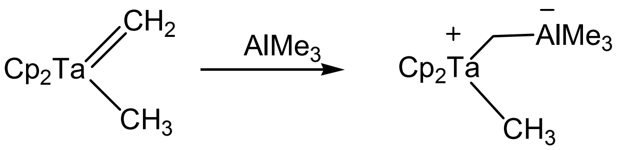

Figure 1.11 Addition of a Schrock carbene complex to a Lewis acid

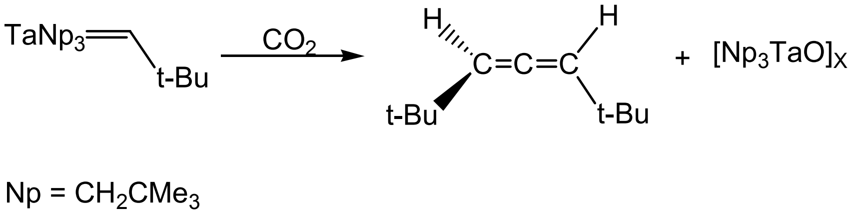

Figure 1.12 Addition of a Schrock carbene complex to carbon dioxide

Schrock working at Du Pont in early 1970's, tried to synthesize [Ta(CH_2CMe_3)$_5$], which was expected to be a stable compound because of the absence of β-hydrogen atoms. Instead he isolated the first stable metal-alkylidene complex, [Ta(CH_2CMe_3)$_3$(=$CHCMe_3$)], which has the formal oxidation state of V.[13] The advantage of Scrock's carbene catalysts, of which the most efficient were reported in 1990,[14-16] is that they are extremely active and are especially known for their role in metathesis reactions.

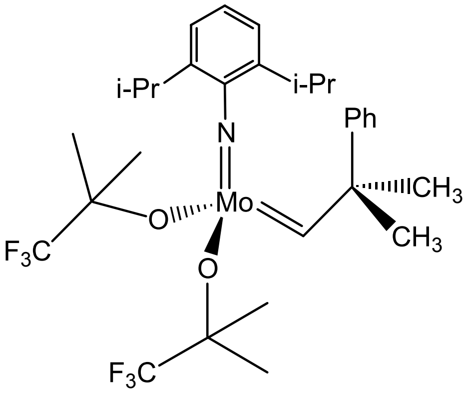

Figure 1.13 Commercially available Schrock carbene catalyst[14-16]

Schrock has invented a variety of catalysts, but the most important of these are arylimido complexes (imido ligands, also referred to as imides or nitrenes) of molybdenum with the general formula (Ar'N)(RO)$_2$Mo=CHR' where Ar' is typically 2,6-diisopropylphenyl, R' can be virtually anything and R is neopentyl (Np) or neophyl (CH_2CMe_2Ph). These catalysts are exceedingly active, metathesizing over 1000 equivalents of cis-2-pentene for one equivalent catalyst. Another advantage of these catalysts is that their reactivity can be tuned.

The Tebbe reagent [$Cp_2Ti(\mu\text{-}Cl)(\mu\text{-}CH_2)AlMe_3$] is particularly useful for the conversion of esters to vinyl ethers. It will olefinate carbonyls without enolizing α-stereocenters.[17] In the presence of a strong base such as pyridine, the reagent is functionally equivalent to $Cp_2Ti{=}CH_2$.

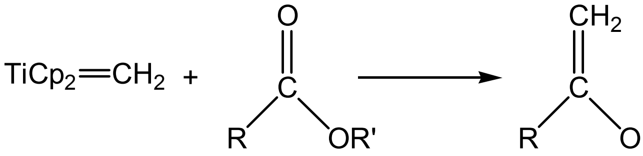

Figure 1.14 The conversion of an ester to vinyl ether, with the use of the Tebbe reagent

Another example where Schrock-type carbene complexes are used is in olefin matathesis. Olefin matathesis was first used in petroleum reformation for the synthesis of higher olefins in the Shell higher olefin process (SHOP). A metathesis reaction is a chain reaction involving a metal-carbene intermediate. The carbene ligand reacts with a coordinated olefin to a metallacyclobutane intermediate. This simple reaction type has enormous application in industry.

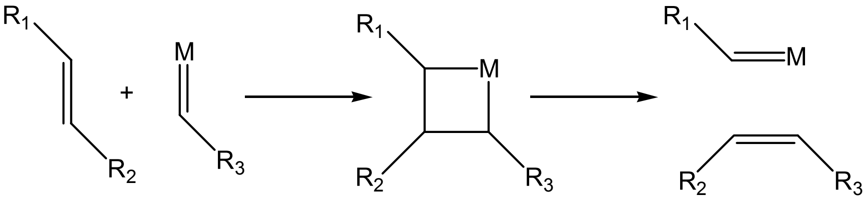

Figure 1.15 An example of a metathesis reaction

Three researchers in carbene chemistry shared this year's (2005) Nobel Prize in Chemistry; they are Y. Chauvin, R.H. Grubbs and R.R. Schrock. The Royal Swedish Academy of Sciences citation runs "for development of the metathesis method in organic synthesis".

Ring Opening Metathesis Polymerization (ROMP) is just another example of numerous metathesis reactions and is a subset of polymerization. The end of a growing chain acts as a reactive center that can react with additional monomers to propagate the chain to form a polymer. In ring-opening polymerization, the monomer is a cyclic compound which causes the chain to propagate through cationic or anionic propagation. Examples of polymers produced by this method are Nylon 6 and polyethylene oxide. The catalysts used for ROMP are the same catalysts used for olefin metathesis.

The Grubbs[18] and Schrock[19] catalysts offer synthetic chemists novel opportunities, due to their tolerance of a large variety of functional groups, combined with their efficiency, and, for Grubbs' catalysts, their ease of handling in air. These catalysts have widespread use in organic chemistry.[20]

Clearly metal carbene complexes are of utmost importance in organic synthesis, by acting as templates and catalysts.[21]

3. Dimetallic Fischer carbene complexes

A lot of interest has developed in compounds containing two or more metals, due to the belief that these compounds could cooperate in catalytic transformations more effectively, because of their ability to promote new processes unknown for one metal acting on its own.[22-25] Principally, three possibilities exist in adding new metal centered fragments (represented by M') to Fischer carbene connecting atoms (Scheme 1.1).

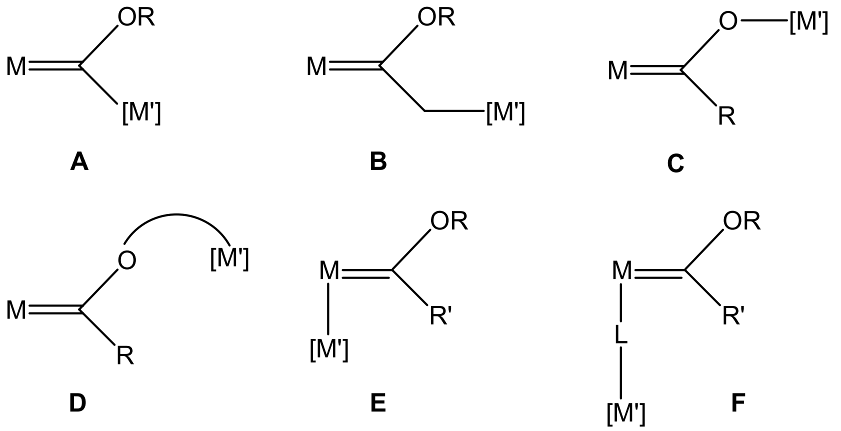

Scheme 1.1 Dimetallic Fischer carbene complexes

The first possibility is on the carbene carbon, either directly joined (**A**) or through a carbon chain or bridging unit (**B**). The second is through the heteroatom connected to the carbene carbon (**C**, directly and **D**, *via* a carbon or connecting chain). Thirdly, directly to the metal center, by a metal-metal bond (**E**) or by a bidentate ligand joining both metal centers (**F**). For compounds analogous to **A** and **B**, the standard synthetic procedures are based on that developed for the preparation of mononuclear carbene complexes; it will follow one of the following methods:

(I) From metal complexes that do not contain a preformed carbene ligand.

(II) A mononuclear metal carbene complex containing a carbanion generated α to the carbene carbon, can be alkylated or acylated.

(III) The additional metal center can be attached on the double or triple bond of metal carbene complexes that have unsaturated substituents.

(IV) A metal nucleophile can be added to a carbyne complex.

(V) Allenyl complexes can be used as precursors.

For compounds analogous to **C** and **D**, the classical Fisher route to carbene complexes is applicable, but alkylation involves a metal. Another possibility exists, and that is by starting with (η^4-diene)metallocenes and metal carbonyls, several dimetallic metaloxy-carbene complexes were afforded.[26-29] As for compounds analogous to that of **E**, the first synthesised carbene of this type was by King in 1963[30] (Figure 1.16). These reactions were carried out by reacting sodium pentacarbonyl manganate(-I) and either 1,3-dibromopropane or 4-butyryl chloride.

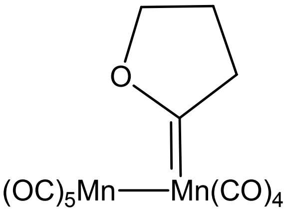

Figure 1.16 King's dimetallic carbene complex[31]

Fischer reported that the reaction of $[Mn_2(CO)_{10}]$ with RLi (R = Me, Ph) followed by treatment with $[R_3O]BF_4$ yielded the first homodimetallic carbene complex that was characterized.[32,33]

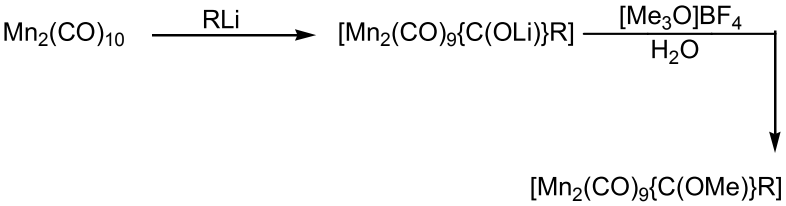

Figure 1.17 Synthesis of one of the first homodimetallic carbene complexes

Complexes of the type **F**, can be generated by attaching metal fragments *via* bidentate ligands.

4. Aim of this study

The synthesis and characterization of Fischer carbene complexes with transition metal containing substituents have not yet been investigated systematically. In this study, the role of independent metal containing substituents in stabilizing the carbene carbon atom was addressed. Substituents were selected if they contained a conjugated π-system, creating a pathway for charge to be transferred from the metal to the carbene carbon atom. A second important factor that could affect the formation and/or stability of the trimetallic carbene complex was the steric bulk of the substituents. These metal-containing substituents may be too bulky and the carbene carbon atom too crowded for stability. Steric complications can be expected when the metal fragments are directly bonded to the carbene carbon (Schrock-type carbene complexes) or slightly less so when attached to a carboxy-carbene (Fischer-type carbene complexes). However, even for Fischer carbene complexes, we were concerned that the non-oxygen substituent may again, because of its bulkiness, cause too much steric hindrance for the trimetallic carbene complex to be stable enough to isolate. It was decided to create some space at the non-oxygen substituent by introducing a heteroaromatic ring that is π-bonded to a $Cr(CO)_3$ fragment. For this study carbene complexes of chromium and tungsten with carbonyl ligands as ancillary ligands were chosen, being representative of classes of carbene complexes of high stability.[7] As alkoxy substituent titanocene chloride was chosen for two reasons. The procedure for the synthesis of titanoxycarbene complexes in bimetallic complexes has been described in literature and the titanium(IV) centre has a high affinity for oxygen atoms.[34] As a third metal-containing fragment benzothiophene π-coordinated to chromium tricarbonyl was chosen for reasons of creating space at the carbene carbon atom as the $Cr(CO)_3$ fragment is π-bonded to the benzene ring which is furthest from the point of attachment.[35] To systematically study the electronic and steric effects of the different metal-containing substituents they were introduced in a stepwise manner.

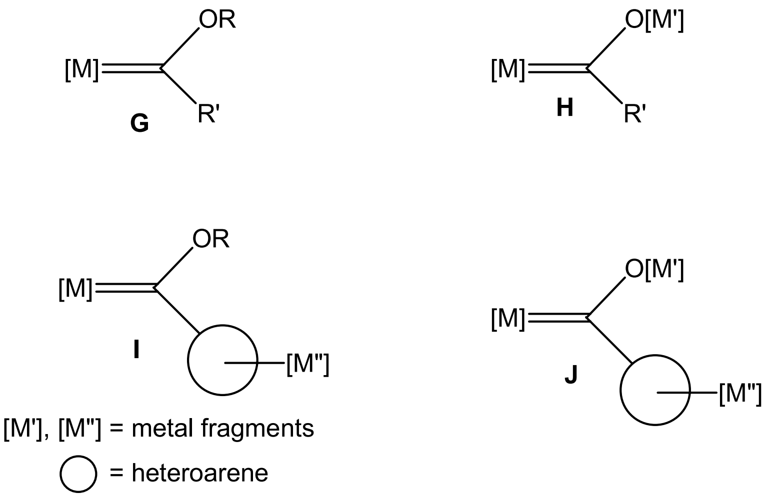

Scheme 1.2 Synthesized metal carbene complexes

The chapters in this thesis were organized in such a way that it deals with each metal substituent as an independent role player in the overall carbene complex.

In Chapter 1 a short overview is given of metal carbene and π-arene complexes. Emphasis is placed on the electronic properties of carbene complexes and their reaction profile. Chapter 2 was dedicated to the synthesis and the molecular structures of the "reference carbene complexes". They contain either components of the metal substituents or will act as reference substituents to unravel the role of the metal-containing substituent. These are shown as carbene complexes of the type **G** (Scheme 1.2). Two different metal hexacarbonyls were used as precursors, lithiated benzo[*b*]thiophene as reactant and alkylation was done by [Et$_3$O]BF$_4$.

In Chapter 3 "alkylation" was performed with titanocene dichloride while benzo[*b*]thienyl remained the third substituent. These complexes are represented by **H** and the objective was to study the role of the titanocene fragment in the carbene complexes. Comparisons were made with respect to the ethoxycarbene complexes in Chapter 2.

In Chapter 4 the focus was on modifying the benzo[*b*]thienyl group to a π-benzo[*b*]thienyl complex and using this as carbene substituent. Complexes represented by **I** were synthesized to study the role of the π-benzo[*b*]thienyl-chromium-tricarbonyl substituent. Comparisons were made with respect to the benzo[*b*]thienyl complexes in Chapter 2. In Chapter 5 the anticipated three-metal-fragment carbene complexes, as represented by **J**, were the focus point of the investigations.

The study also included a large number of crystal structures and detailed NMR and infrared studies to explore the electronic and steric properties of the carbene substituents in the solid state as well as in solution.

5. References

1. F.A.Cotton, C.M.Lukehart, *Prog. Inorg. Chem.*, **1972,** p. 489.
2. A.Wolfgang, C.Kocher, *Angew. Chem* **1997,** *36* 2162.
3. D.Bourissou, O.Guerret, F.P.Gabbai, G.Bertrand, *Chem. Rev.* **2000,** *39* 100.
4. E.O.Fischer, A.Maasböl, *Angew. Chem* **1964,** *76* 645.
5. R.R.Schrock, *Acc.Chem. Res.* **1979,** *12* 98.
6. L.S.Hegedus, *Synthesis of complex organic molecules*, Mill Valley Clifornia **1994**.
7. K.H.Dötz, H.Fischer, P.Hofmann, F.R.Kreissl, U.Schubert, K.Weiss, *Transition metal carbene complexes*, (VCH Verlag Chemie) Weinheim **1983**.
8. M.Schuster, S.Blechert, *Angew. Chem., Int. Ed. Engl.* **1997,** *36* 2036.
9. W.D.Wulff, *Organometallics* **1998,** *17* 3116.
10. R.Aumann, R.Fröhlich, J.Prigge, O.Meyer, *Organometallics* **1999,** *18* 1369.
11. M.M.Abd-Elzaher, H.Fischer, *J.Organomet.Chem.* **1999,** *588* 235.
12. C.P.Casey, A.J.Shusterman, *J. Mol. Catal.* **1980,** *8* 1.
13. R.R.Schrock, *J. Am. Chem. Soc.* **1974,** *96* 6796.
14. J.S.Murdzek, R.R.Schrock, *Organometallics* **1987,** *6* 1373.
15. R.R.Schrock, S.A.Krouse, K.Knoll, J.Feldman, J.S.Murdzek, D.C.Yang, *J. Mol. Catal.* **1988,** *46* 243.

16. R.R.Schrock, J.S.Murdzek, G.C.Bazan, J.Robbins, M.DiMare, M.O'Regan, *J. Am. Chem. Soc.* **1990,** *112* 3875.

17. K.A.Brown-Wensley, S.L.Buchwald, L.Cannizzo, L.Clawson, S.Ho, D.Meinhardt, J.R.Stille, D.Straus, R.H.Grubbs, *Pure Appl.Chem.* **1983,** *55* 1733.

18. P.Schwab, R.H.Grubbs, J.W.Ziller, *J. Am. Chem. Soc.* **1996,** *118* 100.

19. R.R.Schrock, J.S.Murdzek, G.C.Bazan, J.Robbins, M.DiMare, M.O'Regan, *J. Am. Chem. Soc.* **1990,** *112* 3875.

20. R.H.Grubbs, *Handbook of metathesis*, Wiley-VCH, New York **2003**.

21. J.L.Hérisson, Y.Chauvin, *Macromol. Chem.* **1971,** *141* 161.

22. E.K.van den Beuken, B.L.Feringa, *Tetrahedron* **1998,** *54* 12985.

23. E.M.Vogl, H.Gröger, M.Shibasaki, *Angew. Chem., Int. Ed. Engl.* **1999,** *38* 1570.

24. M.Shibasaki, H.Sasai, T.Arai, *Angew. Chem., Int. Ed. Engl.* **1997,** *36* 1237.

25. W.A.Herrmann, B.Cornils, *Angew. Chem., Int. Ed. Engl.* **1997,** *36* 1049.

26. G.Erker, *Angew. Chem., Int. Ed. Engl.* **1989,** *28* 397.

27. G.Erker, *Polyhedron* **1988,** *7* 2451.

28. G.Erker, F.Sosna, U.Hoffmann, *J. Organomet. Chem.* **1989,** *372* 41.

29. R.Beckhaus, *Angew. Chem., Int. Ed. Engl.* **1997,** *36* 686.

30. R.B.King, *J. Am. Chem. Soc.* **1963,** *85* 1922.

31. C.P.Casey, *J. Chem. Soc., Chem. Commun.* **1970,** 1220.

32. E.O.Fischer, E.Offhaus, *Chem. Ber.* **1969,** *102* 2549.

33. G.Hunter, D.Regler, *Chem. Ber.* **1972,** *105* 1230.

34. E.O.Fischer, S.Fontana, *J. Organomet. Chem.* **1972,** *40* 159.

35. E.O.Fischer, H.A.Goodwin, C.G.Kreiter, H.D.Simmons, K.Sonogashira, S.B.Wild, *J. Organomet. Chem.* **1968,** *14* 359.

2 Monometallic Benzo[b]thienyl-carbene Complexes

1. Introduction

Benzo[*b*]thiophene

The first example of a carbene metal complex containing an aromatic substituent is coincidentally also the first reported carbene complex [W(CO)$_5$C(OMe)Ph] prepared by Fischer and Maasböl.[1] After refining the synthetic process[2] they concluded that these carbene complexes are generally quite stable, diamagnetic, soluble in organic solvents, and sublimable. A compound like **G** (Scheme 1.2) is of this kind and contains a single metal-fragment. Benzo[*b*]thiophene (BT) is an example of a heteroarene and has a benzene ring fused to a thiophene ring. Since the 1960s it was agreed that aromatic compounds have the following characteristics:[3]

(I) They have cyclic delocalized π-electron systems and are planar.

(II) They are more stable than their olefinic analogues by an energy called the resonance energy.

(III) Bond lengths between adjacent atoms intermediate between those of typical single and double bonds.

(IV) They have a π-electron ring current induced by an external magnetic field, leading to increased diamagnetic susceptibility and typical diatropic [low field] chemical shifts of exocyclic protons in ^{1}H NMR spectra.

(V) Substitution reactions take place more readily than addition reactions.

(VI) Spectroscopically they show higher energy ultraviolet/visible spectral bands and a more symmetrical structure for their IR spectra.

It is important to note that heterocycles can be classified as π-excessive or π-deficient. π-Excessive heterocycles are compounds in which the number of π-electrons in the conjugated system exceeds the number of atoms forming the cycle. The compounds pyrrole, thiophene, benzo[*b*]thiophene, indole and dibenzothiophene are classical examples of π-excessive heterocycles. In this chapter focus falls on carbene complexes containing BT, of which the molecular orbital calculations of the localized charges for each of the carbon atoms and the sulphur atom have been reported.[4]

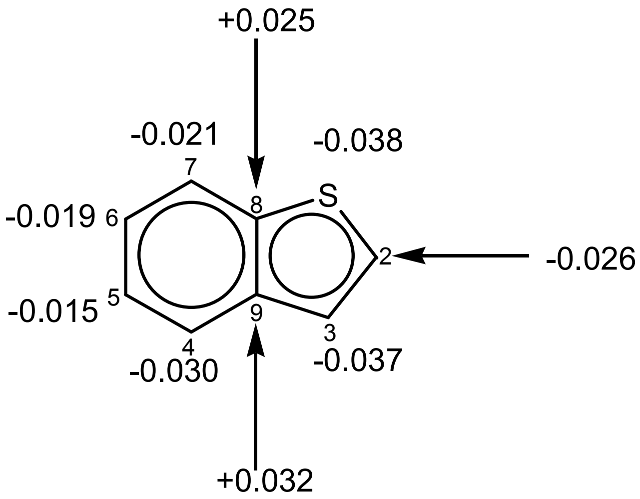

Figure 2.1 Molecular orbital charge calculations and atom numbering for benzo[*b*]thiophene

Molecular orbital calculations for BT have revealed that the highest electron densities are on the sulphur and the C2-C3 carbon atoms, giving rise to the fact that BT is easily deprotonated in high yields in the 2-position of the thiophene ring to give benzothienyllithium. This lithiated precursor can be used to react with transition metal hexacarbonyls.

Stabilization of carbene complexes

A complete study has been conducted on complexes of the type [$M(CO)_5C(X)Y$], where M = Cr or W; X = OR or NR^1R^2, and Y is an organic group, with the aid of NMR spectroscopy. The findings were that the chemical shift of the carbene carbon is more strongly influenced by X than by either M or Y.[5] Mills in cooperation with Fischer and his co-workers carried out a single crystal X-ray structure determination of the carbene complex, pentacarbonyl[methoxy-(phenyl)carbene]-chromium(0).[6] This structure confirmed that the carbene carbon atom is *sp*^{2} hybridized, which also indicates an empty *p*-orbital and an electron-deficient carbon atom.

There are three ways in which the electron deficiency on the carbene carbon atom can be relieved and the carbene complex stabilized. This can be achieved mainly by π-interaction from the substituents with π-bonding facilities. Carbene stabilization is predominantly from the low oxidation state metal and/or from the heteroatom lone pair bonded to the carbene carbon. A *pπ—pπ* bond can form between one of the lone electron pairs on the oxygen atom of the alkoxy group and the unused *p*-orbital of the carbene carbon. In amino carbene complexes this effect is even enhanced to such an extent that geometric isomers exists and can be isolated.[7] Also very important is *dπ—pπ* backbonding from occupied central metal (tungsten or chromium) orbitals to the empty *p*-orbital of the carbene carbon. It is known that the carbonyl ligands in metal-carbonyl complexes may be considered as weak σ-donor and good π-acceptor ligands. This represents a synergic σ-donor and π-acceptor bonding mode and increases the metal-carbon(carbonyl) bond order. Compared to carbonyl ligands, Fischer carbene ligands are stronger σ-donor but weaker π-acceptor ligands. However, the role of the third substituent to π-stabilize the carbene carbon atom *via pπ—pπ* interaction could also be important if the substituent is an aryl. This electron withdrawing effect should be comparable to the effect observed of an ester substituent on an aryl-type ring with a conjugated π-system. Connor and Jones studied the role of the heteroatom in heteroarene substituted carbene complexes.[8] It was assumed that by changing the heteroatom (Figure 2.2) in the herteroarene substituent, the contribution of π-stabilization of the carbene carbon by this substituent should differ.

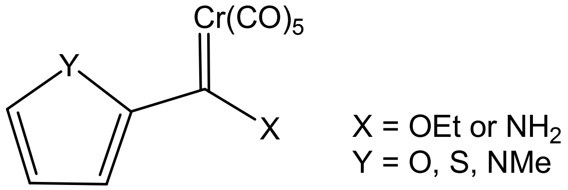

Figure 2.2 A heteroarene substituent with different heteroatoms in carbene complexes[8]

It was found that the heteroarene rings will π-donate electron density to the carbene carbon and the effect will increase in the order Y = O<S<NMe.

In this study the effect of carbene stabilization by all three substituents comes under scrutiny. In this chapter the carbene complexes shown in Figure 2.3 were synthesized and characterized. The carbene carbon is in π-contact with the benzo[*b*]thiophene substituent and the oxygen substituent.

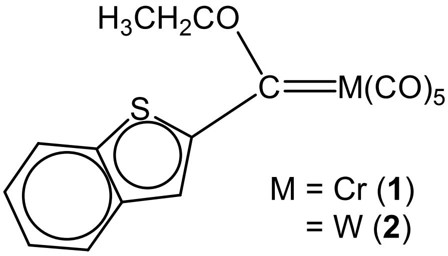

Figure 2.3 Carbene complexes synthesized in this chapter

To study electronic and steric properties in solution, spectroscopic measurements were recorded and in the solid-state crystal structure determinations were performed. Although **1** and **2** represent fairly simple examples of Fischer carbene complexes, they form the basis and reference point of a systematic study of di-and trimetallic carbene complexes. It is reasonable to assume that benzothienyl substituents should be comparable to thienyl substituents in their potential to donate electron density to the carbene carbon. Fischer carbene complexes with thienyl substituents have been prepared and studied before.[8-10]

2. Metallation

Deprotonation of BT is accomplished by the use of a strong base (pK_a>20) e.g. n-BuLi (n-butyllithium). The acidity of the arene protons allows hydrogen-metal exchange to occur on the 2-position, in the thiophene ring, under conditions as specified (Scheme 2.1).

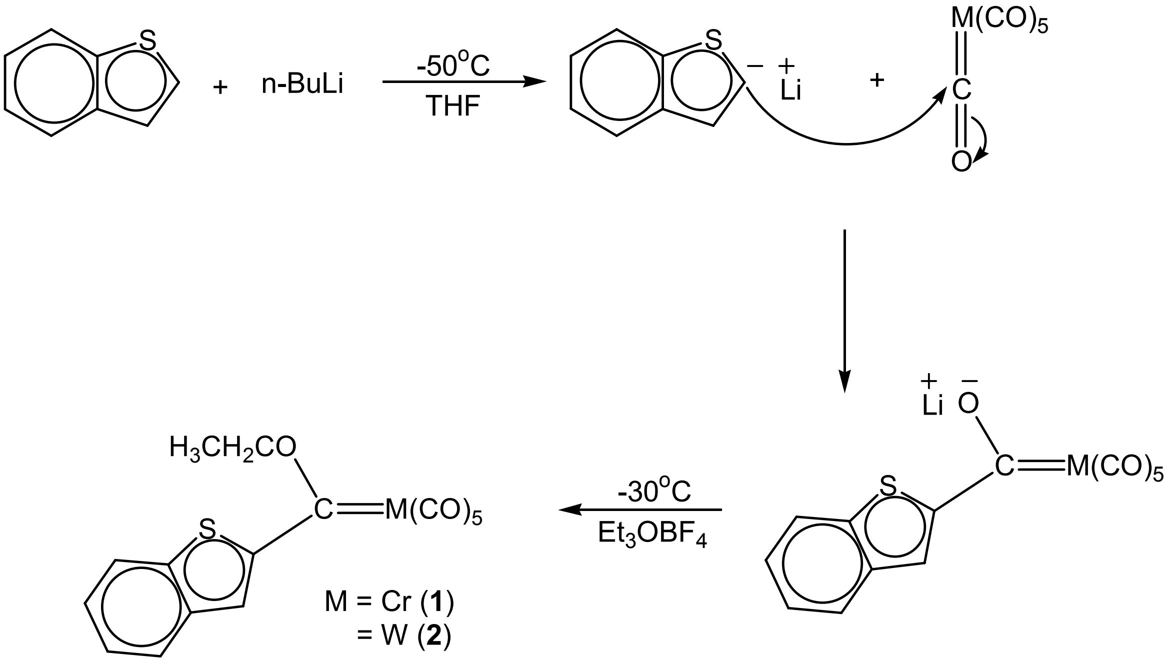

Scheme 2.1

The metallated BT has nucleophilic properties located on the α-carbon of the thiophene ring and attacks an electron deficient carbon atom belonging to the metal hexacarbonyl complex to form a metal acylate. After replacing the solvent with dichloromethane, triethyloxonium salt was added to the metal acylate and the desired neutral carbene complexes formed. The formation of the carbene complexes, **1** (red) and **2** (red-brown), occurred with high yields and the complexes were purified with column chromatography, using silica gel as stationary phase.

3. Spectroscopic characterization

The carbene complexes **1** and **2** were characterized in solution using NMR and infrared spectroscopy and in the solid state by molecular crystal structure determinations.

3.1 NMR Spectroscopy

The chemical shift values of ligand nuclei are affected when coordination of a metal fragment occurs. The resulting coordination shift, defined as the chemical shift difference between the metal bonded ligand and the free ligand is indicated with the symbol Δδ.

3.1.1 ^{1}H NMR spectroscopy

The signals in the ^{1}H NMR spectrum of uncoordinated BT were resolved and a full iterative analysis was carried out.[11] The signals of the protons of BT in deuterated chloroform are given in Figure 2.4.[12,13] and the following system of numbering of the protons and carbon atoms of benzo[*b*]thiophene will be used throughout the whole discussion.

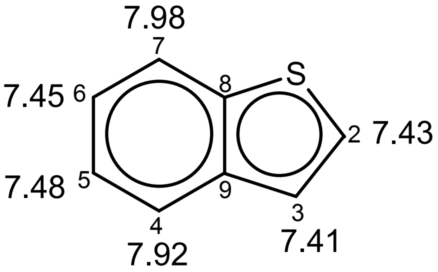

Figure 2.4 Chemical shifts of the protons of BT and atom labelling used for benzo[*b*]thiophene complexes

^{1}H NMR spectra were recorded in $CDCl_3$ as well as C_6D_6 as reported in Table 2.1, the assignment of the chemical shifts to the individual protons was resolved from chemical shift values and a HETCOR experiment along with the chemical shift values obtained for the starting material. In complexes **1** - **2**, the singlet of coordinated BT, (or doublet due to long distance coupling) and the doublet of uncoordinated BT observed for the thienyl protons along with the coupling constants and patterns, prove that the carbene carbon is bonded at the 2-position of the BT ligand. Since H3 is the proton closest to the site of coordination to the metal fragment, the chemical shift of this proton is influenced the most.

Comparing the data of uncoordinated BT (Figure 2.5) with the data of BT in compounds **1** and **2**, it is evident that the metal-fragment and metal type have a significant influence on the ring protons. By comparing only the $CDCl_3$ values, since the ^{1}H NMR spectrum of the uncoordinated BT was only in $CDCl_3$, it is evident that a large down field chemical shift ($\Delta\delta \approx 1$ ppm) for H3 occurs. This is expected due to the electron withdrawing character of the carbene carbon bonded to the 2-position of the BT ring as well as the coordination of the carbene carbon to the $M(CO)_5$ fragment. As a result the withdrawal of electron density from the 3-position was observed, leading to a more deshielded proton, and causing a downfield chemical shift.

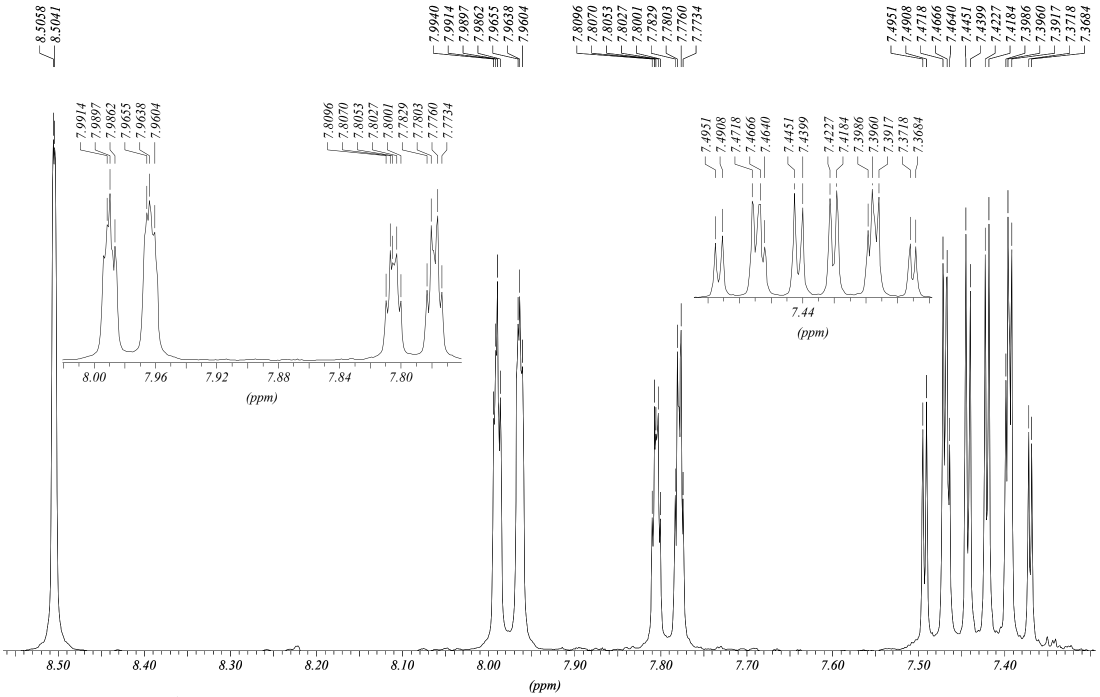

Figure 2.5 ^{1}H NMR spectrum of complex **1** in $CDCl_3$, in the region for the ring protons

When comparing compounds **1** and **2**, one can recognise a more deshielded H3 proton for complex **1** ($\Delta\delta \approx 0.1$ ppm). The methylene protons of the etoxycarbene substituent are also downfield for **1** compared to **2** ($\Delta\delta \approx 0.2$ ppm). This is ascribed to the different metals bonded to the carbene carbon. Interestingly, the benzene protons H4-H7 are little affected compared to the thiophene proton, indicating that little charge is withdrawn from the benzene ring.

Problems were experienced during the effort to determine the coupling constant of the H5-H6 signal due to the overlap of the NMR signals, and no value could be assigned unambiguously. Coupling constants of H5 and H6 to protons H4 and H7 were resolved with the help from the resolutions obtained from the H4 and H7 proton signals, which had clear coupling constants.

Table 2.1 ^{1}H NMR data of complexes **1** and **2**

Assignment	Complexes				
	Chemical shifts (δ, ppm) and coupling constants (J, Hz)				
	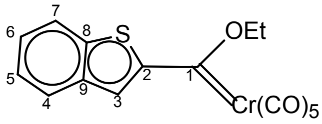 **1**			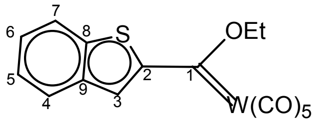 **2**	
Proton	δ	$^3J_{H\text{-}H}$	$^4J_{H\text{-}H}$	δ	$^3J_{H\text{-}H}$
H3[a]	8.50 (d)	-	0.8	8.39 (s)	-
H4	7.80 (dddd)	8.0	1.8 0.8	7.79 (d)	8.2
H5	7.47 (ddd)	8.0	1.03	7.50 (m)	8.2
H6	7.40 (ddd)	7.8	1.8	7.39 (m)	7.9
H7	8.00 (dd)	7.8	1.03	8.00 (d)	7.9
$-CH_2-$	5.25 (q)	7.0	-	5.04 (q)	6.9
$-CH_3$	1.72 (t)	7.0	-	1.69 (t)	6.9
H3[b]	8.51 (s)	-	-	8.40 (s)	-
H4	7.33 (d)	7.9	-	7.31 (dd)	8.1
H5	7.00 (t)	7.9	-	7.01 (m)	8.1
H6	6.95 (t)	7.9	-	6.94 (m)	8.1
H7	7.46 (d)	7.9	-	7.45 (d)	8.1
$-CH_2-$	4.70 (q)	6.9	-	4.51 (q)	7.0
$-CH_3$	1.05 (t)	6.9	-	1.02 (t)	7.0

[a] spectrum was recorded in $CDCl_3$

[b] spectrum was recorded in C_6D_6

3.1.2 ^{13}C NMR spectroscopy

The chemical shifts in the ^{13}C NMR spectrum of uncoordinated BT in deuterated chloroform are known from literature[11-13] and are as follow: 126.1 (C2), 123.7 (C3) 139.5, 134.6 (C8, C9), 123.5 (C4), 124.0 (C5), 124.1 (C6), 122.3 (C7).

The ^{13}C NMR data of complexes **1** and **2** are summarized in Table 2.2 and the chemical shift values were assigned with the help of the information gained from a 2D HETCOR experiment. Due to poor solubility in C_6D_6, the ^{13}C NMR spectrum of compound **1** does not show all the resonances.

Table 2.2 ^{13}C NMR chemical shifts of complexes **1** and **2**

Assignment	Complexes			
	Chemical shifts (δ, ppm)			
	1		**2**	
Carbon	δ^a	δ^b	δ^a	δ^b
C1	320.5	320.2	294.3	294.2
C2	154.0	-	157.0	157.5
C3	141.9	139.5	142.5	143.2
C4	122.8	122.7	122.9	122.9
C5	128.9	129.1	128.8	129.0
C6	125.1	125.2	125.2	125.4
C7	126.8	128.6	126.9	127.1
C8, C9	138.7, 139.2	-	139.0, 139.5	139.3, 139.7
$-CH_2-$	76.5	76.6	79.0	79.1
$-CH_3$	15.1	14.5	14.9	14.3
CO	216.9 (cis) 223.4 (trans)	217.4 (cis) 223.8 (trans)	197.5 (cis), (sattelites) 202.6 (trans)	197.9 (cis), (sattelites) 203.1 (trans)

[a] spectrum was recorded in $CDCl_3$

[b] spectrum was recorded in C_6D_6

Notable differences are observed when comparing the ^{13}C NMR chemical shift values of the uncoordinated BT with those of the complexes **1** and **2**. It is obvious that the thiophene ring, where the carbene carbon is attached (C2) and other thiophene carbons (C3,C8,C9), are more affected than those of the benzene ring fragment. Again, this is due to the electron withdrawing effect of the carbene carbon C1 and charge delocalization of the thiophene ring, which in itself has the highest down field chemical shift due to electron deficiency. In free BT charge delocalization is mostly within the thiophene ring with a resulting shielding effect. When BT is attached to a carbene carbon atom, delocalization is outwards towards the carbene carbon with a resulting deshielding effect.

For both compounds the $M(CO)_5$ resonances are depicted as two signals of different intensities, indicating a difference in chemical shifts of the CO carbons. This is due to the fact that one carbonyl is *trans* to the carbene ligand where the other four ligands are found *cis* to the carbene carbon or opposite carbonyl ligands. The interesting pattern observed at 197.5 ppm in $CDCl_3$ and 197.9 ppm in C_6D_6, for the *cis* carbonyl resonance of complex **2** (Figure 2.6), is ascribed to ^{13}C—^{183}W coupling (J = 63.3 Hz). Other examples of ^{13}C—^{183}W coupling have been reported.[14]

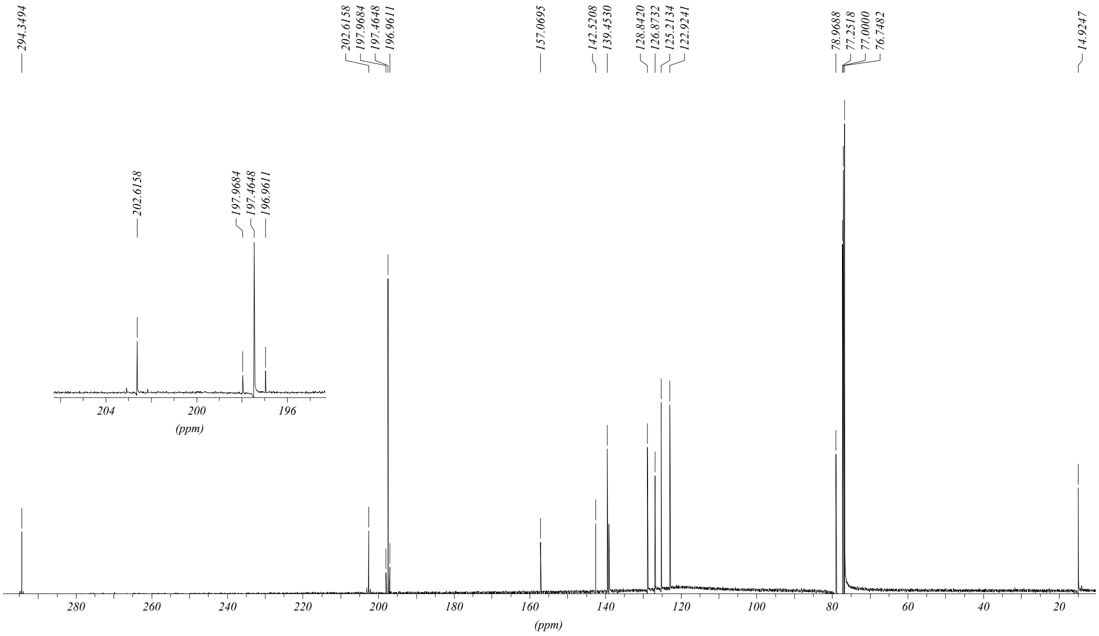

Figure 2.6 ^{13}C NMR spectrum in $CDCl_3$ of complex **2** with the enlarged CO region

3.1.3 2D HETCOR Experiment

In this experiment one-bond ^1H-^{13}C couplings are used to show directly which protons are attached to which carbon atoms. In Figure 2.7 the HETCOR spectra of complex **2** is represented. The chemical shifts of H (δ_H) are stipulated on the x-axis, while the chemical shifts of C (δ_C) are introduced on the y-axis. From this data it was possible to assign C3, C4-C7 to the corresponding protons in ^1H NMR spectrum.

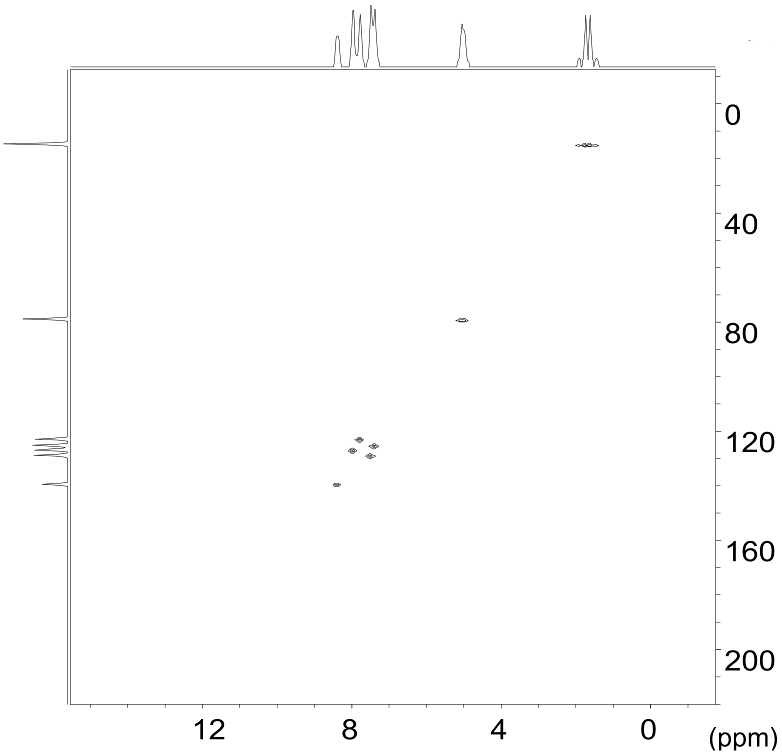

Figure 2.7 2D HETCOR spectrum of compound **2**

3.2 Infrared Spectroscopy

A lot of structural and electronic information of ligands can be obtained from the infrared spectra in the carbonyl region of metal carbonyl complexes. The transition metal-CO bond of a terminal carbonyl ligand is described as a resonance hybrid and the bond order for the M-C and C-O bonds are determined by the electronic properties of the metal and other ligands in the compound. The bond order for the M-C bond can either be 1 (a) or 2 (b) and the bond order for the C-O bond varies accordingly from 3 (a) to 2 (b) as seen in figure 2.8.

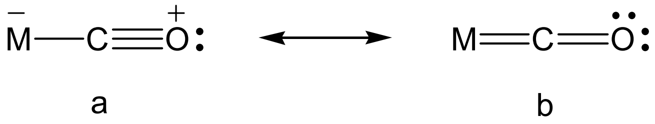

Figure 2.8 Resonance structures for the M-C-O bonds in metal carbonyl complexes

The resonance effect observed in **a** is due to the electron density donation from the carbonyl ligand to the metal *via* a σ-donor interaction. In return, the metal can donate electron density to the carbonyl *via* π-interaction (backbonding) shown by **b**. The magnitude of the backbonding depends on the nature of the transition metal and other non-carbonyl ligands. Obviously when late transition metals are concerned or complexes have a net negative charge, backbonding will play a decisive role, since the electron density on these metals are considerably higher than for early transition metals. C-O stretching vibrational frequencies can be regarded as being independent from other vibrations in the molecule, thus a qualitative correlation between CO stretching vibrational frequencies and the bond order of the C-O bond can be made.[15] As backbonding from the metal to the carbonyl ligand increases, the M-C bond becomes stronger and thus shorter. The C-O bond weakens accordingly and becomes longer. This increase in bond order of the M-C bond, prompts the carbonyl stretching frequency to shift to a lower wavenumber on the IR spectrum.

The number and intensities of carbonyl stretching frequencies are dependent on the local symmetry of the carbonyl ligands around the central atom. According to the method of local symmetry[16] a pentacarbonyl complex of the type $M(CO)_5L$, belongs to the symmetry group C_{4v}, which can perform four vibrations namely $A_1^{(1)}$, $A_1^{(2)}$, B_1 and E. As seen in Figure 2.9, only two vibrational bands are IR active and they are the E and $A_1^{(2)}$ bands, the other bands can be detected with Raman spectroscopy, however the $A_1^{(1)}$ band may become IR active due to coupling with the vibrational modes of the $A_1^{(2)}$ band vibrations and since complexes in discussion do not exhibit absolute C_{4v} symmetry, distortions in the carbonyl plane are possible, resulting in an IR-active B_1 band. Aspects related to tricarbonyl fragments will be discussed in Chapter 4.

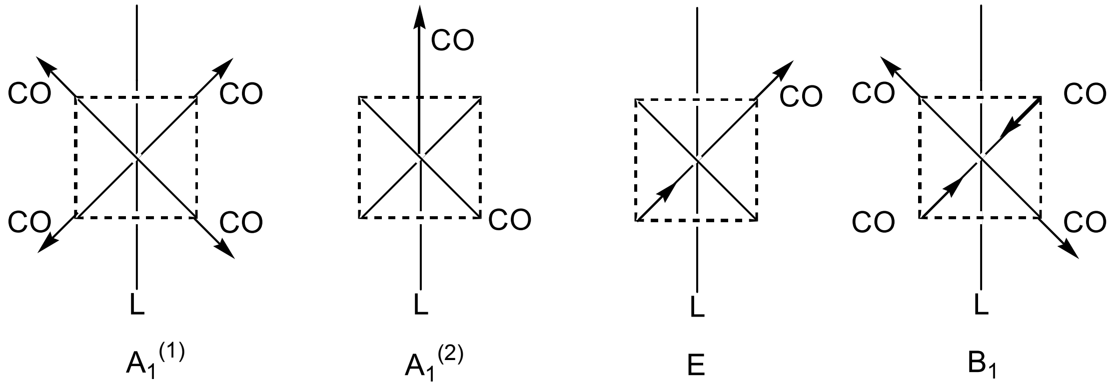

Figure 2.9 Stretching vibration modes of [M(CO)$_5$L] complexes

From Figure 2.9 it is clear that the $A_1^{(2)}$ and the E bands will display the highest intensities on the IR spectrum. The $A_1^{(2)}$ band is often observed as a "shoulder" on the spectrum, at the higher frequency side of the E band when the unique ligand is a good π-acceptor ligand (carbene) and on the lower frequency side when the unique ligand is a poor π-acceptor ligand (amine).

The IR spectra for complexes **1** and **2** were recorded in hexane; the A_1^1, A_1^2, B_1 and E bands can easily be identified as observed in Figure 2.10. The pattern and intensities of bands are characteristic for a M(CO)$_5$ fragment of an octahedral complex.

The wavenumbers of the carbonyl bands for compounds **1** and **2** lie between 2128 and 1718 cm^{-1}, which indicates the presence of terminal carbonyl groups only.

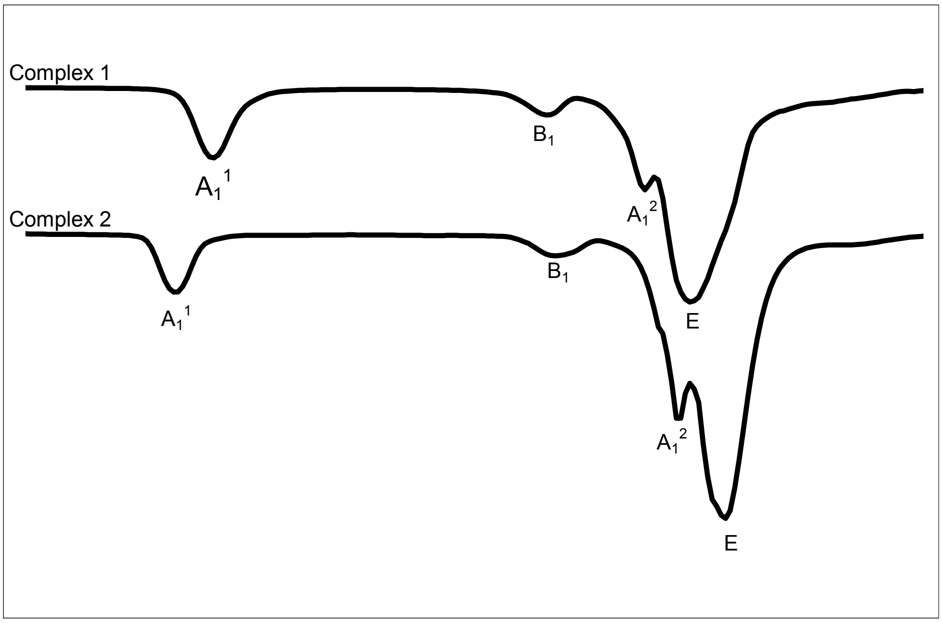

Figure 2.10 Stacked infrared spectrum of compounds **1** and **2** in the carbonyl region

Table 2.3 IR-data[a] in the carbonyl region of complex **1** and **2**

Complex	Carbonyl vibrating frequencies (ν_{CO}, cm^{-1})			
	$A_1^{(1)}$	B_1	$A_1^{(2)}$	E
1	2058m	1984w	1959s	1948vs
2	2067m	1981vw	1955s	1945vs

[a] Hexane as solvent

3.3 X-ray Crystallography

Final confirmation of the structures of **1** and **2** was obtained from single crystal X-ray diffraction studies. The complexes were crystallised from a layered 1:1 dichloromethane:hexane solution. This method gave dark red-brown crystals of good quality for both complexes. Figures 2.11 and 2.12 represent the ORTEP[17] + POV-Ray[18] plots of the geometry of **1** and **2**, which also indicate the atom numbering scheme that was used for the structural data. Compound **1** crystallized in the space group P 21/m with a = 9.2928(11), b = 7.6330(9), c = 12.4413(15) Å, Z = 2, compound **2** also crystallized in the space group P 21/m with a = 9.3964(6), b = 7.7430(5), c = 12.5316(7) Å and Z = 2. The most important bond lengths and angles are listed in Table 2.4, whilst the most important torsion angles are listed in Table 2.5. Other structural information is captured on the supplementary CD.

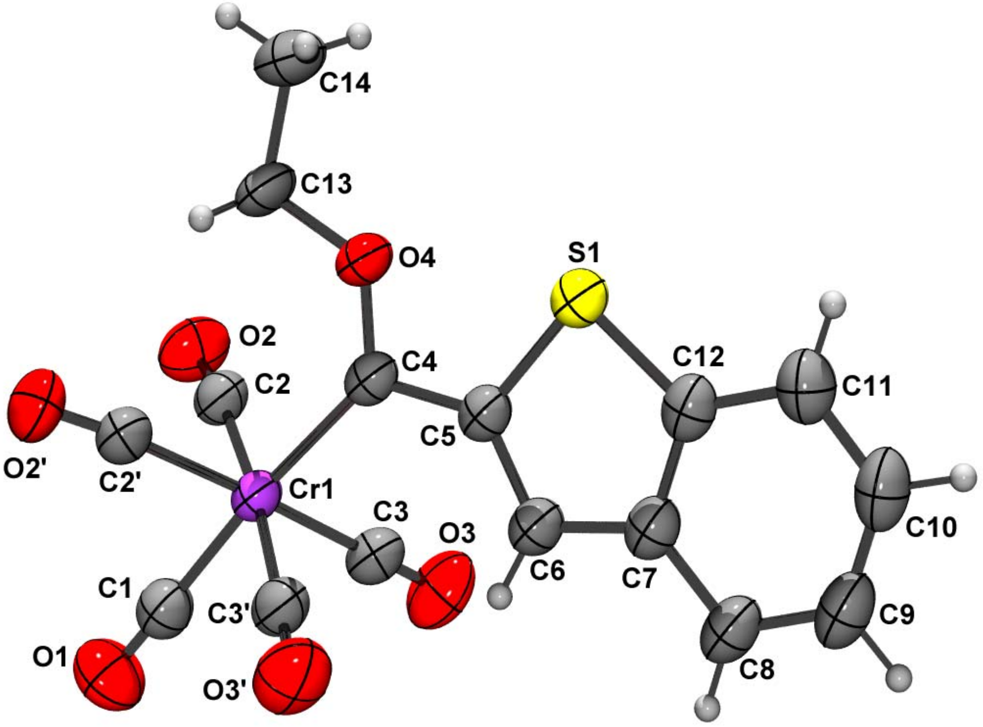

Figure 2.11 ORTEP + POV-Ray plot of the geometry of complex **1**

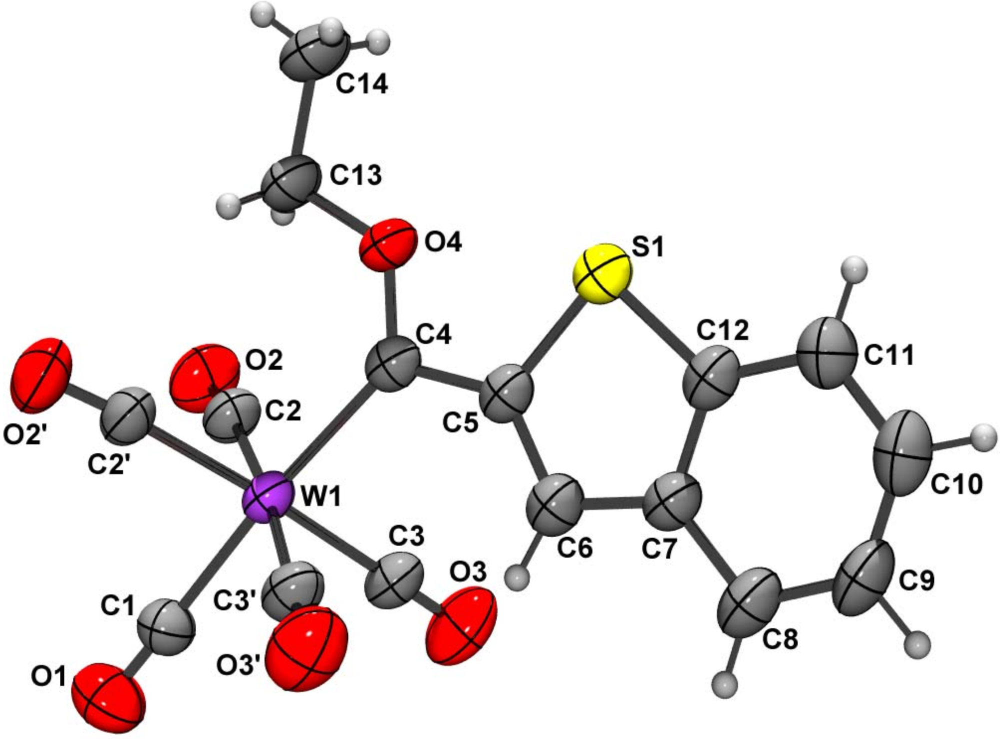

Figure 2.12 ORTEP + POV-Ray plot of the geometry of complex **2**

Table 2.4 Selected bond lengths and angles of **1** and **2**

Bond	Bond Lengths (Å)		Bond	Bond angles (°)	
	1 (M = Cr)	**2** (M = W)		**1** (M = Cr)	**2** (M = W)
M(1)-C(4)	2.067(3)	2.201(5)	C(1)-M(1)-C(4)	175.08(10)	175.01(19)
C(4)-O(4)	1.319(3)	1.315(6)	O(4)-C(4)-C(5)	105.2(2)	105.7(4)
C(4)-C(5)	1.462(3)	1.468(7)	O(4)-C(4)-M(1)	129.92(17)	130.1(4)
O(4)-C(13)	1.449(3)	1.448(6)	C(5)-C(4)-M(1)	124.89(17)	124.2(4)
M(1)-C(1)	1.875(3)	2.018(6)	C(4)-O(4)-C(13)	123.3(2)	122.3(4)
M(1)-C(2,2',3,3')[a]	1.9044(19)	2.036(4)	C(4)-C(5)-S(1)	119.52(18)	119.4(4)
C(5)-C(6)	1.368(3)	1.356(7)			
C(6)-C(7)	1.421(4)	1.426(7)			
C(7)-C(12)	1.399(4)	1.403(7)			
C(12)-S(1)	1.727(3)	1.733(5)			
C(5)-S(1)	1.758(3)	1.757(5)			

[a] mean value

Table 2.5 Selected torsion angles of **1** and **2**

Bond	Torsion angle (°)	
	1 (M = Cr)	**2** (M = W)
C(2)-M(1)-C(4)-O(4)	44.17(6)	43.97(11)
M(1)-C(4)-O(4)-C(13)	0.0	0.0
O(4)-C(4)-C(5)-S(1)	0.0	0.0
M(1)-C(4)-C(5)-S(1)	180.0	180.0

Structural information shows that complexes **1** and **2**, in the solid state, have nearly octahedral geometries of ligands surrounding the metals. A mirror plane, with the carbene ligand in the plane, bisects two sets of carbonyls in the equatorial plane. This can be seen by looking at torsion angles C(2)-M(1)-C(4)-O(4) (**1** = 44.17(6), **2** = 43.97(11)) and C(2)-M(1)-C(4)-C(5) (**1** = -135.83(6), **2** = -136.03(11)). In both complexes two of the equatorial carbonyls bend away from the carbene carbon towards the trans carbonyl as seen by looking at angles C(2)-M(1)-C(4) (**1** = 96.37(7), **2** = 96.52(15)) and two bend towards the carbene ligand as seen by angles for C(3)-M(1)-C(4) (**1** = 87.98(7), **2** = 88.06(15)).

For complexes **1** and **2** the sulphur atom of the thiophene ring is on the same side as the oxygen atom of the etoxy substituent, indicating restricted rotation around the C4-C5 bond or a preferred packing order in the solid state. This may be as a result of the stabilization of the metal acylate by a five membered ring containing the lithium ion in close contact to the hetero atoms as seen in Figure 2.13.

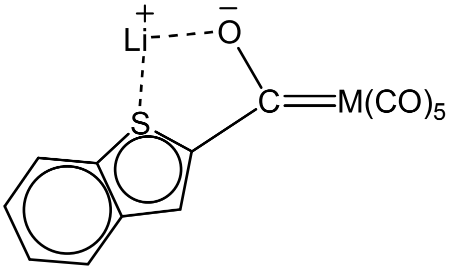

Figure 2.13 Proposed stabilization of the metal acylate

M═C(carbene) distances for alkoxy carbene complexes with two alkyl or aryl substituents are between 2.00 and 2.13 Å for [Cr(CO)$_5$(carbene)] and 2.15 and 2.25 Å for [W(CO)$_5$ carbene].[19] Distances for **1** and **2** fall within these ranges and are comparable with a distance of 2.053(1) Å for [Cr(CO)$_5${C(OEt)}Me] and 2.221(8) Å for [W(CO)$_5${C(OEt)thienothiophene}].[20] The Cr-C(carbene) distance of 2.067(3) Å for **1** is significantly shorter than a C*sp*^{2}-Cr single bond distance of 2.21(2) Å showing metal to carbene carbon back-bonding.[21]

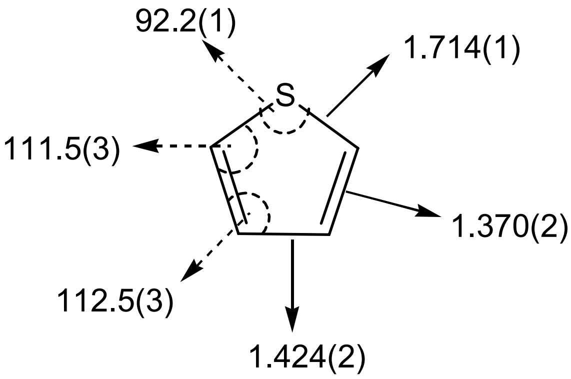

Figure 2.14 Bond lengths (Å) and bond angles (°) of free thiophene[22]

When comparing the bond lengths for the carbene substituents of **1** and **2**, the following conclusions can be made:

(i) The C(4)-O(4) distances are around 1.317(4) Å for **1** and **2**, which is significantly shorter than a Csp^2-O single bond distance of 1.336 Å, typical for organic esters.

(ii) The C(carbene)-C(thienyl) bond (Cr : 1.462 Å) is slightly shorter than a distance of 1.48 Å accepted for a Csp^2-Csp^2 single bond. The distances in the thiophene rings of **1** and **2** are very similar to those in a free thiophene ring and represent a similar degree of delocalization in **1** and **2**.

(iii) Significant, however is the much shorter C-S distances (1.714(1) Å) in free thiophene compared to the corresponding distances of BT in **1** and **2**.

In summary, delocalization of electron density in the thiophene ring remains more or less the same for the carbon atoms, but is disrupted to the sulphur and spills over to the carbene carbon.

4. References

1. E.O.Fischer, A.Maasböl, *Angew. Chem.* **1964,** *76* 645.

2. R.Aumann, E.O.Fischer, *Chem. Ber.* **1968,** *101* 954.

3. T.M.Krygowski, M.K.Crañski, Z.Czarnocki, G.Häfelinger, A.R.Katritzky, *Tetrahedron* **2000,** *56* 1783.

4. P.Geneste, A.Guicla, D.Levaché, *Bull. Chem. Soc. Fr.* **1983,** *5-6* 136.

5. J.A.Connor, E.M.Jones, E.W.Randall, E.Rosenberg, *J. Chem. Soc., Dalton Trans.* **1972,** 2419.

6. O.S.Mills, A.D Redhouse, *J. Chem. Soc. A* **1968,** *3* 642.

7. E.O.Fischer, E.Moser, *J. Organomet. Chem.* **1968,** *15* 157.

8. J.A.Connor, E.M.Jones, *J. Chem. Soc. A* **1971,** 1974.

9. Y.M.Terblans, H.M.Roos, S.Lotz, *J. Organomet. Chem.* **1998,** *566* 133.

10. E.O.Fischer, W.Held, F.R.Kreissl, A.Frank, G.Huttner, *Chem. Ber.* **1977,** *110* 656.

11. K.D.Bartle, R.S.Matthews, D.W.Jones, *Tetrahedron* **1971,** *27* 5177.

12. P.D.Clark, D.F.Ewing, R.M.Scrowston, *Org. Magn. Reson.* **1976,** *8* 252.

13. R.Meyer, S.Brink, E.J.van Rensburg, G.K Jooné, H.Görls, S.Lotz, *J. Organomet. Chem.* **2005,** *690* 117.

14. F.H.Köhler, H.J.Kalder, E.O.Fischer, *J. Organomet. Chem.* **1975,** *85* C19.

15. C.Elsenbroich, A.Salzer, *Organometallics: A Concise Introduction*, VCH Verlagsgesellschaft, Weinheim, Germany **1992,** p. 227.

16. L.M.Haines, M.H.B.Stiddard, *Adv. Inorg. Chem. Radiochem.* **1969,** *12* 53.

17. L.J.Farrugia, *J. Appl. Crystallogr.* **1997,** *30* 565.

18. The POV-Ray Team, POV-Ray 2004 . URL: http://www.povray.org/download/.

19. K.H.Dötz, H.Fischer, P.Hofmann, F.R.Kreissl, U.Schubert, K.Weiss, *Transition metal carbene complexes*, (VCH Verlag Chemie) Weinheim **1983**.

20. M.Landman, Synthesis of metal complexes with thiophene ligands, PhD thesis, University of Pretoria **2000**, p86.

21. J.A.Connor, O.S.Mills, *J. Chem. Soc.A* **1969,** 334.

22. J.Chen, L.M.Daniels, R.J.Angelici, *Polyhedron* **1990,** *9* 849.

3

Bimetallic Titanoxycarbene Complexes

1. Introduction

The metallation of a transition metal acylate with a second transition metal complex containing an activated halide or even a cationic metal complex with a vacant coordination site, has been documented.[1-4] Beck and co-workers[5] showed that it was possible to synthesize heteronuclear bimetallic monocarbene complexes by reacting [Re(CO)$_5$FBF$_3$] and NEt$_4$[Cr(CO)$_5${C(O)R}]. More generally exploited is the use of titanocene dichloride as metallation reagent with chromium pentacarbonyl acylates as carbene complex precursors (Figure 3.1).

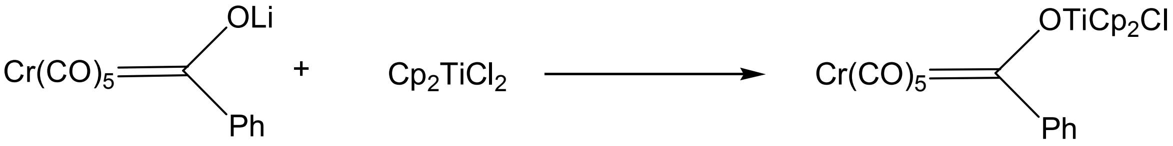

Figure 3.1 Reaction yielding a dimetallic titanoxy carbene complex

Interest in organotitanium(IV) compounds developed after the discovery that certain organotitanium(IV) compounds show higher carbanion selectivity than organolithium compounds. Classical organic C-C bond formation reactions e.g. Grignard-type or Wittig olefination reactions are very useful reactions but have certain limitations. These reagents are basic and extremely reactive, affording wide application but low chemoselectivity and limiting the number of additional functional groups that can be used. It was discovered that titanation of carbanions using TiCl$_2$X$_3$ leads to species with reduced basicity and reactivity.[6] In reactions with organic compounds such as aldehydes, ketones and alkyl halides, the stereoselectivity, regioselectivity as well as chemoselectivity are increased. Stereochemical predictions can therefore be made in many C-C bond-forming reactions, because the ligand X can be varied to control the electronic and steric nature of the reagents.

The arrival of Ziegler-Natta catalysts and the relevance of these compounds in organic syntheses, gave impetus to research in the field of organotitanium compounds. These heterogeneous catalysts are formed by mixing triethylaluminium and titanium tetrachloride and are used in the polymerization of ethylene, propylene and other α-olefins.[7,8]
The syntheses of various monomeric alkyl-titanium compounds was spurred on by the Ziegler-Natta polymerization process, one of them include $TiCH_3Cl_3$.[9]

A large number of η^5-cyclopentadienyltitanium compounds have been prepared, containing either one or two Cp ligands.[10] These Cp-groups are said to have a "stabilizing" effect on titanium-alkyl bonds due to their strong electron donating effect. This stabilizing effect can be very useful in adjusting carbanion-reactivity and selectivity . It was found that, when replacing a chlorine in compounds of the type $TiRCl_3$ by Cp-groups, the reactivity was reduced considerably.

The geometry of the titanocene dichloride complex is a distorted tetrahedron, with the two cyclopentadienyl rings tilted toward each other to form an open sandwich configuration and in complexes where titanocene dichloride (or probably other metallocenes of this type) is added, the halide moieties can easily be substituted for other groups such as alkyl or aryl groups (Figure 3.2). Also, when used with metal acylates by displacing one of the chloro ligands from titanocene dichloride the remaining chloro ligand becomes activated and can lead to the formation of two chromium carbene acylates being bridged by a titanocene fragment (Figure 3.2).[11]

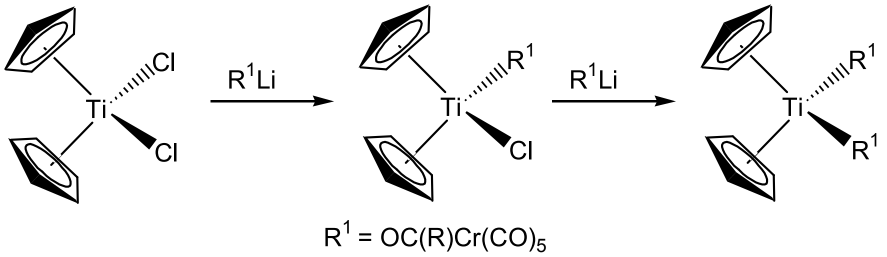

Figure 3.2 Substitution of a chlorine moiety in $TiCp_2Cl_2$

In this study, only titanocene dichloride was used for metallation and the products displayed two metal fragments, titanium(IV) and chromium(0) or tungsten(0). In order not to complicate matters and to control electronic and steric factors, the third substituent was again benzo[*b*]thiophene.

In the following compounds (**3** and **4**) two metal fragments are present, titanium(IV) (d^0), an early transition metal which can be classified as electron-deficient, as well as chromium(0) (d^6) or tungsten(0) (d^6), which are middle transition metals.

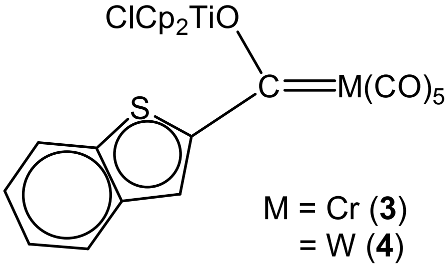

M = Cr (**3**)
= W (**4**)

Figure 3.3 Bimetallic titanoxycarbene complexes synthesized in this chapter

By replacing an ethyl group with a titanocene group the oxygen of the carbene carbon should be affected electronically as well as sterically. The titanium(IV) centre is hard and will bind strongly to the hard oxygen atom.

2. Synthesis

Lithiation of the benzo[*b*]thiophene was achieved by the use of the strong base, n-butyllithium. The addition of the transition metal compounds $M(CO)_6$, with M = Cr or W afforded the metal acylates after which metallation with one equivalent titanocene dichloride took place. Metallation with titanocene dichloride is easily achieved due to the lability of a chloro ligand to afford the titanoxycarbene complexes **3** and **4** (Scheme3.1).

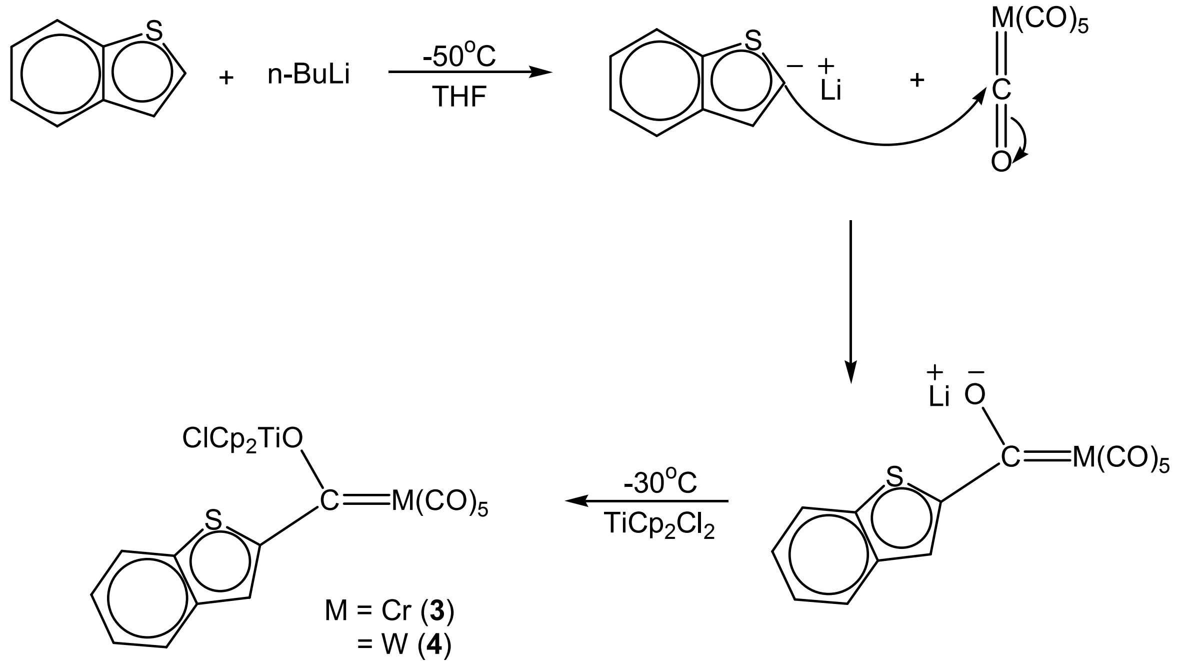

Scheme 3.1

The formation of the desired products, **3** (red-pink) and **4** (dark red), occurred with high yields and the complexes were purified and isolated using column chromatography with silica gel as stationary phase.

3. Spectroscopic characterization

3.1 NMR Spectroscopy

^{1}H NMR spectra were recorded in $CDCl_3$ and C_6D_6. ^{13}C NMR spectra were only recorded in $CDCl_3$ due to poor solubility in C_6D_6. The same system of numbering of the carbon atoms and protons of benzo[b]thiophene used in Chapter 2 was applied to **3** and **4**.

^{1}H NMR Spectroscopy

The ^{1}H NMR data of the starting compound, benzo[*b*]thiophene, is summarized in chapter 2, while the ^{1}H NMR data of complexes **3** and **4** are reported in Table 3.1.

Table 3.1 ^1H NMR data of complexes **3** and **4**

Assignment	Complexes					
	Chemical shifts (δ, ppm) and coupling constants (J, Hz)					
	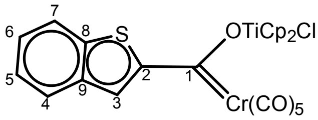 **3**			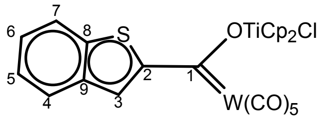 **4**		
Proton	δ	$^3J_{H\text{-}H}$	$^4J_{H\text{-}H}$	δ	$^3J_{H\text{-}H}$	$^4J_{H\text{-}H}$
H3[a]	8.43 (s)	-	-	8.35 (s)	-	-
H4	7.87 (dd)	8.1	-	7.85 (dd)	8.1	1.8
H5	7.50 (m)	8.1	1.2	7.52 (m)	8.1	-
H6	7.45 (m)	7.1	-	7.44 (m)	7.9	1.8
H7	8.04 (d)	7.1	1.2	8.03 (d)	7.9	-
Cp	6.55 (s)	-	-	6.55 (s)	-	-
H3[b]	8.64 (s)	-	-	8.56 (s)	-	-
H4	7.51	-	-	7.48 (d)	8.3	-
H5	7.09 (m)	-	-	7.00 (m)	8.3	-
H6	7.02 (m)	8.9	-	7.10 (m)	7.8	-
H7	7.53 (d)	8.9	-	7.52 (d)	7.8	-
Cp	5.88 (s)	-	-	5.87	-	-

[a] spectrum was recorded in $CDCl_3$

[b] spectrum was recorded in C_6D_6

When comparing chemical shift values of **3** and **4** with those of **1** and **2** in Chapter 2, a downfield shift (Δδ>0.1) can be recognised for the H3 protons. This can be ascribed to the

Ti-fragment that replaced the Et-fragment in the previous examples. The downfield signals of H3 indicate that the thiophene substituent in both **3** and **4** donates more electron density to the electron deficient carbene carbon (C1) in comparison with **1** and **2**. A possible reason for this is the competition between the electro positive Ti-fragment and the electron deficient carbene carbon atom to obtain electron density from the oxygen atom. Electron density shared between oxygen and C1 is polarized towards the oxygen. The ethyl groups on the other hand have an σ-inductive effect that increases the electron density of the oxygen assisting lone pair interaction of the oxygen with the carbene carbon atom.

When comparing all the other protons in the same manner, that is H4 - H7, a clear downfield shift for all the protons in benzothiophene can be recognised. This then indicates an electron withdrawing effect of the carbene carbon that influences the thiophene ring as well as the benzene ring (Figure 3.3). Thus, having a net electron withdrawing effect from the whole aromatic substituent (BT).

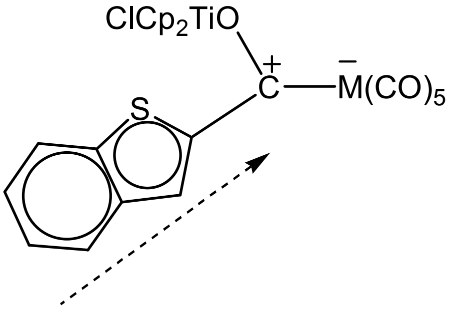

Figure 3.3 Net electron donation from benzo[*b*]thiophene

Free $TiCp_2Cl_2$ has a chemical shift of 6.57 ppm for the protons of the Cp-rings while the Cp's in **3** and **4**, resonate at 5.88 and 5.87 ppm. Once again a clear downfield shift is caused by the electron donation of the Cp rings to the electron deficient titanium supporting a resonance structure with a positive charge on the titanium ($TiCp_2Cl^+$).

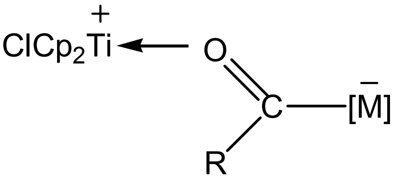

Figure 3.4 Electropositive character of Titanium[3]

^{13}C NMR spectroscopy

The ^{13}C NMR data of complexes **3** and **4** are reported in Table 3.2. The ^{13}C NMR data for complex **4** proved to be not as good as those of complex **3**, it was not possible to detect the signals for the carbene carbon (C1), that of C8 or C9, neither did the spectra indicate a resonance for the trans carbonyl of compound **4**.

Table 3.2 ^{13}C NMR data[a] of complexes **3** and **4**

Assignment	Complexes Chemical shifts (δ, ppm)	
	3	**4**
C1	324.5	-
C2	140.8	141.1
C3	139.5	139.4
C4	122.9	123.1
C5	128.4	128.4
C6	125.4	125.5
C7	126.9	127.1
C8, C9	138.1	-
Cp's	118.7	118.7
CO	217.9 (cis) 224.9 (trans)	199.0 (cis)

[a] spectrum was recorded in $CDCl_3$

When looking at the ^{13}C NMR spectra of compound **3**, it is possible to distinguish between the individual carbons of the arene region, those are the carbons of the benzene ring and the thiophene ring individually (Figure 3.4) as well as those from the cyclopentadienyl ligands. The Cp-rings rotate freely in solution as is evident of single resonances for the protons as well as the carbons in the NMR spectra.

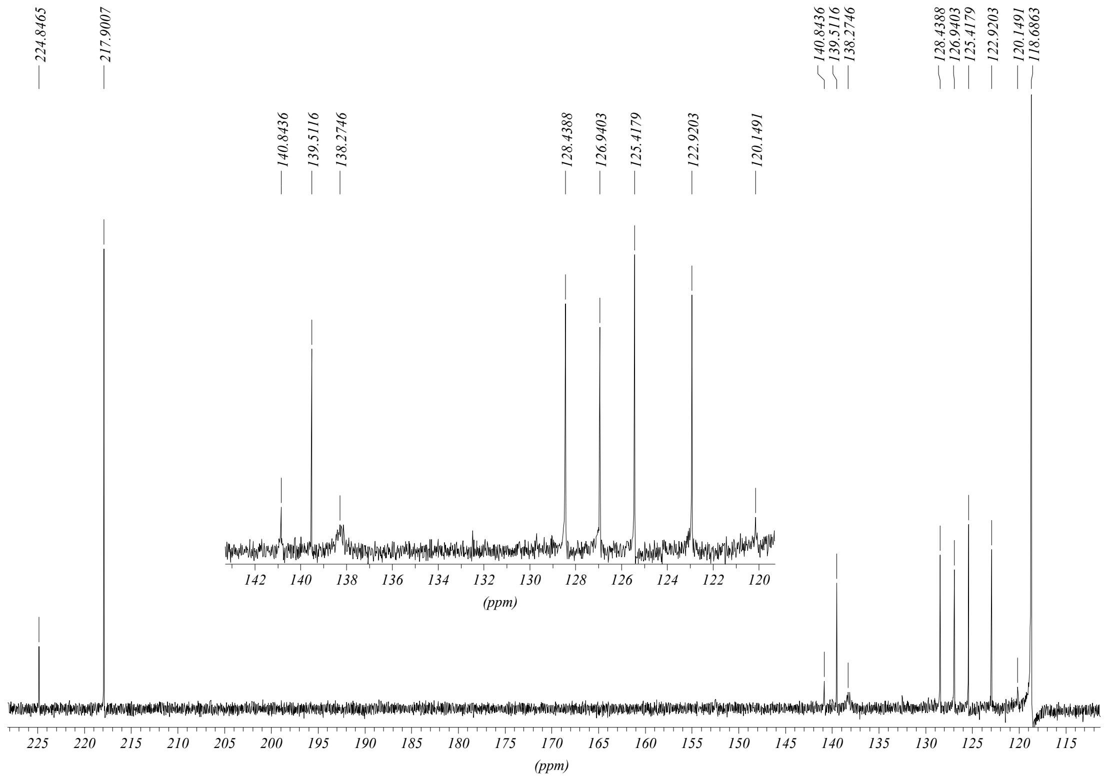

Figure 3.4 ^{13}C NMR spectrum of complex **3** in $CDCl_3$ showing the arene region

3.2 Infrared Spectroscopy

The data of the infrared spectra of compounds **3** and **4** are summarized in Table 3.3, the spectra of the compounds were recorded in hexane and dichloromethane, in order to see the difference of the vibrational spectra in the different solvents, complex **4** was used as example in Figure 3.4 to illustrate this.

The typical pattern for a $M(CO)_5$ (C_{4v}, square pyramidal geometry) is seen in the spectra recorded in dichloromethane in the CO region, but not in a non-polar hexane solution. Hexane is more inert towards the vibrational modes of the compounds and displays a greater resolution power in the spectra. In hexane the degeneracy associated with the E-band is lifted leading to the splitting of the E-band into two separate bands indicated as X and Y (Figure 3.5) of different vibrational frequencies. One of them will be of E-symmetry, while the other band can be either of general A or B symmetry.[12] This seems to indicate a deviation from C_{4v} symmetry and a distortion of the equatorial plane of carbonyl ligands. Also significant is the relatively large difference between the wavenumbers of A_1^2

and the two bands of the E band. These observations are ascribed to a significant distortion of the equatorial plane by the bulky carbene ligand in solution.

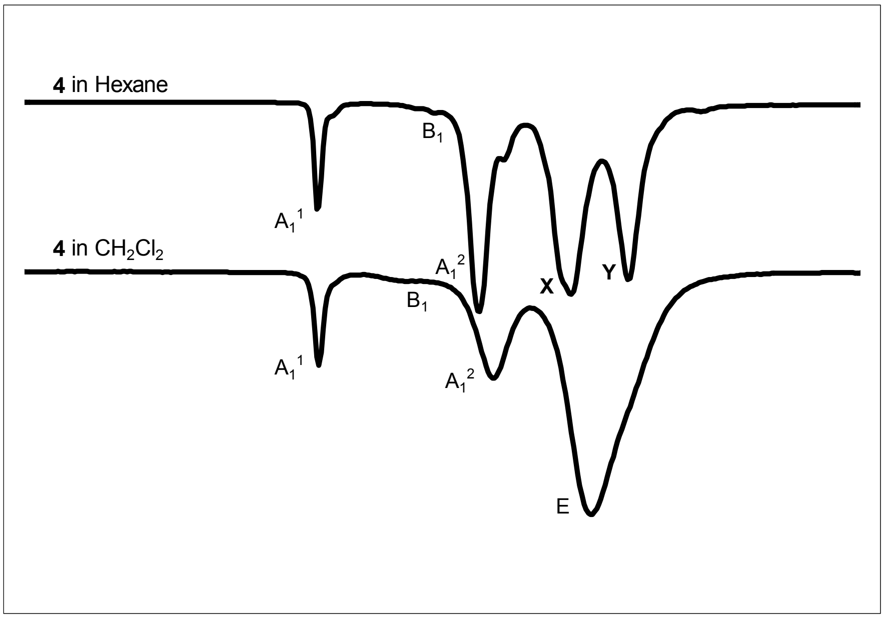

Figure 3.5 Stacked infrared spectrum of compound **4** in hexane and dichloromethane

Table 3.3 IR-data in the carbonyl region of complex **3** and **4**

Complex	Carbonyl vibrating frequencies (ν_{CO}, cm^{-1})			
	$A_1^{(1)}$	B_1	$A_1^{(2)}$	E
3[a]	2050m	1987w	1948s	1936vs, 1915s
3[b]	2050m	-	-	1931vs
4[a]	2050m	2000vw	1982vs	1938vs, 1911s
4[b]	2059m	2018vw	1975s	1929vs

[a] Hexane as solvent

[b] Dichloromethane as solvent

3.3 X-ray Crystallography

Final confirmation of the structure of **4** was obtained from a single crystal X-ray diffraction study. The complex were crystallised from a layered 1:1 dichloromethane:hexane solution. This method gave dark red-brown crystals of good quality for both complexes. Figure 3.6 represents the ORTEP[13] + POV-Ray[14] plot of the geometry of **4**, which also indicates the atom numbering scheme that was used for the structural data. Compound **4** crystallized in the space group P⏋ with a = 11.3533(6), b = 11.6696(6), c = 12.3627(7) Å, Z = 2. The most important bond lengths and angles are listed in Table 3.4 while the most important torsion angles are listed in Table 3.5. Other structural information is captured on the supplementary CD.

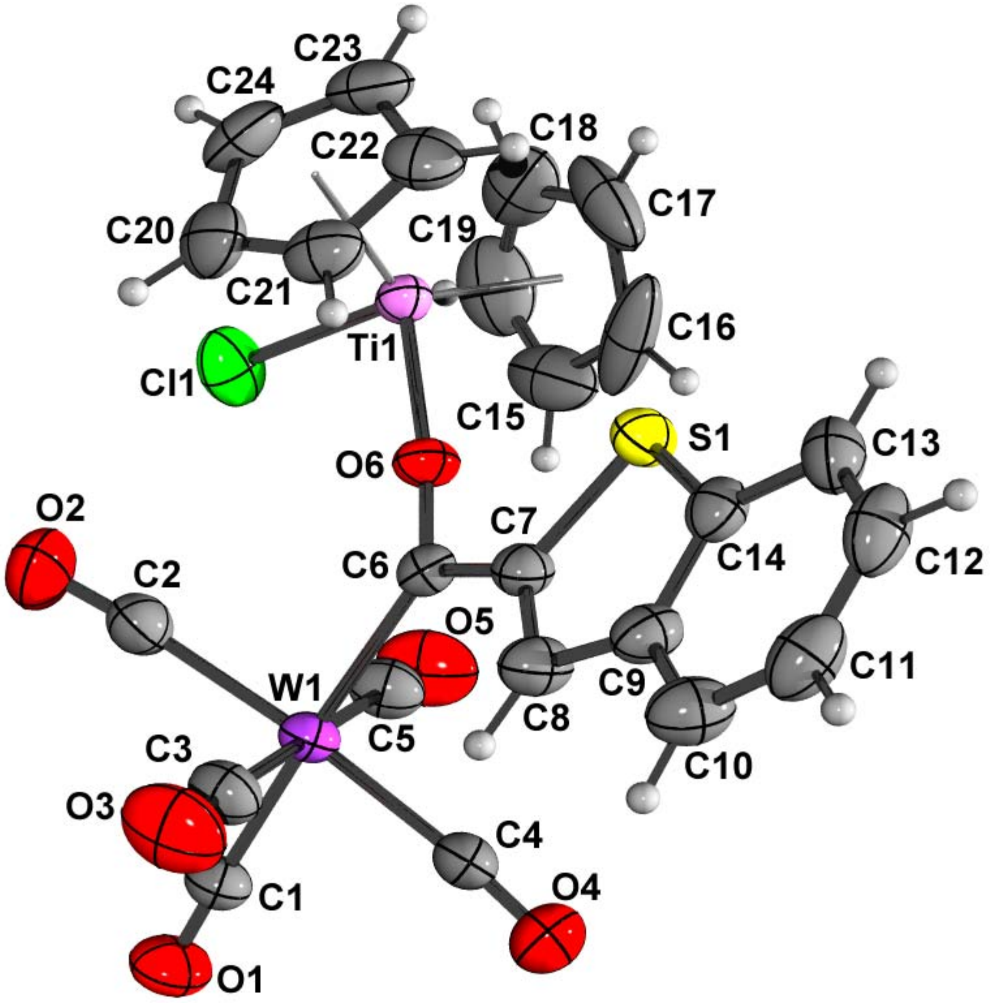

Figure 3.6 ORTEP + POV-Ray plot of the geometry of complex **4**

Table 3.4 Selected bond lengths and angles of **4**

Bond	Bond Lengths (Å)	Bond	Bond angles (º)
W(1)-C(6)	2.211(4)	C(1)-W(1)-C(6)	174.00(13)
C(6)-O(6)	1.279(4)	O(6)-C(6)-C(7)	112.7(3)
C(6)-C(7)	1.474(5)	O(6)-C(6)-W(1)	121.2(3)
O(6)-Ti(1)	1.931(2)	C(7)-C(6)-W(1)	125.9(2)
W(1)-C(1)	2.007(4)	C(6)-O(6)-Ti(1)	171.7(3)
W(1)-C(2,3,4,5)[a]	2.033(4)	C(6)-C(7)-S(1)	120.9(3)
C(7)-C(8)	1.368(5)		
C(8)-C(9)	1.436(5)		
C(9)-C(14)	1.394(6)		
C(14)-S(1)	1.730(4)		
C(7)-S(1)	1.755(4)		

[a] mean value

Table 2.5 Selected torsion angles of **4**

Bond	Torsion angle (°)
	1
C(2)-W(1)-C(6)-O(6)	-49.2(3)
O(6)-C(6)-C(7)-C(8)	169.7(4)
O(6)-C(6)-C(7)-S(1)	-9.8(4)
W(1)-C(6)-C(7)-S(1)	165.53(18)

Structural information shows that the carbene ligand in complex **4**, in the solid state, does not lie in a plane. This is seen by looking at the torsion angle O(6)-C(6)-C(7)-S(1) of 169.7(4)°. The BT substituent is planar with a torsion angle of only 0.8(5)° for S(1)-C(14)-C(9)-C(10). In this complex two of the carbonyl ligands bend away from the carbene carbon towards the trans carbonyl as seen by looking at C(3)-W(1)-C(6) (94.68(15)°) and C(4)-W(1)-C(6) (92.12(14)°).

The Ti(1)-O(6) bond in **4** is much longer than those of typical terminal titanium(IV) alkoxides (1.855 Å in $TiCp_2(OC_2H_5)Cl$)[15] and is in the same range as the bridging Ti-O-*i*-Pr interactions (1.918(2) Å in $\{(CO)_5CrC[OTi(O\text{-}i\text{-}Pr)_3][n\text{-}Bu]\}_2$.[3] This supports the notion that O(6)→C(6) π donation occurs at the expense of O(6)→Ti(1) π donation. It was suggested that π delocalization in the M-C-O-Ti unit is increased for titanoxycarbene complexes by virtue of the π acidity of the d^0 metal center, illustrated by the resonance structures in Figure 3.7.

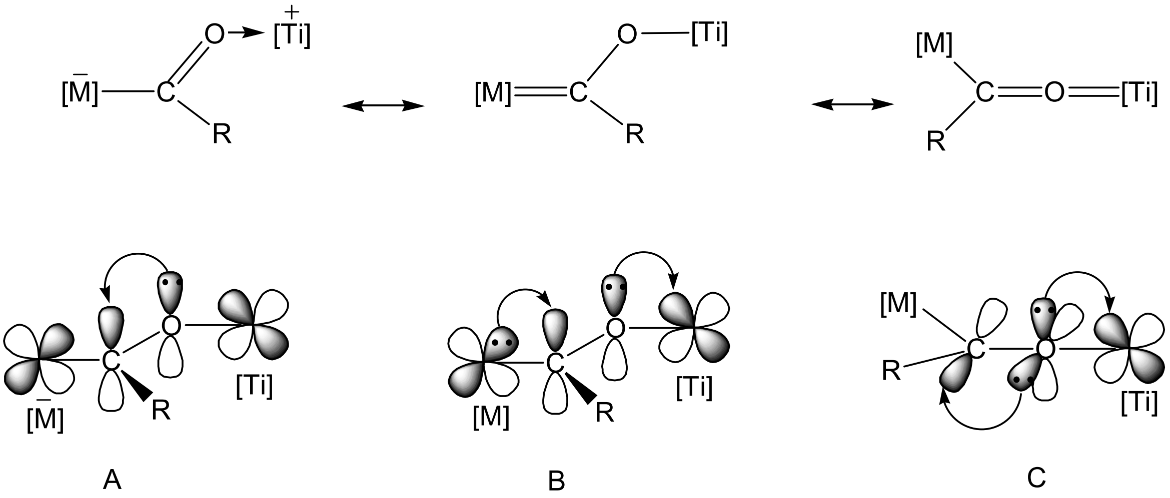

Figure 3.7 Orbital interactions in acyl (A) and carbene (B) resonance forms of titanoxycarbene complexes,[3] and the proposed interaction causing the near linear angles of titanoxycarbene complexes (C).

The combination of A and B suggests that π-electron density may be delocalized over the titanoxycarbene moiety to a greater extent than in alkoxycarbene systems. When looking at the near linear bond angle C(6)-O(6)-Ti(1) of 171.7(3)°, it is possible that electronic factors may play a role as also observed in previous work.[3] This angle suggests almost sp hybridization at O(6), allowing O(6)-Ti and O(6)-C(6) π overlap to occur using both p orbitals of O(6). This seems unlikely because of the long Ti-O bond distance. Steric considerations may well hold the key to the long Ti-O distance as the O(6)-C(6)-C(7) angle (112.7(3)°) is large compared to the corresponding angle in **2** (105.7(4)°).

When comparing bond C(6)-O(6) (1.279(4)) with that of an average alkoxycarbene system, being ±1.35 Å (1.315(6) Å for **2**), a stronger bond is identified for **4**, this stronger C-O interaction suggests that the "acyl" resonance structure A (Figure 3.7) is an important contributor to the bonding in these species, as has been noted by Erker for a series of zirconoxycarbene complexes.[16] The bond distances in the thiophene ring and the W-C(carbene) distance correspond well with those of **2** and the free thiophene molecule.

4. References

1. E.O.Fischer, S. Fontana, *J. Organomet. Chem.* **1972,** *40* 159.
2. H.G.Raubenheimer, E.O.Fischer, *J. Organomet. Chem.* **1975,** *91* C23.
3. M.Sabat, M.F.Gross, M.G.Finn, *Organometallics* **1992,** *11* 745.
4. M.Sabat, M.F.Gross, M.G.Finn, *Organometallics* **1994,** *13* 2084.
5. P.M.Fritz, M.Steimann, W.Beck, *Chem. Ber.* **1987,** *120* 253.
6. M.T.Reetz, *Organotitanium Reagents in Organic Synthesis*, Springer Verlag, Berlin **1986** .
7. H.Sinn, W.Kaminsky, *Adv. Organomet. Chem.* **1980,** *18* 99.
8. P.Pino, R.Mülhaupt, *Angew. Chem., Int. Ed. Engl.* **1980,** *19* 857.
9. C.Beerman, H.Bestian, *Angew. Chem.* **1959,** *71* 618.
10. Gmelin Handbuch, "*Titan-Organische Verbindungen*". Part 1 (**1977**), Part 2 (**1980**), Part 3 (**1984**), Part 4 (**1984**), Springer Verlag, Berlin
11. E.V.Anslyn, B.D.Santarsiero, R.H.Grubbs, *Organometallics* **1988,** *7* 2137.
12. K.Nakamoto, *Infrared and Raman Spectra of Inorganic and Coordination Compounds Part A*, 5th edition, John Wiley & Sons, New York **1997**.
13. L.J.Farrugia, *J. Appl. Crystallogr.* **1997,** *30* 565.
14. The POV-Ray Team, POV-Ray 2004 . URL: http://www.povray.org/download/.
15. J.C.Huffman, K.G.Moloy, J.A.Marsella, K.G.Caulton, *J. Am. Chem. Soc.* **1980,** *102* 3009.
16. G.Erker, *Angew. Chem., Int. Ed. Engl.* **1989,** *28* 397.

4

Bimetallic π-bonded Benzo[*b*]thienylcarbene Complexes

1. Introduction

Coordination through the π-cloud of aromatic molecules causes a localization of the double bonds leading to an electron deficiency of the rings of arene-transition metal complexes that was already recognised in the 1950s.[1] This property aids in the addition of nucleophiles to the arene ligand and deprotonation of acidic arene protons. Several reasons exist for the interest in investigating arene complexes of transition elements. The arene ligand is uncharged and because it can donate an even number of electrons will thus not affect the charge of the complex. The creation of vacant coordination positions can be achieved more easily than in the case of negatively charged ligands e.g. cyclopentadienyl. The hapticity of the arene ligand can be varied e.g. $\eta^6 \rightarrow \eta^4 \rightarrow \eta^2$, by changing or adding additional ligands, this property empowers these complexes to vacate coordination sites and to act as precursors for catalysts in e.g. hydrogenation or polymerization processes.[2-5]

An important feature of heteroarene metal complexes is the competition between heteroatom-metal σ bonds and arene-metal π bonds. A possible explanation for σ-bond formation in pyrroles and pyridines is attributed to the lower ionization energies of unbonded electron pairs of the heteroatom compared to the π-electrons of the arene ring. Thus, the unbonded electron pairs are more accessible for bonding than the electrons in the π-system. Another trait of π-heteroarene complexes is their stability relative to their carbocyclic analogues. In general, the more electronegative atoms such as N and S form π-heteroarene complexes that tend to be more air sensitive.[6,7] Modification of the chemical and physical properties of the metal centre upon coordination to the heteroarene ligand can occur.

The first example[8] of the synthesis of heterodimetallic carbene complexes following the route depicted in Scheme 4.1 (vide infra) was the addition of ferrocenyl lithium (FcLi) to $[M(CO)_6]$ (M = Cr, W) to yield the ate complexes that were alkylated with $[Me_3O]BF_4$ or $[Et_3O]BF_4$ to yield complexes $[(CO)_5M{=}C(OR)Fc]$ (R = Me or Et). Other examples of bimetallic complexes of the type $[(CO)_5M{=}C(OEt)C_6H_5Cr(CO)_3]$ (M = Cr,W) were synthesized by Fischer in 1980.[9] More related to the work of this study is (η^6-benzo[*b*]thiopene)-tricarbonylchromium(0) complexes, of which complex **5** was already synthesised in our laboratories during preliminary investigations.[10]

The η^5-heterocyclic metal carbonyl complexes e.g. with η^5-thiophene[11] and η^5-pyrrole[12] rings have been studied thoroughly. More recently the interest shifted to the benzannulated derivatives of these five membered monoheterocycles, e.g. benzo[*b*]thiophene (BT) and indole,[12] which were π-coordinated to transition metals. In these cases coordination of the benzene ring takes preference to coordination of the heteroarene ring (Figure 4.1). $Li[Cr(\eta^5\text{-thienyl})(CO)_3]$ reacts with $[M(CO)_6]$ (M = Cr, W) and $[Re(CO)_5Br]$ to yield after subsequent alkylation with $[Et_3O]BF_4$, the carbene complexes $[M(CO)_5\{C(OEt)\eta^5\text{-thienylCr(CO)}_3\}]$[13] and $[Re(CO)_4(Br)\{C(OEt)\eta^5\text{-thienylCr(CO)}_3\}]$,[14] respectively. The synthesis of these tricarbonylchromium compounds are known and these complexes were fully characterized by Fischer *et al.*[15]. In addition BT is known to coordinate through the sulphur atom, as seen for $Cp(CO)_2Re(BT)$,[16] or through the 2,3-double bond, e.g. (η^2-2,3-BT)$ReCp(CO)_2$.[17]

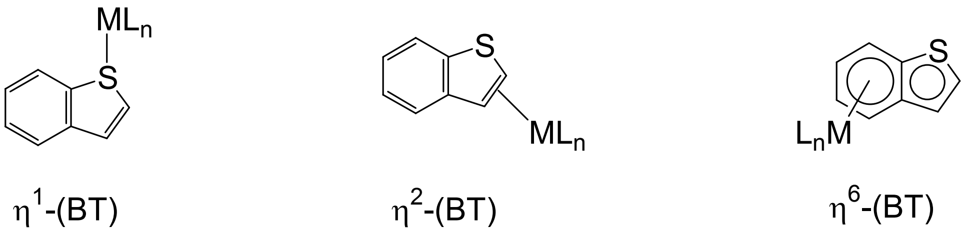

η^1-(BT) η^2-(BT) η^6-(BT)

Figure 4.1 Bonding modes of benzo[*b*]thiophene

In this study the synthesis of new bimetallic carbene complexes were investigated by making use of π-coordinated tricarbonylchromium complexes of BT. Bimetallic carbene complexes **5** and **6** were synthesized to study the effect of π-bonded benzo[*b*]thiophene as a carbene substituent.

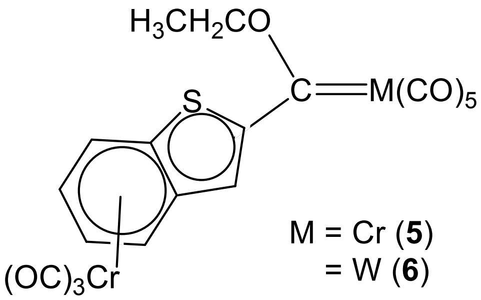

Figure 4.2 Bimetallic π-bonded BT carbene complexes synthesized in this chapter

To focus on the electronic and steric properties of this substituent, alkylation was achieved by using $[Et_3O]BF_4$. Comparison with **1** and **2** in Chapter 2 will reveal the effect of π-coordination of BT by $Cr(CO)_3$ on the carbene carbon atom. It is anticipated that the $Cr(CO)_3$ unit will remove electron density from the BT ring, disrupt the conjugation of double bonds in BT and decrease the amount of electron density available to stabilize the carbene carbon atom.

2. Synthesis

The (η^6-benzo[*b*]thiopene)tricarbonylchromium(0) precursor was prepared according to known literature methods.[18] The preparation involved the displacement of the amine-ligands in the complex $[Cr(NH_3)_3(CO)_3]$ by the heteroarene in the presence of boron trifluoride diethyl etherate in boiling dibutyl ether. The harder ammonia base will preferentially coordinate to the harder Lewis acid BF_3, thereby facilitating its substitution and the coordination of the heteroarene.

$$[Cr(NH_3)_3(CO)_3] + BT \rightarrow [Cr(\pi\text{-}BT)(CO)_3] \quad (BT = \text{benzo}[b]\text{thiophene})$$

The coordination of a transition metal to an arene ligand in a π-complex modifies the reactivity of the arene ligand. A definite result is the acidification of the ring protons, which allows direct proton abstraction from the ring. The first observation of metallation of arene ligands was reported in 1968[19] and the first examples with chromiumtricarbonyl activation followed soon afterwards.[20] An important property of (π-arene)tricarbonylchromium complexes is the displacement of the arene hydrogens under mild conditions. Despite the fact that the tricarbonylchromium moiety is coordinated to the benzene ring in the π-complex of BT, the α-proton on the thiophene ring remains the most acidic.[21]

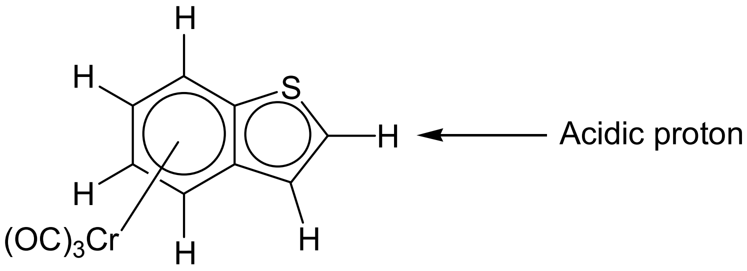

Deprotonation of the (π-benzo[*b*]thiophene)tricarbonylchromium(0) complex is accomplished by the use of a strong base (pK_a>20) e.g. n-butyllithium and hydrogen-metal exchange occurs under conditions where the uncoordinated substrate is still not reactive.

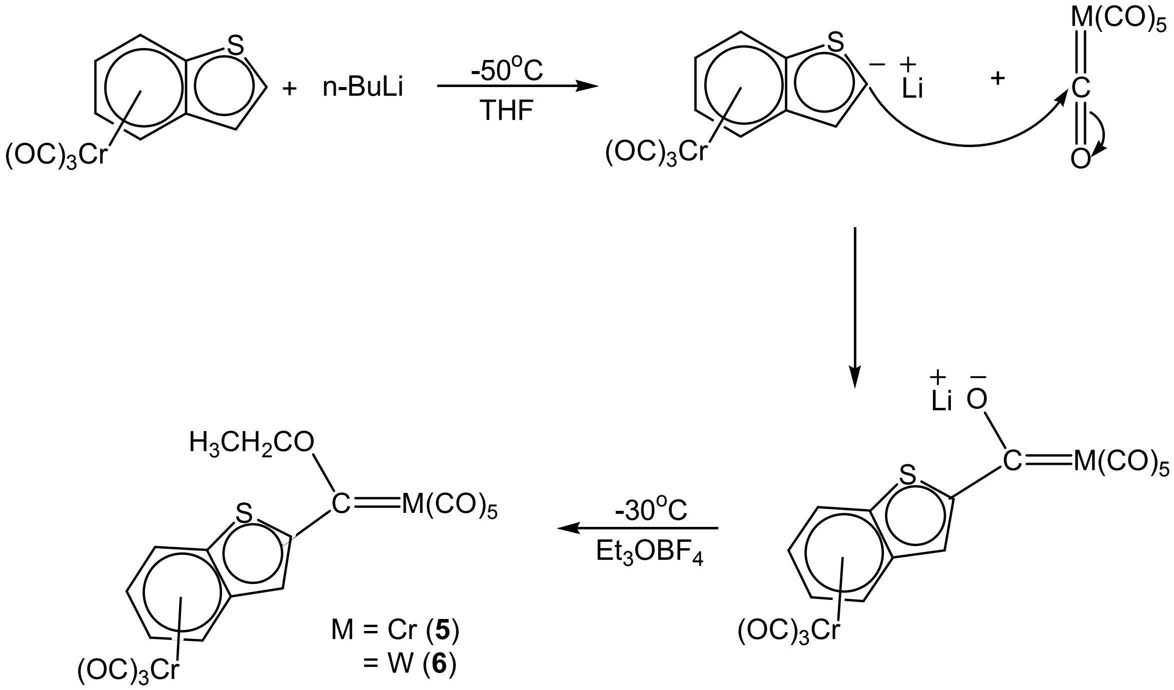

Scheme 4.1

The desired products **5** (red-pink) and **6** (red-orange) were obtained in high yields after purification using column chromatography with silica gel as stationary phase. The $Cr(CO)_3$ and $Cr(CO)_5$ metal fragments can communicate electronically *via* a connecting conjugated π-system in the bridging BT-carbene ligand. It is possible from spectroscopic measurements to look at the role of each substituent to stabilize the carbene carbon atom in the complex. Also, the introduction of a π-bonded $Cr(CO)_3$ fragment on the BT substituent will introduce additional steric strain to the bimetallic carbene complex compared to the complexes **1** and **2** in Chapter 2.

3. Spectroscopic characterization

3.1 NMR Spectroscopy

π-Coordination of an arene ring to a $Cr(CO)_3$ fragment leads to the localization of the double bonds and the disruption of the aromaticity of the ring. The ring current, the induced magnetic lines of force that result from the flow of charge, is destroyed and the result is a significant upfield change in chemical shift. The reactivity and aromaticity of heteroaromatic compounds can be studied by nuclear resonance spectroscopy by measuring the chemical shifts and coupling constants of the arene protons and carbons.

All ^1H NMR spectra were recorded in $CDCl_3$ and in C_6D_6. ^{13}C NMR spectra were only recorded in $CDCl_3$ due to their poor solubility in C_6D_6 and the only useful ^{13}C NMR spectrum was obtained for **5**.

^{1}H NMR Spectroscopy

The signals of the protons of (η^6-benzo[*b*]thiophene)tricarbonylchromium(0) in deuterated chloroform are given in Figure 4.3. The same system of numbering of the protons and carbon atoms was used as before. The ^1H NMR data of complexes **5** and **6** are summarized in Table 4.1. Figure 4.4 represents the ^1H NMR spectrum of **5**.

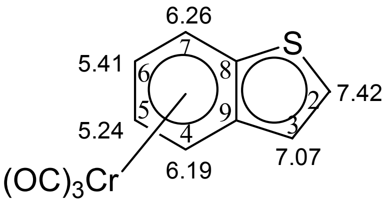

Figure 4.3 Chemical shifts of the protons of (η^6-benzo[*b*]thiophene)tricarbonyl-chromium(0).[22]

Two important observations of the chemical shifts in the ^1H NMR spectra of **5** and **6** are seen when compared to the corresponding complexes **3** and **4** in Chapter 3. The spectra display an upfield shift of almost 2.0 ppm for the benzene protons because of the π-coordination to the $Cr(CO)_3$-fragment and also an upfield shift for H3 of around 0.3 ppm in C_6D_6 and 0.6 ppm in $CDCl_3$. The latter is still 1.0 ppm downfield from the same resonance in uncoordinated BT emphasizing deshielding at C3 caused by the electron-withdrawing effect of the carbene carbon atom. This effect, however, is less important in these compounds. The same observations were recognised when comparing **5** and **6** with **1** and **2** in chapter 2. An overall upfield shift is observed, for the benzene protons once again a shift of about 2.0 ppm can be seen and the upfield shift for H3 is around 0.5 ppm.

For complex **5** in C_6D_6, the coupling constant of the CH_2 group could not be resolved from the CH_2 signal, due to the overlap of signals with the H6 resonances. Coupling constants was obtained from the H4 and H7 resonances.

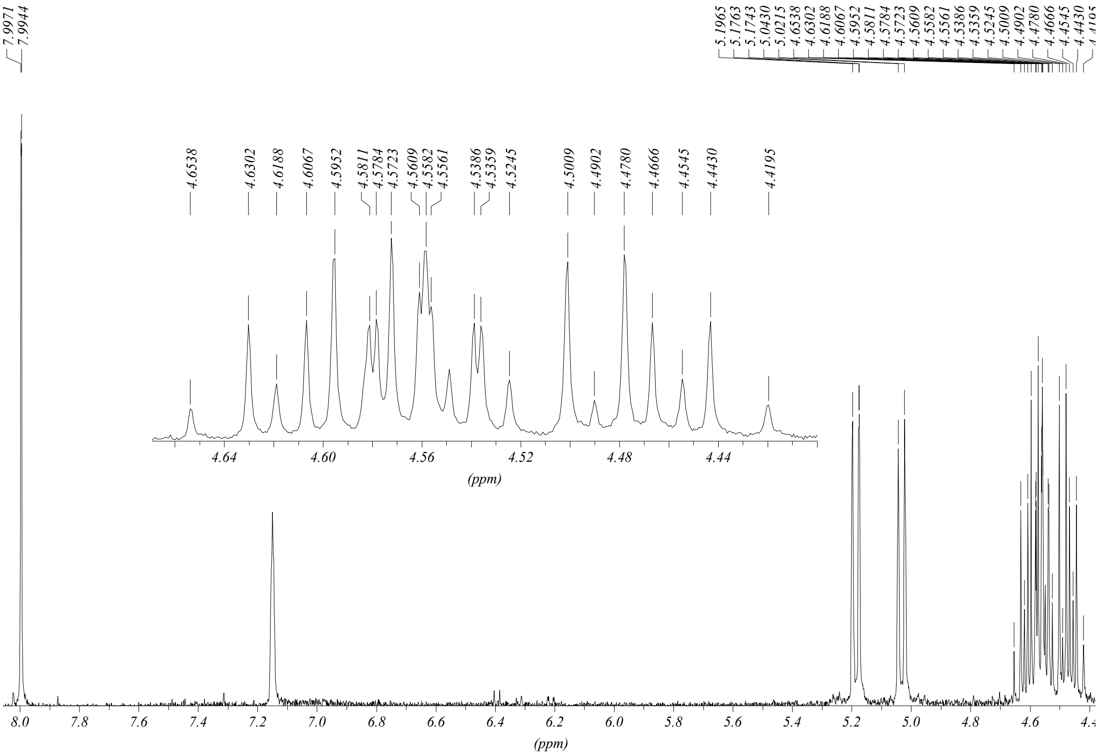

Figure 4.4 ^{1}H NMR spectrum of complex **5** in C_6D_6, in the region for the ring protons

Table 4.1 ^{1}H NMR data of complexes **5** and **6**

Assignment	Complexes				
	Chemical shifts (δ, ppm) and coupling constants (J, Hz)				
	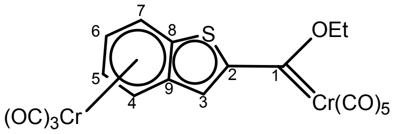 **5**			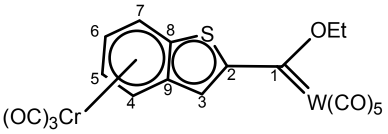 **6**	
Proton		$^3J_{H-H}$	$^4J_{H-H}$		$^3J_{H-H}$
H3[a]	8.13 (s)	-	-	8.05 (d)	-
H4	6.07 (d)	6.8	-	6.07 (d)	6.7
H5	5.61 (m)	6.8	0.9	5.64 (m)	6.7
H6	5.26 (m)	6.6	-	5.25 (m)	6.5
H7	6.29 (d)	6.6	0.9	6.29 (dd)	6.5
$-CH_2$	5.19 (q)	7.0	-	4.98 (q)	7.1
$-CH_3$	1.69 (t)	7.0	-	1.67 (t)	7.1
H3[b]	8.00 (d)	-	0.8	7.91 (s)	-
H4	5.03 (d)	6.5	0.8	5.00 (d)	7.0
H5	4.56 (m)	6.5	0.6	4.56 (m)	7.0
H6	4.19 (m)	6.7	-	4.17 (m)	6.5
H7	5.19 (dd)	6.7	0.6	5.14 (d)	6.5
$-CH_2-$	4.54 (q)	-	-	4.34 (q)	-
$-CH_3$	0.97 (t)	7.0	7.0	0.94 (t)	7.0

[a] recorded in $CDCl_3$, [b] spectrum was recorded in C_6D_6,

^{13}C NMR spectroscopy

^{13}C NMR chemical shift values for (η^6-benzo[*b*]thiophene)tricarbonylchromium(0) are captured in Figure 4.5 and the ^{13}C NMR spectrum for **5** was measured in deuterated chloroform (Figure 4.6). It was not possible to obtain a useful spectrum for **6** due to poor solubility and decomposition of the compound during measurements.

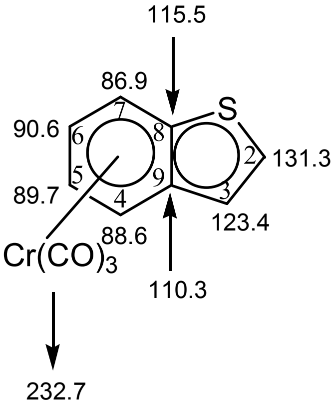

Figure 4.5 Chemical shifts of the carbons of (η^6-benzo[*b*]thiophene)tricarbonyl-chromium

Chemical shifts (δ, ppm, $CDCl_3$) of **5**: 318.2 (C1), 231.4 ($Cr(CO)_3$), 223.4 (trans) and 216.5 (cis) ($Cr(CO)_5$),155.6 (C2), 138.2 (C3), 88.9(C4), 89.8 (C5), 92.2 (C6), 84.3 (C7), 118.1 and 126.6 (C8, C9), 76.8 (CH_2), 15.0 (CH_3).

The signals in the ^{13}C NMR spectrum of **5** follow the same pattern as the signals of the ^{1}H NMR and display upfield changes in chemical shift of approximately 30 ppm for the benzene protons because of π-coordination to the $Cr(CO)_3$-fragment. The shifts of the thienyl carbons are downfield from those observed in [Cr(η^6-BT)$(CO)_3$] due to attachment to the carbene carbon atom. When comparing C2 of **1** and **3** with C2 of **5**, a large downfield shift is observed in **5** in comparison with **1** Δδ = 16.4 ppm and **3** Δδ = 35.4 ppm, at the same time an upfield shift is observed when comparing chemical shifts of C3, in comparison with **1** Δδ = 0.5 ppm and **3** Δδ = 1.3 ppm. The carbonyl resonances of $Cr(CO)_3$ are the same as in [Cr(η^6-BT)$(CO)_3$] and those of $Cr(CO)_5$ the same as in **3**.

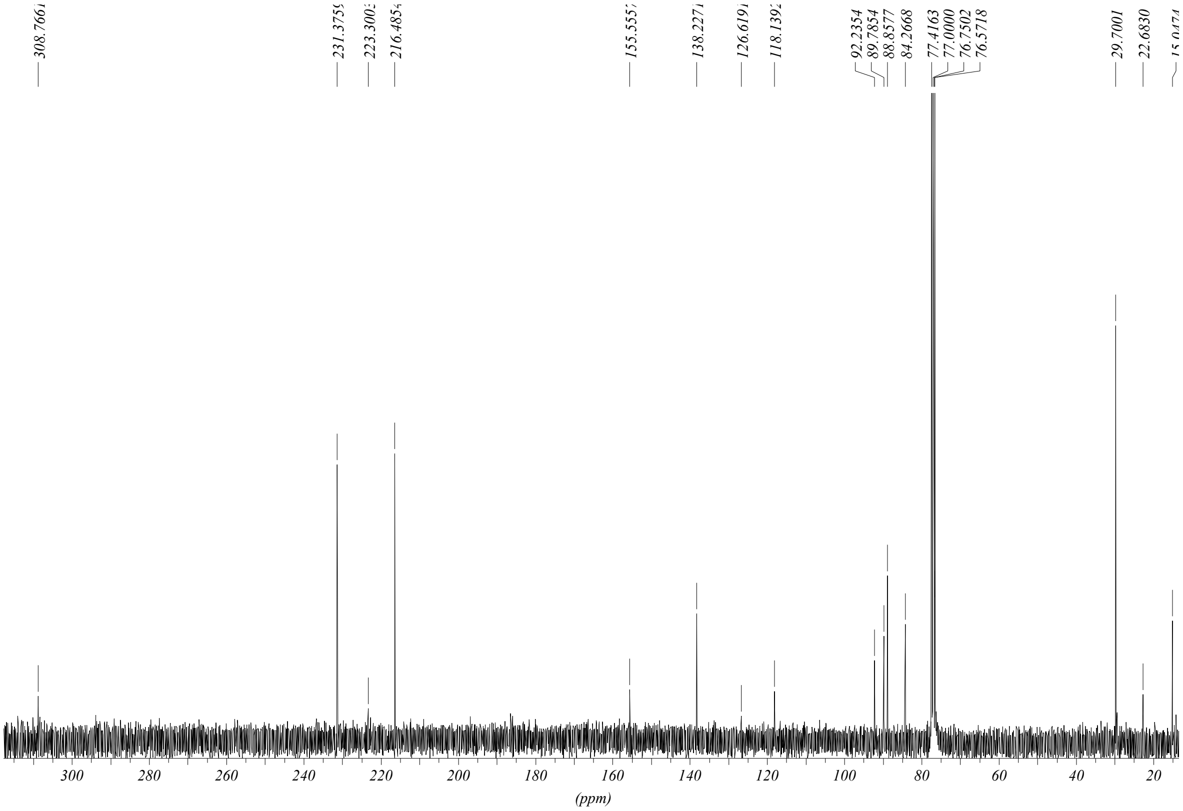

Figure 4.6 ^{13}C NMR spectrum of complex **5** in $CDCl_3$

3.2 Infrared Spectroscopy

Distinct patterns are observed for the bands of the different metal carbonyl fragments. The number, intensities and region of the bands in the spectrum is a valuable aid for the characterization of the products. The individual vibrational modes are assigned to specific bands by taking a local symmetry of the carbonyls into consideration. Since complexes of the general composition $ML_3(CO)_3$ belong to the symmetry group C_{3v}, two IR-active bands are observed in the spectrum, they correspond to the A_1 and the E vibrational modes. The first sharp A_1 band is observed at higher wavenumbers than the stronger E band and is associated with the symmetrical stretching vibrations while the E band, at lower wavenumbers, is associated with the unsymmetrical stretching vibrations in the molecule. Aspects related to the vibrational modes of a metalpentacarbonyl fragment were discussed in Chapter 2.

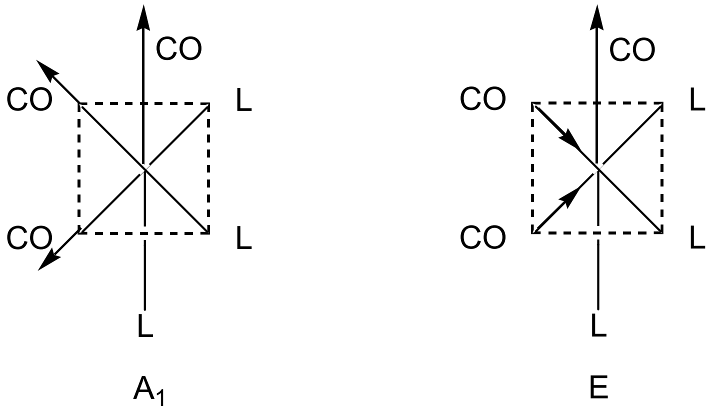

Figure 4.7 Stretching vibrational modes of $M(CO)_3L_3$

All IR spectra were recorded in hexane and dichloromethane.

The wavenumbers of the carbonyl bands for compounds **5** and **6** lie between 1900 and 2070 cm^{-1}, which indicate the presence of terminal carbonyl groups only. Because of the overlap of the pentacarbonyl and the tricarbonyl moieties in these compounds, it was almost impossible to unambiguously allocate a specific wavenumber to the A_1 band of the $Cr(CO)_3$-fragment in compound **6**.

Table 4.3 IR-data in the carbonyl region of complex **5** and **6**

Complex	Carbonyl vibrating frequencies (ν_{CO}, cm^{-1})					
	$Cr(CO)_3$		$Cr(CO)_5$			
	A_1	E	$A_1^{(1)}$	B_1	$A_1^{(2)}$	E
5[a]	1928m	1905s 1914s	2059m	1989vw	1950*vs	1950vs
5[b]	1947s	1901m	2060m-s	-	1969vs	1947s
6[a]	1945vs	-	2067w	1980vw	1954m[c]	1945vs
6[b]	1942vs	1903w	2068m-s	-	1969s	1942vs

[a] Hexane as solvent, [b] Dichloromethane as solvent, [c] observed as a shoulder,

*$A_1^{(2)}$ and E overlap

3.3 X-ray Crystallography

Final confirmation of the structures of **5** and **6** was obtained from single crystal X-ray diffraction studies. The complexes were crystallised from a layered 1:1 dichloromethane:hexane solution. This method gave dark purple crystals of good quality for both complexes. Figures 4.8 and 4.9 represent the ORTEP[23] + POV-Ray[24] plots of the geometry of **5** and **6**, which also indicate the atom numbering scheme that was used for the structural data. Compound **5** crystallized in the space group Pī with a = 8.3523(11), b = 10.7547(15), c = 13.0118(17) Å, Z = 2, compound **6** crystallized in the space group P⏋ with a = 8.4597(6), b = 10.8010(8), c = 13.1159(10) Å, Z = 2. The most important bond lengths and angles are listed in Table 4.4. Other structural information is captured on the supplementary CD.

An important feature of the structures of **5** and **6** that differentiate them from the structures in the previous chapters are the two possible positions of the sulphur atom in the thienyl ring with respect to the ethoxy substituent and the C9-C10 bond. The major isomer (Cr 88.0 %, W 84.4 %) is the one with the sulphur on the same side as the ethoxy substituent, similar to the structures of **1** and **2** and the same arguments used in Chapter 2 may be valid. The question to answer is why does a second, minor isomer (Cr 12 %, W 15.6 %) exist with the sulphur on the opposite side of the ethoxy substituent. The existence of the second isomer can be explained by placing the $Cr(CO)_3$ fragment on one of two different sides of the flat benzene ring when the ring is attached to a substituent in the 2-position. Rotation round this C2-substituent bond to get the $Cr(CO)_3$ fragment on the same side for both isomers, will mean that the sulphur will have to move to the other side of the molecule (Figure 4.8).[25]

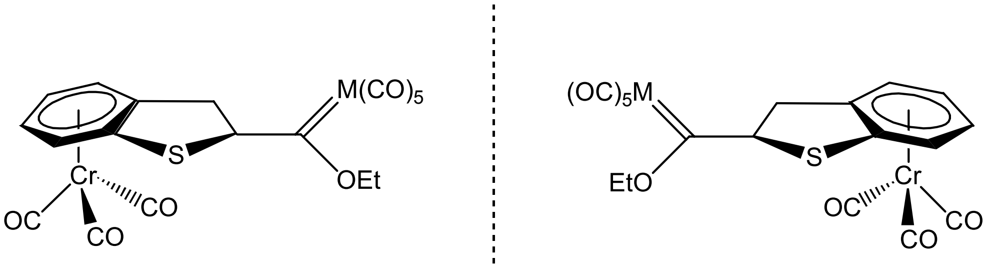

Figure 4.7 Planar chirality in π-BT carbene complexes

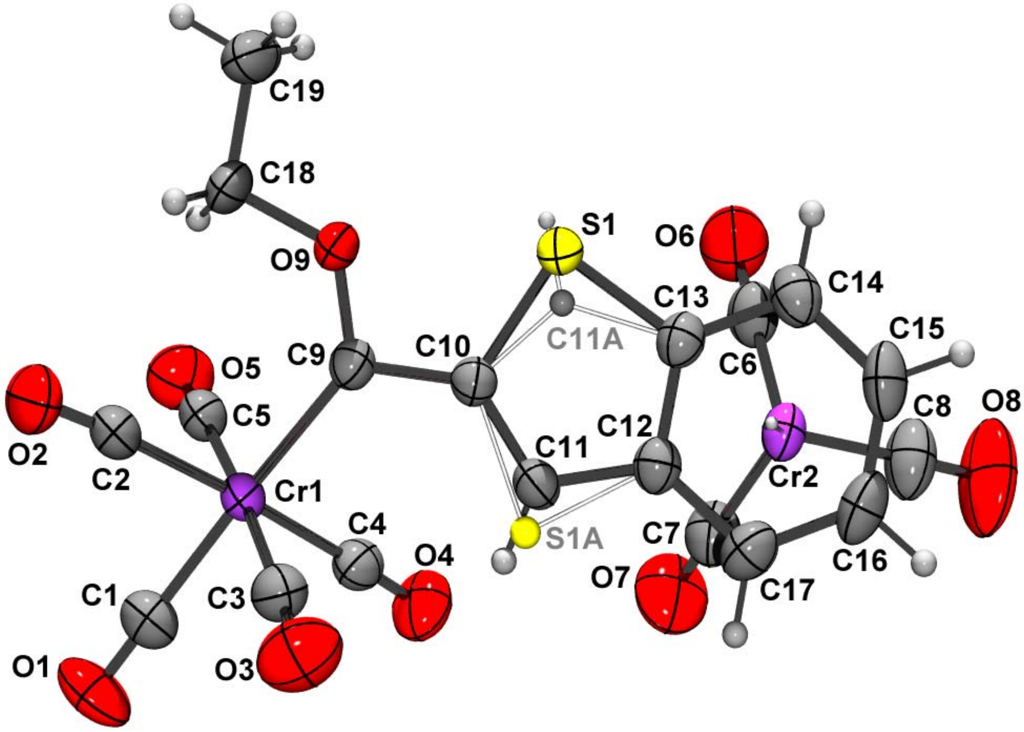

Figure 4.8 ORTEP + POV-Ray plot of the geometry of complex **5**

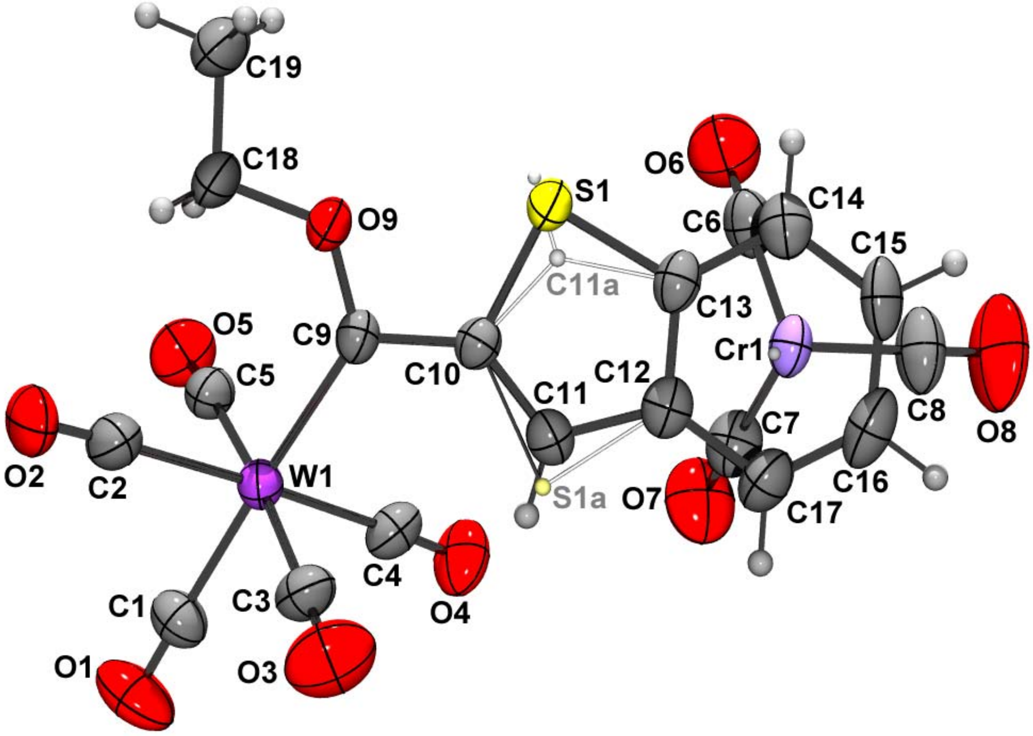

Figure 4.9 ORTEP + POV-Ray plot of the geometry of complex **6**

This phenomenon, described as planar chirality,[25] has been described before in literature and is relevant for asymmetrically substituted π–arene complexes. Assuming that the attack on the carbonyl is such that both isomers will form it is not clear on steric grounds why the sulphur is not in the normal position and the $Cr(CO)_3$ fragment on both sides of the benzene ring. This again raises the question whether free rotation exists around the C9-C10 bond in solution, and not in the solid state.

Table 4.4 Selected bond lengths and angles of **5** and **6**

Bond	Bond Lengths (Å)		Bond	Bond angles (°)	
	5 (M = Cr)	**6** (M = W)		**5** (M = Cr)	**6** (M = W)
M(1)-C(9)	2.050(2)	2.179(7)	C(1)-M(1)-C(9)	177.75(10)	177.4(2)
C(9)-O(9)	1.324(3)	1.318(8)	O(9)-C(9)-C(10)	104.52(18)	105.5(5)
C(9)-C(10)	1.472(3)	1.471(8)	O(9)-C(9)-M(1)	130.04(15)	130.0(4)
O(9)-C(18)	1.453(3)	1.458(7)	C(10)-C(9)-M(1)	125.36(15)	124.4(4)
M(1)-C(1)	1.884(3)	2.011(7)	C(9)-O(9)-C(18)	124.28(18)	123.3(5)
M(1)-C(2,3,4,5)[a]	1.905(3)	2.058(8)	C(9)-C(10)-S(1)	117.69(15)	117.0(4)
C(10)-C(11)	1.354(4)	1.353(9)	C(9)-C(10)-S(1A)	118.4(2)	118.8(5)
C(11)-C(12)	1.439(3)	1.441(9)			
C(12)-C(13)	1.408(3)	1.399(8)			
C(13)-S(1)	1.726(2)	1.735(6)			
C(10)-S(1)	1.763(2)	1.778(5)			
C(10)-C(11A)[m]	1.356(9)	1.355(9)			
C(11A)-C(13)[m]	1.455(9)	1.449(9)			
C(12)-S(1A)[m]	1.707(5)	1.725(6)			
C(10)-S(1A)[m]	1.782(4)	1.776(5)			

[a] mean value

[m] minor product

Table 4.5 Selected torsion angles of **5** and **6**

Bond	Torsion angle (°)	
	5 (M = W)	**6** (M = W)
C(2)-M(1)-C(9)-O(9)	-42.0(2)	-41.3(6)
M(1)-C(9)-O(4)-C(18)	3.5(4)	2.1(9)
O(9)-C(9)-C(10)-S(1)	-8.2(2)	-8.2(6)
O(9)-C(9)-C(10)-S(1A)^m	169.5(3)	169.5(5)
O(9)-C(9)-C(10)-C(11)	174.7(3)	175.3(6)
O(9)-C(9)-C(10)-C(11A)^m	-10.5(13)	-11(2)
M(1)-C(9)-C(10)-S(1)	168.59(11)	169.7(3)
M(1)-C(9)-C(10)-S(1A)^m	-13.7(3)	-12.7(7)
C(10)C(11)-C(12)-C(17)	-179.2(2)	-178.8(6)
C(10)-S(1A)-C(12)-C(17)^m	-177.4(2)	-176.9(5)

^{m} minor isomer

Structural information shows that the carbene ligand in the complexes **5** and **6** does not lie in a flat plane, one can see this by looking at the torsion angles O(9)-C(9)-C(10)-S(1) (**5** = -8.2(2) and **6** = -8.2(6)) for the major isomer and O(9)-C(9)-C(10)-S(1A) (**5** = 169.5(3) and **6** = 169.5(5)) for the minor isomer, in the solid state. The BT rings in both complexes, including the major and minor isomers, may be considered as flat, since the minimal distortion is present (all torsion angles are smaller than 2°). There is believed to be little steric hindrance in these complexes, since the etoxy group is a lot smaller than the titanoxy group in complex **4** and the O(9)-C(9)-C(10) angles are around 105° and similar to the corresponding angles in **1** and **2** in Chapter 2. In these complexes two of the four carbonyls bend away from the carbene carbon, towards the trans carbonyl as seen by looking at C(9)-M(1)-C(2) (**5** = 94.17(9)° and **6** = 94.7(3)°) and C(9)-M(1)-C(5) (**5** = 93.18(9)° and **6** = 93.6(3)°). Furthermore, it was observed that the major isomer has less distortion overall in comparison with the minor isomer.

The carbonyl conformations in (η^6-arene)Cr(CO)$_3$ complexes were studied and it was concluded that the conformation of the arene ligand is dependent is on the electronic characteristics of the arene ligand.[26,27] As shown in Figure 4.7, the ML$_3$ fragment of a condensed aromatic ligand can adopt one of three orientations within the *ortho* substitution. The three different orientations are known as the E orientation in which three ring carbon atoms and the three ligands, L, are eclipsed (a) and the S orientation in which the ring carbon atoms are staggered with respect to the ligands, L, and an M-L bond does not project onto the C-C bond containing S1 and S2 (b).

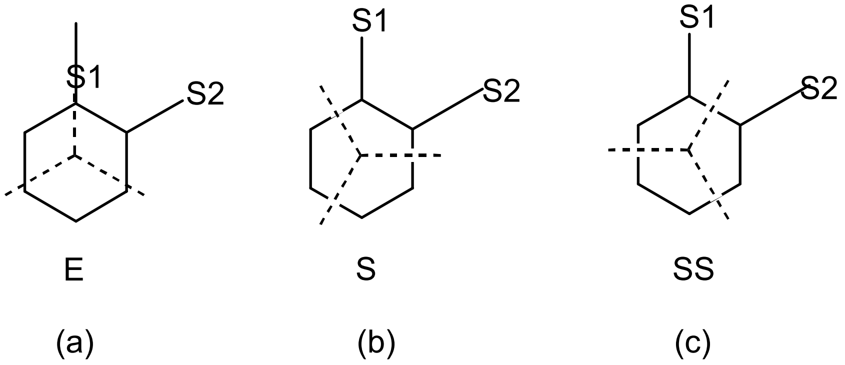

Figure 4.10 Conformational possiblities for disubstituted η^6-arene-ML_3 complexes[27]

Among the *ortho*-substituted-arene-ML_3 structures that exhibit the E orientation, the more electron-donating substituent is eclipsed while the more electron-withdrawing substituent is not eclipsed, as would be expected, based on electronic arguments found in literature.[27] When looking at the crystal structures of **5** and **6**, it is clear that the two complexes also took on the expected staggered (b) conformation since the carbene carbon *via* the condensed thiophene ring (S1, S2) is electron withdrawing.

When comparing the metal-carbene bond lengths obtained for complexes **5** and **6** with the distances in Chapter 2, the Cr-C(carbene) distances are the same but the W-C(carbene) is significantly shorter in **6**. For the thiophene ring the bond C(10)-C(11) for the major products as well as that of the minor products is shorter than that of free thiophene and the C(11)-C(12) bonds are longer than that of free thiophene. This indicates the disruption of the delocalization of electron density within the thiophene ring itself, π-coordination of benzene in BT eliminates one of the double bonds of thiophene and results in only one olefinic bond in thiophene and no conjugated π-system. Both the C-S bonds in **5** and **6** for the major and minor products are longer than that of free thiophene (except for the S(1A)-C(12) bond of complex **5**). This can be explained by looking at the localization of the benzene protons, since the $Cr(CO)_3$-fragment will cause this phenomenon. Thus, stabilization of the carbene carbon can only be supported by the thiophene ring (Figure 4.11), and no longer by the benzene ring as seen for complexes **1-4** (Figure 3.3).

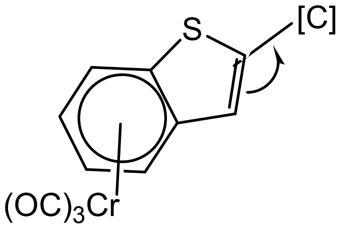

Figure 4.11 Stabilization of the carbene carbon by the thiophene ring

4. References

1. H.H.Zeiss, P.J.Wheatly, H.J.S.Winkler, *Benzenoid-Metal Complexes*, Ronald Press, New York **1966**.
2. M.Y.Darensbourg, El.Muetterties, *J. Am. Chem. Soc.* **1978,** *100* 7425.
3. T.W.Bell, M.Helliwell, M.G.Partridge, R.N.Perutz, *Organometallics* **1992,** *11* 1922.
4. A.M.Morken, D.P.Eyman, M.A.Wolff, S.J.Schauer, *Organometallics* **1993,** *12* 725.
5. C.Pellecchia, A.Grazzi, A.Immirizi, *J. Am. Chem. Soc.* **1993,** *115* 1160.
6. M.Novi, G.Giuseppe, C.Dell'Erba, *J. Heterocycl. Chem.* **1975,** *12* 1055.
7. G.E.Herberich, J.Hengesback, V.Kolle, W.Oschmann, *Angew. Chem., Int. Ed. Engl.* **1977,** *16* 42.
8. J.A.Connor, J.P.Lloyd, *J. Chem. Soc., Dalton Trans.* **1972,** 1470.
9. E.O.Fischer, F.J.Gammel, D.Neugenberger, *Chem. Ber.* **1980,** *113* 1010.
10. M.A.Sierra, *Chem. Rev.* **2000,** *100* 3591.
11. C.H.Langford, *Inorg. Chem.* **1965,** *4* 326.
12. K.K.Joshi, P.L.Pauson, *Proc. Chem. Soc.* **1962,** 326.
13. Y.M.Terblans, S.Lotz, *J. Chem. Soc., Dalton Trans.* **1997,** 2177.
14. T.A.Waldbach, R.van Eldik, P.H.van Rooyen, S.Lotz, *Organometallics* **1997,** *16* 4056.

15. E.O.Fischer, H.A.Goodwin, C.G.Kreiter, H.D.Simmons, K.Sonogashira, S.B.Wild, *J. Organomet. Chem.* **1968,** *14* 359.

16. K.Choi, R.J.Angelici, *Organometallics* **1992,** *11* 330.

17. J.A.Rudd, R.J.Angelici, *Inorg. Chim. Acta* **1995,** *240* 393.

18. M.Novi, G.Guanti, *J. Heterocycl. Chem.* **1975,** *12* 1055.

19. C.Elschenbroich, *J. Organomet. Chem.* **1968,** *14* 157.

20. M.D.Rausch, *Pure Appl. Chem.* **1972,** *30* 523.

21. J.Davidson, H.Patel, P.Preston, *J. Organomet. Chem.* **1987,** *336* C44.

22. M.Landman, Novel heteroarene complexes of chromium(0), MSc dissertation, University of Pretoria **1997**, p76.

23. L.J.Farrugia, *J. Appl. Crystallogr.* **1997,** *30* 565.

24. The POV-Ray Team, POV-Ray 2004 . URL: http://www.povray.org/download/.

25. K.Schlögl, *J. Organomet. Chem.* **1986,** *300* 219.

26. G.Erker, R.Schlund, C.J.Krüger, *J. Organomet. Chem.* **1988,** *338* C4.

27. E.L.Muetterties, J.R.Bleeke, E.J.Wuckerer, T.A.Albright, *Chem. Rev.* **1982,** *82* 499.

5 Trimetallic Titanoxy-Benzo[b]-thienylcarbene Complexes

1. Introduction

In the previous chapters, a lot of attention was drawn to Fischer carbene complexes, containing one or two metal fragments. As discussed, a number of other examples of these types of complexes exist. In this chapter however, the focus will be on Fischer carbene complexes containing three metal fragments attached to the carbene carbon atom. Examples of polymetallic Fischer carbene complexes are found in literature,[1] and these were obtained by different synthetic routes. Trinuclear complexes are only one example of a polymetallic carbene complex but the ratio of carbene ligand to metal fragment is 1:1. There is no electronic contact between the metals and this type of complex can better be described by a chain of monocarbene complexes.

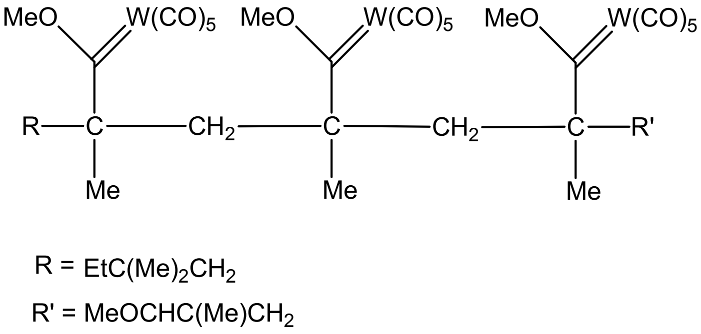

Figure 5.1 Trinuclear tris carbene complex[2]

Examples exist in literature where all carbene substituents contain a transition metal unit, but two substituents will form part of a ring system in heterodimetallic carbene complexes.[1,3-5]

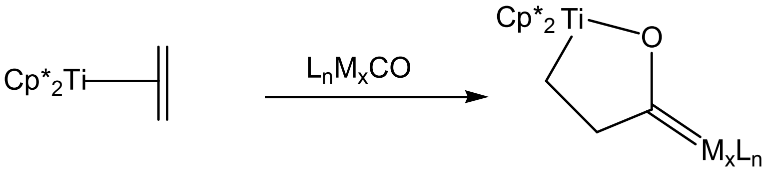

M_xL_n = $Cr(CO)_5$; $Mo(CO)_5$;$W(CO)_5$;
trans-$Mn_2(CO)_9$; *trans*-$Re_2(CO)_9$

Figure 5.2 Example of cyclic heterodimetallic carbene complexes

The metalloxycarbene complexes can be prepared without a nucleophilic addition to a metal carbonyl by using very reactive η^2-olefin precursors.

Similarly the reaction of η^4-coordinated dienes with metal carbonyls afford dimetallic η^3-allyl metaloxycarbene complexes (Figure 5.3).[1,3,4]

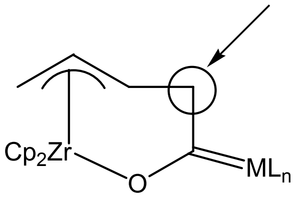

ML_n = $Cr(CO)_5$; $Mo(CO)_5$; $W(CO)_5$; $Fe(CO)_4$; $Fe(CO)_3PPh_3$; Rh(CO)Cp;
Co(CO)Cp; Co(CO)(η-C_5H_4Cl); $Ni(CO)_3$; $Zr(CO)Cp_2$; $Hf(CO)Cp_2$;
$V(CO)_3Cp$

Figure 5.3 Example of dimetallic metalloxycarbenes

The Cp_2Zr fragment acts as a link between two carbene substituents, but these complexes differ in two ways from the complexes discussed in this chapter. Although Zr is π-bonded to an allyl, no electronic connection exists with ML_n because of a CH_2-unit in this substituent (as indicated by the arrow in Figure 5.3). Secondly the same fragment Cp_2Zr is the metal containing fragment of two substituents and forms part of a metallocycle.

On the other hand, electronic communication through the π-system of the bridging ligand exists in the product obtained starting with a reactive aryne precursor (Figure 5.4).[1] These complexes have all the features and requirements of metal-metal communication but have only two metals as one of them links two substituents of the carbene in a five membered ring.

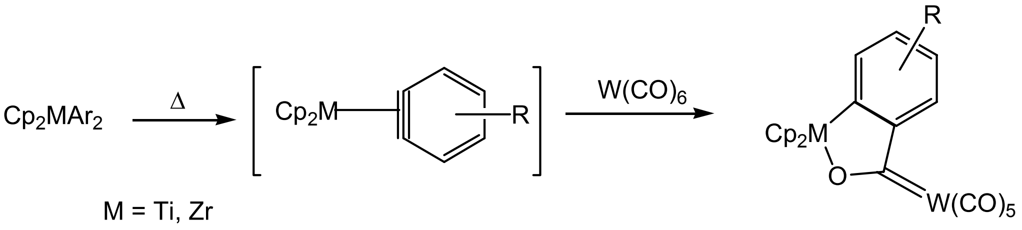

Figure 5.4 Example of metalloxycarbene complexes with electronic communication

Our purpose was to "surround" a single carbene carbon with three transition metal fragments as depicted in Chapter 1 (Scheme 1.2, structure **J**). This makes the complexes discussed in this chapter unique from the examples found in literature and represents the one type of a Fischer carbene complex without a precedent in literature. Not only was it possible to obtain stable complexes but also to record some reasonable spectra and manage to isolate crystals for crystal structure determinations of both **7** and **8**. An important fact of the complexes obtained in this chapter, is the different metal substituents attached to the carbene carbon, especially in **8** where all the transition metals contained in the fragments attached to the carbene carbon are unique, in **7** Cr appears twice.

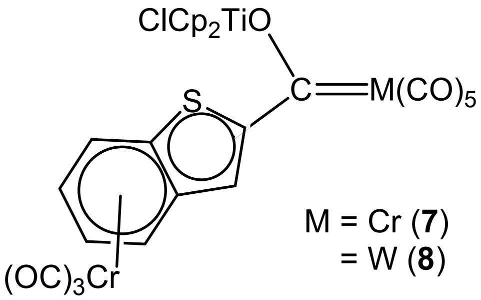

Figure 5.5 Complexes **7** and **8**, showing the three metal fragments that surround a carbene carbon

2. Synthesis

The same procedure was followed as described in Chapter 4. In this instance titanocene dichloride was added instead of triethyloxonium tetrafluroborate to the metal acylate, and the neutral trimetallic carbene complexes formed.

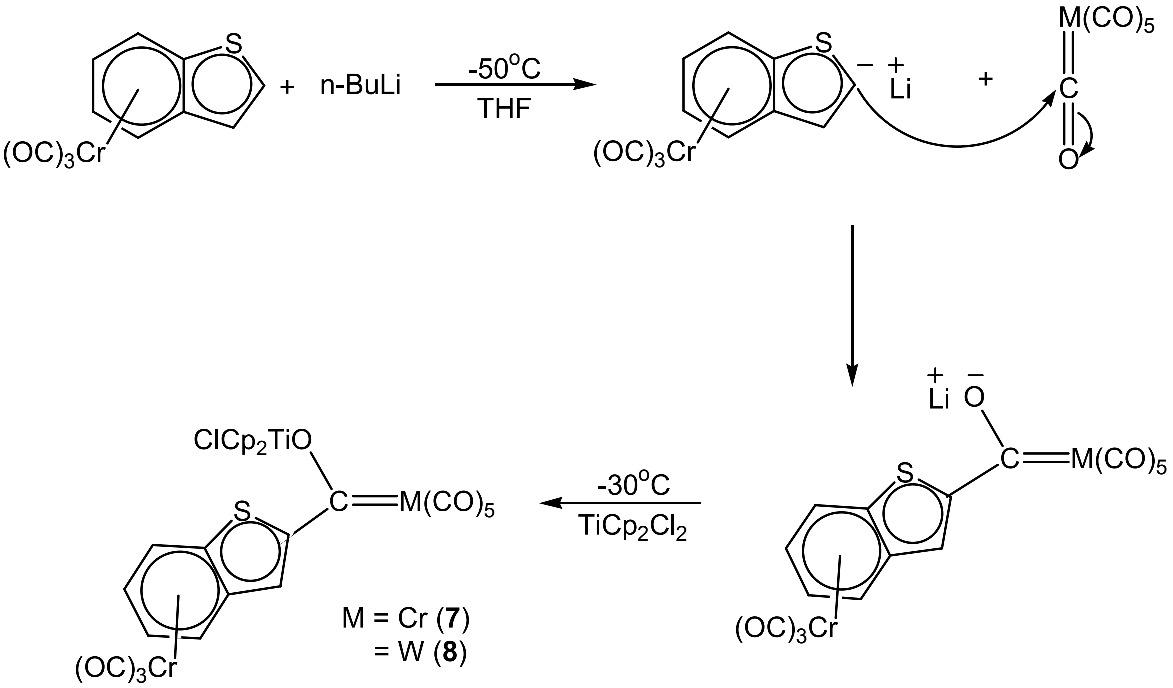

Scheme 5.1

The desired products **7** (dark purple) and **8** (dark purple) were obtained after purification using column chromatography with aluminium oxide as stationary phase. It was found that the complexes were more stable on alox compared tot silica gel during purification. The $Cr(CO)_3$, $Cr(CO)_5$ and the Ti- metal fragments can communicate electronically *via* a connecting conjugated π-system. The π-conjugated linker includes the BT-substituent, the carbene carbon atom and the oxygen as heteroatom. It is possible from spectroscopic measurements to look at the role of each substituent to stabilize the carbene carbon atom and the complex. Also, the introduction of a bulky $TiCp_2Cl$ fragment on the oxygen substituent will introduce additional steric strain within the trimetallic carbene complex.

3. Spectroscopic characterization

^{1}H NMR Spectroscopy

All ^{1}H NMR spectra were recorded in C_6D_6 only, due to decomposition in $CDCl_3$, which is an indication of the poor stability of these complexes in solution. No ^{13}C NMR spectra were obtainable due to poor solubility in C_6D_6.

A spectrum of poor quality was obtained for complex **7**, and no coupling constants could be calculated. The spectrum obtained for complex **8** shows fully resolved resonances and can be seen in Figure 5.6.

Chemical shifts (δ, ppm, C_6D_6) of **8**: 7.95 (d) (H3) with 0.8 ($^4J_{H\text{-}H}$), 5.11 (d) (H4) with 6.7 ($^3J_{H\text{-}H}$), 4.57 (m) (H5), 4.15 (m) (H6), 5.21 (dd) (H7) with 6.7 ($^3J_{H\text{-}H}$) and 0.8 ($^4J_{H\text{-}H}$) and 5.88 and 5.85 (Cp's).

When comparing the chemical shifts of **8** with the analogous **6**, it is clear that H3 in these complexes is very similar ($\Delta\delta = 0.04$). This can be ascribed to a dominating electron withdrawing effect of the $Cr(CO)_3$ fragment that controls the electron density on the BT ring without much interference from the carbene carbon, whilst the ethoxy group in the prior complexes (**5** and **6**) was electron donating, rather than withdrawing. An interesting observation for **8** is that there are two resonance signals for the Cp rings attached to the titanium, indicating that the two rings are in different electronic environments. This was not observed in **4**, which is ascribed to a more sterically crowded complex for **8** with restricted rotation around the Ti-O bond. Hence although the rings can rotate freely (sharp singlet), they are locked in a specific region of space because of the bulkiness of the π-BT substituent. The Cp-rings in **8**, again show a more electron positive titanium centre similarly to complex **4** in Figure 3.4[3] because of the down field shift compared to $TiCp_2Cl_2$ (experimentally determined in $CDCl_3$ has a value of 6.57 ppm).

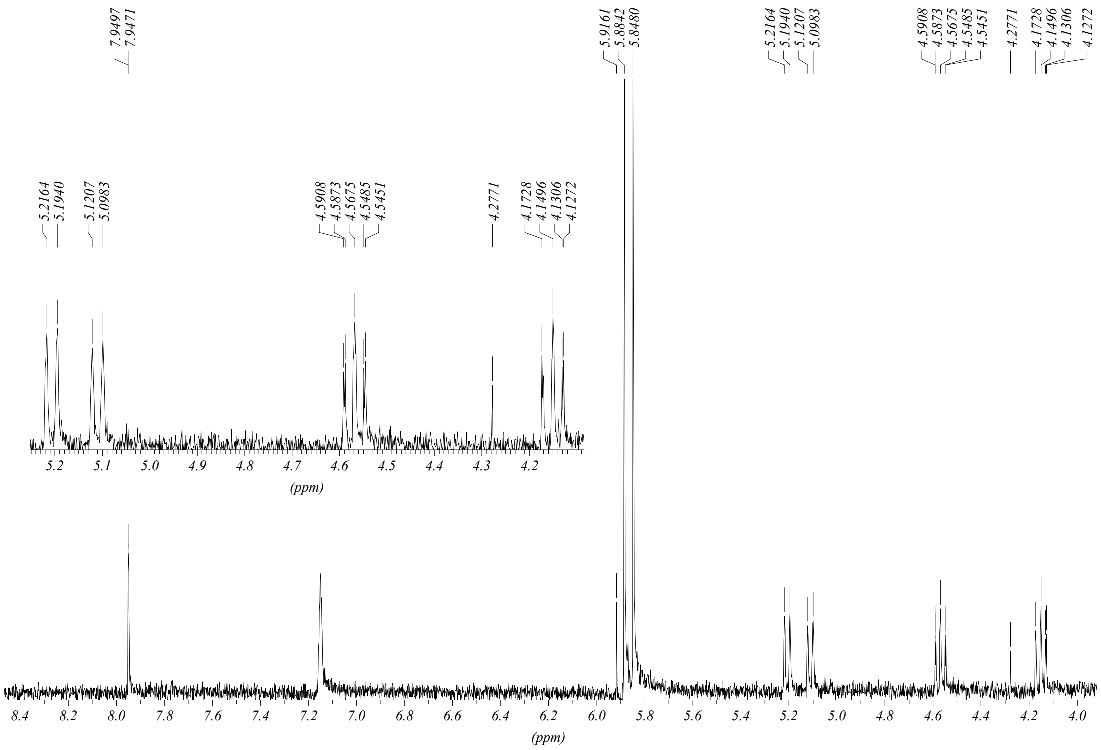

Figure 5.6 ^{1}H NMR spectrum of complex **8** in C_6D_6

3.2 Infrared Spectroscopy

The carbonyl data of the infrared spectra of complexes **7** and **8** are summarized in Table 5.1, the spectra of the compounds were recorded in dichloromethane due to not being soluble in hexane.

Complexes **7** and **8** contain metalpentacarbonyl and metaltricarbonyl fragments, aspects related to these metal fragments were discussed in Chapters 2 and 4. Due to the overlap of bands of the pentacarbonyl and tricabonyl moieties in these compounds, it was difficult to unambiguously assign a specific wavenumber to the A_1 band of the $Cr(CO)_3$-fragment of both complexes. The spectra are also indicative of large distortions in the complexes and a lowering of the carbonyl symmetry eventhough bands are broadened because of interaction with the polar solvent.

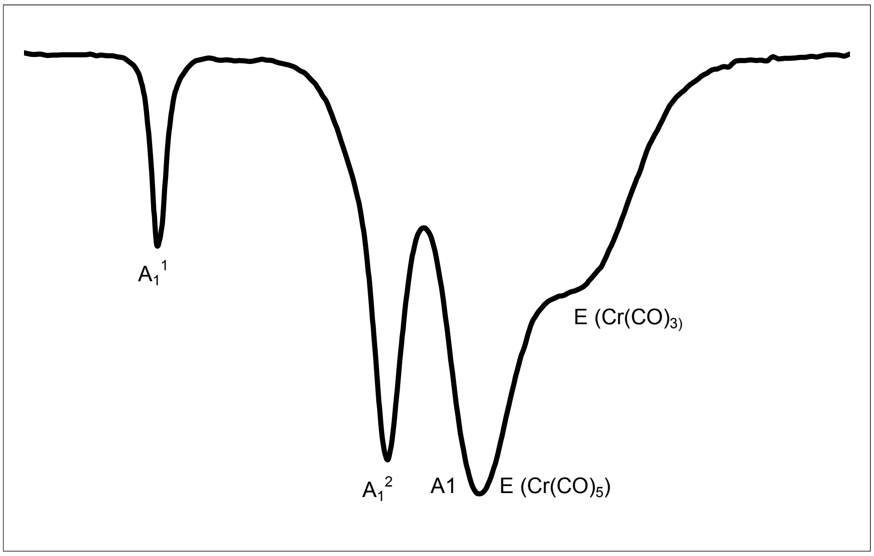

Figure 5.7 Infrared spectrum of **7** in the carbonyl region

Table 5.1 IR-data[b] of complex **7** and **8**

Complex	Carbonyl vibrating frequencies (ν_{CO}, cm^{-1})					
	$Cr(CO)_3$		$Cr(CO)_5$			
	A_1	E	$A_1^{(1)}$	B_1	$A_1^{(2)}$	E
7	1935*vs	1895m[c]	2052m	-	1968s	1935*vs
8	1930*vs	-	2060m	-	1969s	1930*vs

[b] Dichloromethane as solvent *A_1 ($Cr(CO)_3$) and E ($Cr(CO)_5$) overlap

[c] observed as a shoulder

3.3 X-ray Crystallography

Final confirmation of the structures of **7** and **8** was obtained from single crystal X-ray diffraction studies. The complexes were crystallised from a layered 1:1 dichloromethane:hexane solution. This method gave dark purple crystals of good quality for both complexes. Figures 5.8 and 5.9 represent the ORTEP[6] + POV-Ray[7] plot of the geometry of **7** and **8**, which also indicates the atom numbering scheme that was used for the structural data. Compound **7** crystallized in the space group P 21/c with a = 11.260(2), b = 12.083(2), c = 23.804(4) Å, Z = 4, compound **8** crystallized in the space group $P2_1/c$ with a = 11.2280(5), b = 12.2398(5), c = 23.9446(11) Å, Z = 4. The most important bond lengths and angles are listed in Table 5.2, whilst the most important torsion angles involving the carbene ligand are listed in Table 5.3. Other structural information is captured on the supplementary CD.

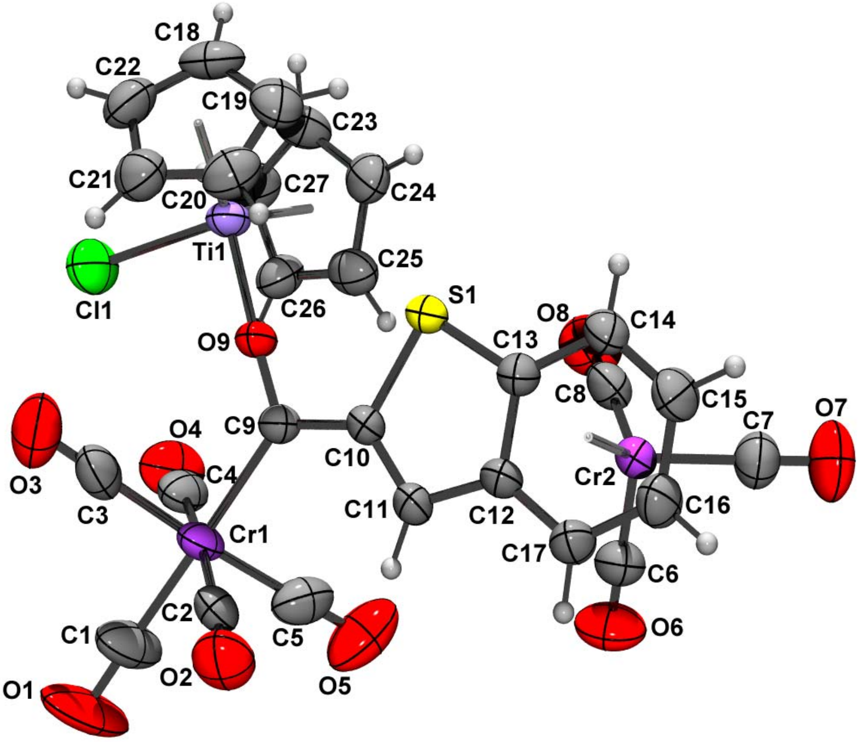

Figure 5.8 ORTEP + POV-Ray plot of the geometry of complex **7**

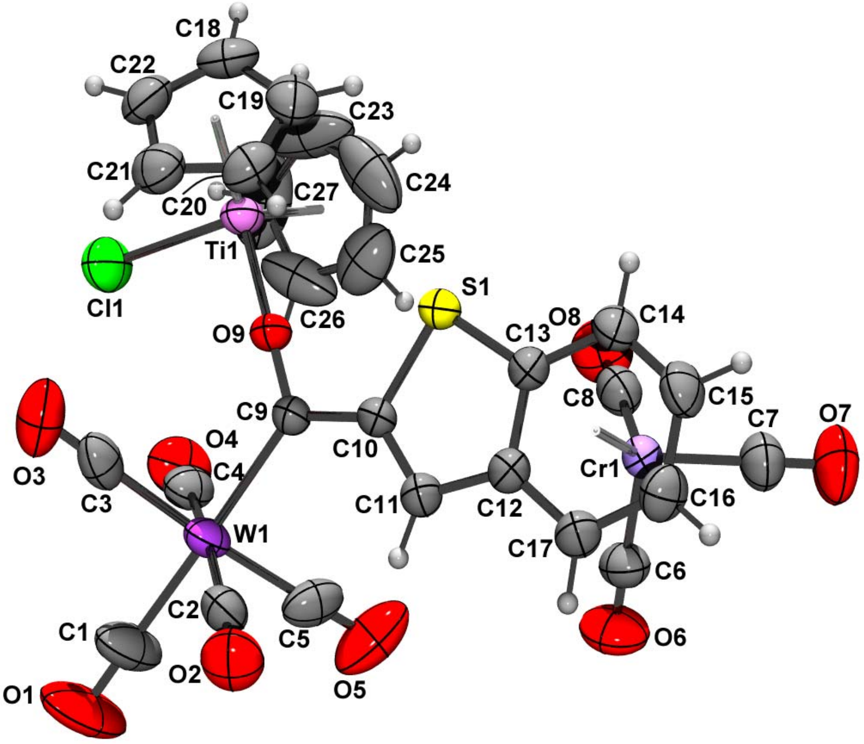

Figure 5.9 ORTEP + POV-Ray plot of the geometry of complex **8**

Table 5.2 Selected bond lengths and angles of **7** and **8**

Bond	Bond Lengths (Å)		Bond	Bond angles (°)	
	7 (M = Cr)	**8** (M = W)		**7** (M = Cr)	**8** (M = W)
M(1)-C(9)	2.077(4)	2.207(4)	C(1)-M(1)-C(9)	178.0(3)	177.2(3)
C(9)-O(9)	1.285(5)	1.280(5)	O(9)-C(9)-C(10)	112.7(4)	112.5(3)
C(9)-C(10)	1.463(6)	1.461(6)	O(9)-C(9)-M(1)	120.9(3)	121.4(3)
O(9)-Ti(1)	1.925(3)	1.921(3)	C(10)-C(9)-M(1)	126.4(3)	126.1(3)
M(1)-C(1)	1.859(6)	2.000(6)	C(9)-O(9)-Ti(1)	174.0(3)	174.6(3)
M(1)-C(2,3,4,5)[a]	1.897(7)	2.074(7)	C(9)-C(10)-S(1)	119.8(3)	119.7(3)
C(10)-C(11)	1.363(6)	1.361(6)			
C(11)-C(12)	1.438(6)	1.440(6)			
C(12)-C(13)	1.414(6)	1.424(6)			
C(13)-S(1)	1.724(5)	1.723(4)			
C(10)-S(1)	1.770(4)	1.775(4)			

[a] mean value

Table 5.3 Selected torsion angles of **7** and **8**

Bond	Torsion angle (()	
	7 (M = Cr)	8 (M = W)
C(4)-M(1)-C(9)-O(9)	42.1(4)	40.9(4)
O(9)-C(9)-C(10)-C(11)	-179.5(4)	179.9(4)
O(9)-C(9)-C(10)-S(1)	-1.7(5)	-1.3(5)
M(1)-C(9)-C(10)-S(1)	178.8(2)	177.6(2)

Structural information shows that the carbene ligand of the complexes **7** and **8** lies in a flat plane. One can see this by looking at the torsion angles given in Table 5.5 i.e, O(9)-C(9)-C(10)-S(1) (**7** = -1.7(5) and **8** = -1.3(5)) and M(1)-C(9)-C(10)-S(1) (**7** = 178.8(2) and **8** = 177.6(2)). The plane of the carbene ligand bisects two *cis* carbonyl ligands. These angles are much smaller than those of complexes **4**, **5** and **6**. The BT ligand in both complexes may be considered as flat, since distortion (torsion angles < 1°) is minimal. In these complexes two of the four carbonyls bend away from the carbene carbon, towards the *trans* carbonyl as seen by looking at C(3)-M(1)-C(9) (**7** = 87.5(2) and **8** = 87.01(18)) and C(5)-M(1)-C(9) (**7** = 89.2(2) and **8** = 89.5(2)).

Looking at the crystal structures of **7** and **8** the expected conformation for the $Cr(CO)_3$-fragment was obtained as indicated in Chapter 4, the $Cr(CO)_3$ fragment, once again took on a staggered conformation (Figure 4.10), since this is the energetically favoured conformation.

When comparing the bond lengths obtained for complexes **7** and **8** with known distances from literature[8] and those discussed in Chapter 2-4, some delocalization of electron density is observed since the C(9)-O(9) (**7** = 1.285(5); **8** = 1.280(5) Å) and C(9)-C(10) (**7** = 1.463(6); **8** = 1.461(6)Å) bonds are shorter than those of single bonds (Csp^2-O(2) in enol esters: C=C-O-C* = 1.354 Å and Csp^2-Car (overall) = 1.483 Å), but still longer than double bonds. For the thiophene ring the bonds C(10)-C(11) (**7** = 1.363(6); **8** = 1.361(6)Å) are in the same range as those of free thiophene (1.362 Å) and the C(11)-C(12) (**7** = 1.438(6); **8** = 1.440(6)Å) bonds are longer than those of free thiophene (1.424 Å). Both the C-S bonds in **7** and **8** are longer than those of free thiophene (1.712Å), this observation can be ascribed to the bulkiness of the carbene substituents and poorer conjugation within the thiophene ring. The C-S bond closer to the carbene carbon (C(10)-S(1)) is much longer than those, on the side of the benzene ring (C(13)-S(1)). This can be ascribed to the fact that the ring protons in the benzene ring are no longer available for delocalization due to the bonded $Cr(CO)_3$-fragment, while in complexes **1-4** this was not the case. (See Chapter 4, Figure 4.11)

In Chapter 4 we saw two possible structures for the complexes (**5** and **6**) in the solid state, where the positions for the sulphur atom with respect to the ethoxy substituent differ. This observation was explained by means of planar chirality of the π-BT substituent due to the coordination of the $Cr(CO)_3$-group. The ethoxy substituent is relatively small, and both isomers formed. For complexes **7** and **8**, however, only one isomer is observed because of the bulkiness of the titanoxy substituent and this isomer agrees with the main product in Chapter 4.

4. References

1. M.A.Sierra, *Chem. Rev.* **2000,** *100* 3591.
2. D.W.Macomber, M.-H.Hung, *J. Organomet. Chem.* **1989,** *366* 147.
3. M.Sabat, M.F.Gross, M.G.Finn, *Organometallics* **1992,** *11* 745.
4. G.Erker, *Angew. Chem., Int. Ed. Engl.* **1989,** *28* 397.
5. G.Erker, F.Sosna, U.Hoffmann, *J. Organomet. Chem.* **1989,** *372* 41.
6. L.J.Farrugia, *J. Appl. Crystallogr.* **1997,** *30* 565.
7. The POV-Ray Team, POV-Ray 2004 . URL: http://www.povray.org/download/.
8. F.H.Allen, O.Kennard, D.G.Watson, L.Brammer, A.G.Orpen, R.Taylor, *J. Chem. Soc. Perkin. Trans.II* **1987,** S1.

6

Conclusion

1. Stability of complexes

The stabilities of the complexes **1–8** were not formally investigated, but the rates of decomposition of the different complexes in solution and on exposure to air were used as criteria. It was found that the stability of the complexes decreased on increasing the number of metal fragments surrounding the carbene carbon atom. For instance, the carbene complexes containing three metal fragments decomposed within hours in an inert atmosphere in solution, while the analogous carbene complex containing only one metal fragment was stable for several days under the same conditions. Carbene complexes are sensitive towards oxygen and the substitution of a metal fragment by oxygen is a common occurrence in reactive carbene complexes.[1-3] Also, in reactive carbene complexes under inert conditions with the exclusion of oxygen or oxygen containing solvents, carbene-carbene carbon-carbon coupling reactions have been observed.[4,5] Neither of these two decomposition pathways were observed from studying NMR spectra in $CDCl_3$ of **5–8** that have changed their composition. The most important routes for complexes losing their identity was the substitution of the carbene ligand to afford $M(CO)_6$ complexes and the π-coordination mode for $Cr(CO)_3$ fragments (Scheme 6.1). The stability of the different complexes was found to follow the trend depicted in Figure 6.1 (The top complex, being the more stable one).

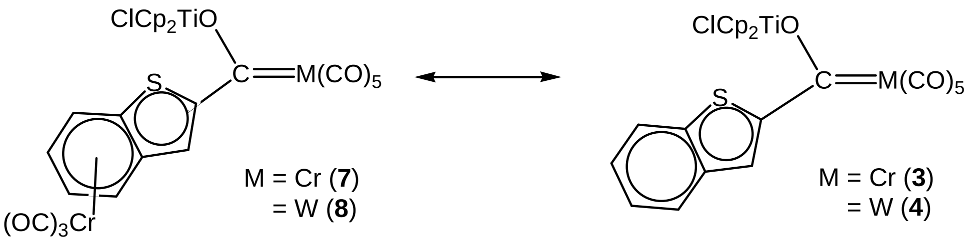

Scheme 6.1

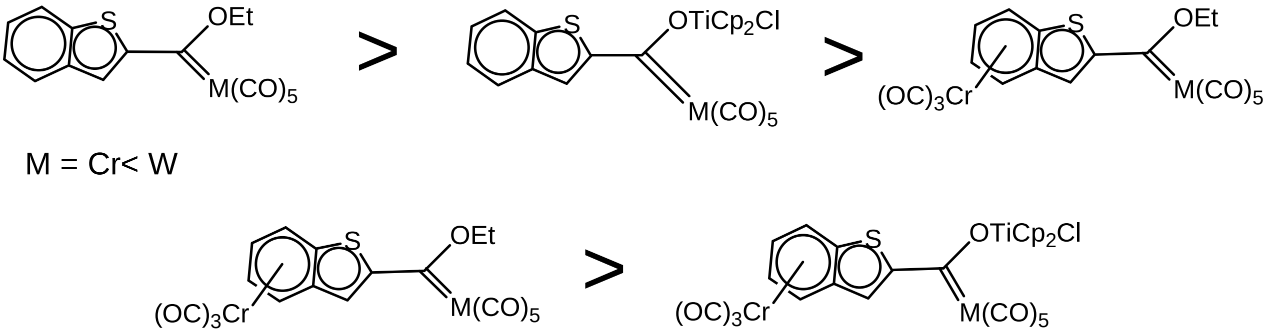

Figure 6.1 Decreasing order for the stability of complexes **1-8**.

2. Electronic spectra

The UV-spectra of the complexes containing a $W(CO)_5$-fragment were recorded in dichloromethane. The electronic data of the series **2**, **4**, **6** and **8** are produced in Table 6.1 The electronic spectrum of complex **2** is presented by Figure 6.2. All the complexes exhibit very strong ligand-based absorption bands between 223 and 245 nm. Intense characteristic absorption bands with $?_{max}$ in the range 325 to 380 nm are assigned to the benzo[*b*]thiophene-based p-p* transitions. In benzo[*b*]thiophene this transition is observed at 265 nm when measured in dichloromethane. Coordination to metal fragments shifts this band to higher wavelengths, indicating interaction of the metal carbene p-system with that of the thiophene substituent. This means that the energies of the p-p* transitions in the benzo[*b*]thiophene substituent are reduced. Displacement of the p-p* transitions to lower energies upon metallation has been observed for p-metal complexes of oligothiophenes end-capped with ruthenium units.[6-8] The absorption band at lowest energy is assigned to the d-p metal-to-ligand charge transfer transition. Since the colours of the different complexes are characteristic to the number of metal moieties coordinated to the carbene carbon, it is not surprising that the values of this transition are very similar for the different types of complexes. Complexes containing one metal fragment all have a red colour, those containing two metal fragments are of a darker colour varying between red-brown and purple, while the complexes containing three metal fragments are a very dark purple.

Table 6.1 UV data of complexes **2**, **4**, **6** and **8**

Complex	Colour	Ligand p-p* transition (?, nm)	Metal-ligand transition (?, nm)
2	Red-brown	334	458
4	Red-orange	334, 381	483
6	Dark brown	325	449, 569
8	Purple	325	494, 567

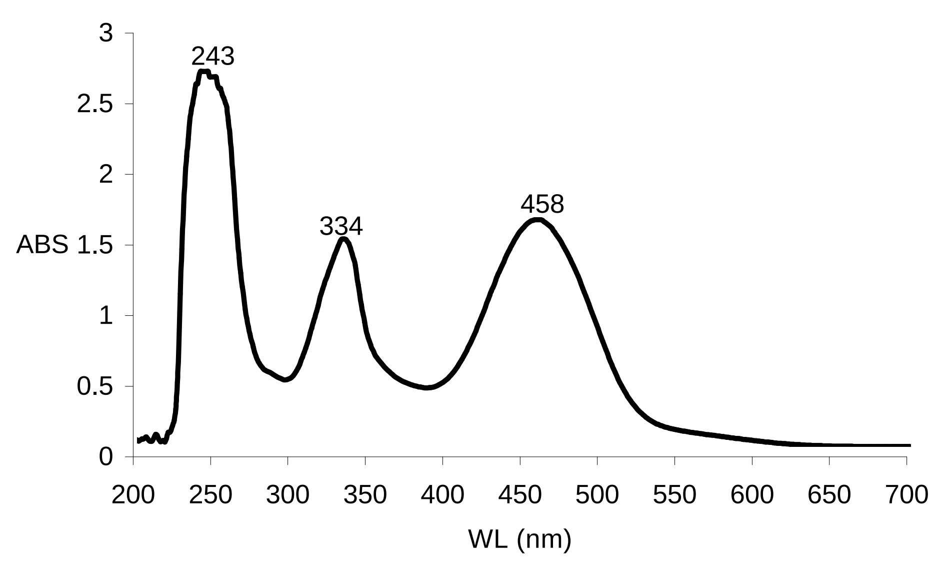

Figure 6.2 UV-spectrum of complex **2**

3. NMR Spectroscopy

The bridging ligands were such in **3-8** that metal-metal communication exists in all the complexes. Surrounding the $M(CO)_5$ carbene carbon are two substituents that were chosen to create competitive demands on electrons vital to stabilize the carbene carbon atom. In all the complexes prepared in this study a flow of electron density can be recognised. For the complexes containing one metal fragment (**1** and **2**), the electron flow is from the oxygen and from the BT-substituent towards the carbene carbon, once a titanoxy-fragment is added (**3** and **4**), a competition for electron density between the positive titanium(IV) and the carbene carbon is introduced and when a p-fragment of $Cr(CO)_3$ is added on the benzene ring, this fragment will withdraw electron density (**5** and **6**) from the BT-substituent and cause competition. Surrounding the carbene carbon atom by three metal fragments (**7** and **8**), causing push-pull effects, this will affect the whole complex (Figure 6.3), causing the most dramatic scenario. Figure 6.2 shows the flow of electron density to the carbene carbon atom as well as competitive processes by the titanocene chloride and $Cr(CO)_3$ fragments. It is clear that the metal-fragments of **7** and **8** can "communicate" electronically with each other.

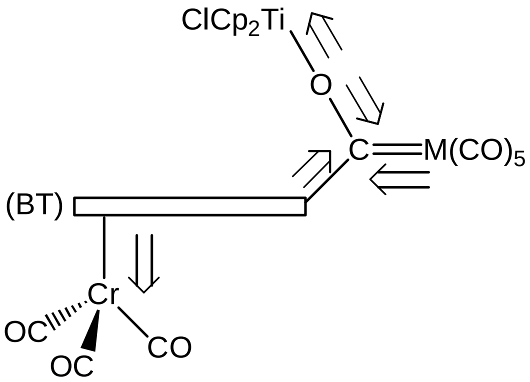

Figure 6.3 Effect of metal fragments on electron flow in the carbene complexes **7**and **8**

Table 6.1 ^{1}H NMR Spectra of complexes **1-8** for the BT-substituent

Proton	Chemical shifts (d, ppm)						
	[Cr(CO)$_5$]-complexes			[W(CO)$_5$]-complexes			
	1	**3**	**5**	**2**	**4**	**6**	**8**
H3[a]	8.50	8.43	8.13	8.39	8.35	8.05	
H4	7.80	7.87	6.07	7.79	7.85	6.07	
H5	7.47	7.50	5.61	7.50	7.52	5.64	
H6	7.40	7.45	5.26	7.39	7.44	5.25	
H7	8.00	8.04	6.29	8.00	8.03	6.29	

H3[b]	8.51	8.64	8.00	8.40	8.56	7.91	7.95
H4	7.33	7.50	5.03	7.31	7.48	5.00	5.11
H5	7.00	7.09	4.56	7.01	7.10	4.56	4.57
H6	6.95	7.02	4.19	6.94	7.00	4.17	4.15
H7	7.46	7.53	5.19	7.45	7.52	5.14	5.21

[a] spectrum was recorded in $CDCl_3$

[b] spectrum was recorded in C_6D_6

A downfield shift in the resonances of the following pairs of complexes: **1? 3** or **2? 4** and **5 ? 7** or **6? 8** in C_6D_6 is observed for the H3 chemical shift value in the ^{1}H NMR spectra of the complexes. The corresponding change in the structure of the complexes for these groupings is Et? $TiCp_2Cl$, while the other substituents were kept the same. The observed downfield shift is ascribed to the electropositive Ti-fragment that withdraws electron density from the oxygen and forces the carbene carbon to “get” more electron density from the BT-substituent. This will influence the H3 proton in such a manner that H3 becomes more deshielded.

In grouping the following pairs of complexes: **1? 5** or **2? 6** and **3? 7** or **4? 8** and by studying their H3 chemical shift values in the ^{1}H NMR spectra in C_6D_6 for these complexes, an upfield shift appears for every pair. The corresponding change in structure that appears in these pairs is BT? p-BTCr$(CO)_3$, while the other substituent was kept the same. The observed upfield shift is ascribed to the $Cr(CO)_3$-fragment which because of its coordination to BT retains electron density on the rings, causing the H3 proton to be more shielded. The same observations in the chemical shifts values in the ^{1}H NMR spectra of the complexes dissolved in $CDCl_3$, were not observed.

In conclusion, the most dramatic downfield shift for H3 in the ^{1}H NMR spectra of the complexes is for **3** and **4**, demonstrating the electronic effect of the $TiCp_2Cl$ substituent and the most dramatic upfield shift for H3 is for **5** and **6**, demonstrating the electronic effect of the $Cr(CO)_3$ fragment.

The chemical shift of the carbonyl ligands in ^{13}C NMR spectra are very insensitive to changes in the substituents of the carbene ligand and mostly effected only by the type of ligand and the number of carbonyl ligands attached to the metal.

Table 6.2 ^{13}C NMR Spectra[a] of complexes **1-5**

Carbon	Chemical shifts (d, ppm)				
	[Cr(CO)$_5$]-complexes			[W(CO)$_5$]-complexes	
	1	**3**	**5**	**2**	**4**
C1	320.5	324.5	318.2	294.3	-
C2	154.0	140.8	155.6	157.0	141.1
C3	141.9	139.5	138.2	142.5	139.4
C4	122.8	122.9	88.9	122.9	123.1
C5	128.9	128.4	89.8	128.8	128.4
C6	125.1	125.4	92.2	125.2	125.5
C7	126.8	126.9	84.3	126.9	127.1
C8, C9	138.7, 139.2	138.1	118.1, 126.6	139.0, 139.5	-
M(CO)$_5$	216.9 (cis) 223.4 (trans)	217.9 (cis) 224.9 (trans)	216.5 (cis) 223.4 (trans)	197.5 (cis), (triplet) 202.6 (trans)	199.0 (cis)
M(CO)$_3$	-	-	231.4	-	-

[a] spectrum was recorded in $CDCl_3$

4. Structural features of the carbene complexes

On comparing the structural data obtained for the complexes in the solid state, it is evident that the heteroaromatic ligand is planar and only very small distortions were observed for all of the complexes except **1** and **2**. With a planar heteroaromatic ligand, it is possible to facilitate the delocalization of electron density through the p-system of the ligand. In these Fischer carbene complexes, metal-metal communication through this delocalized system seems plausible. Bond lengths and angles surrounding the carbene carbon in solid state are summarized in Tables 6.3 and 6.4. Figure 6.4 indicates the bond angles referred to in Table 6.4.

Table 6.3 Selected bond lengths (Å) of the carbene complexes

Bond	[Cr(CO)$_5$]-complexes			[W(CO)$_5$]-complexes			
	1	**5**	**7**	**2**	**4**	**6**	**8**
M-C$_{carb}$	2.067(3)	2.050(2)	2.077(4)	2.201(5)	2.211(4)	2.179(7)	2.207(4)
M-CO$_t$	1.875(3)	1.884(3)	1.859(6)	2.018(6)	2.007(4)	2.011(7)	2.000(6)
M-CO$_{av}$	1.9044(19)	1.905(3)	1.897(7)	2.036(4)	2.033(4)	2.058(8)	2.074(7)
C$_{carb}$-O	1.319(3)	1.324(3)	1.285(5)	1.315(6)	1.279(4)	1.318(8)	1.280(5)
C$_{carb}$-C	1.462(3)	1.472(3)	1.463(6)	1.468(7)	1.474(5)	1.471(8)	1.461(6)

$_{carb}$ = carbene, $_t$ = trans, $_{av}$ = average

The shortest metal-carbene distances, and these are significantly shorter, are associated with complexes **5** and **6** in solid state. This again highlights the role of the π-coordinated Cr(CO)$_3$ fragment within an arene carbene substituent and supports conclusions drawn from the NMR spectroscopy for these complexes in solution. The Cr(CO)$_3$ fragment retains the electronic charge on the BT-substituent and decreases the amount of charge transfered to the carbene carbon atom for **5** and **6** compared to the other complexes. As a result, more π-backdonation from the M(CO)$_5$ fragment is required to stabilize the electrophilic carbene carbon atom. One would expect the same observation for **7** and **8** because of the presence of the π-coordinated Cr(CO)$_3$ fragment, but instead these complexes represent the longest M-C(carbene) distances. This is ascribed to steric crowding around the carbene carbon atom that is greatest for **7** and **8** and would tend to lengthen the metal carbene distance to create more space for the bulky substituents. At the same time the M-CO(trans) bond increases its distance to compensate for the shorter M-C(carbene) distances. The metal-carbene distances fall within the range that are characteristic for alkoxy carbene complexes of M(CO)$_5$.[9]

The shortest carbene-oxygen distances, and these are significantly shorter, are associated with complexes **4**, **7** and **8**. These complexes all display the very electropositive TiCp$_2$Cl fragment on the one hand with a high affinity for the oxygen electron density, but this fragment is the most bulky substituent surrounding the carbene carbon atom. As a result the C(carbene)-O and O-Ti distances are the net result of strong competition between $TiCp_2Cl$ fragment and the electrophilic carbene carbon for electron density on the one hand and steric interactions of the $TiCp_2Cl$ fragment on the other hand. This manifests in a short C(carbene)-O distance and a long Ti-O distance. The C(carbene)-C(BT) distances are the same for all the complexes, showing some delocalisation from the thienyl of the BT-substituent, but are more or less constant in magnitude.

A second aspect of importance is the bond angles surrounding the carbene carbon atom. These are shown in Figure 6.4 and the data given in Table 6.4. The sterically greatest substituent will impact on the two adjacent bond angles. From the data it is clear that the bond angle 2 remains more or less the same showing the very little steric interaction between the $M(CO)_5$ fragment and the BT-substituent. Especially important the fact that the introduction of the π-coordinated $Cr(CO)_3$ plays no role.

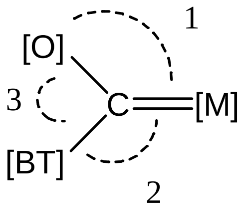

Figure 6.4 Bond angles referred to in Table 6.4

Table 6.4 Bond angles (°) shown in Figure 6.4 of the carbene complexes.

Angle	$[Cr(CO)_5]$-complexes			$[W(CO)_5]$-complexes			
	1	**5**	**7**	**2**	**4**	**6**	**8**
1	129.92(17)	130.04(15)	120.9(3)	130.1(4)	121.2(3)	130.0(4)	121.4(3)
2	124.89(17)	125.36(15)	126.4(3)	124.2(4)	125.9(2)	124.4(4)	121.4(3)
3	105.2(2)	104.52(18)	112.7(4)	105.7(4)	112.7(3)	105.5(5)	112.5(3)

The biggest steric effect is displayed in complexes **4**, **7** and **8** where the angles described by angle 1 are almost 10° smaller and those by angle 3 around 8° greater than the average values of the other complexes. In **4**, **7** and **8** the OEt-group was replaced by a much more bulky OTiCp$_2$Cl-group and thus occupying a greater volume of space. Since the Cr(CO)$_3$-fragment was relatively far away from the carbene carbon in comparison to the other metal centers, the occupied space at substituent 3 was not as crowded as that of substituent 2.

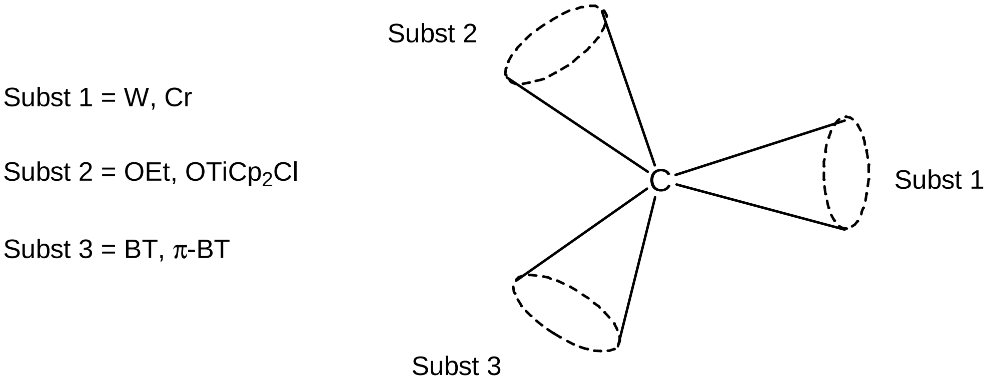

Figure 6.5 Steric demands of metal substituents surrounding the carbene carbon

When looking closely at the structures of the synthesized complexes in the solid state, it appears as though there is some space available directly underneath the thiophene ring as indicated in Figure 6.6.

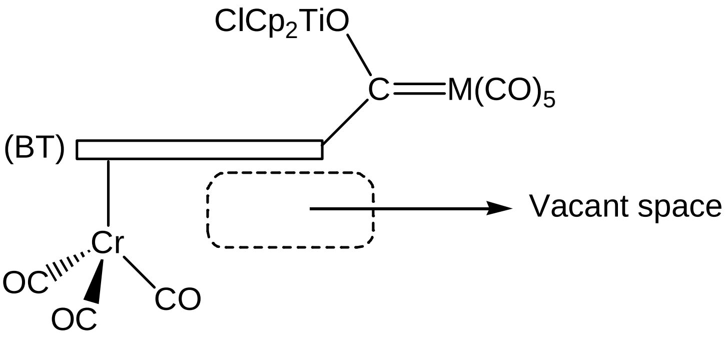

Figure 6.6 Vacant space in synthesized trimetallic carbene complexes

In the quest to bind the metal-fragments as close as possible to the carbene carbon and evidently filling the "vacant space", one other complex was synthesized (**9**), containing a ferrocene fragment in the place of the p-BT, evidently forcing the iron metal centre to be closer to the carbene carbon than the chromium metal centre of the p-BT.

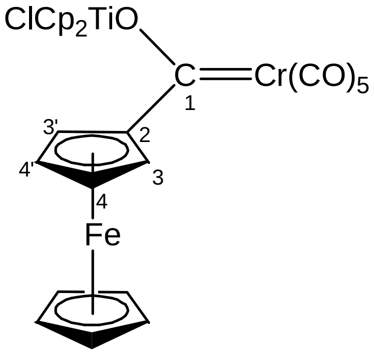

Figure 6.7 Structural representation and numbering of carbene complex **9**

A fairly good spectrum was obtained for **9**, but as expected, this complex was less stable than the other previously synthesized trimetallic carbene complexes (**7** and **8**).

Chemical shifts (d, ppm, CDCl$_3$) of **9**: 4.70 (H3 and H3'), 4.53 (H4 and H4'), 6.70 (Ti-Cp), 4.14 (Fe-Cp).

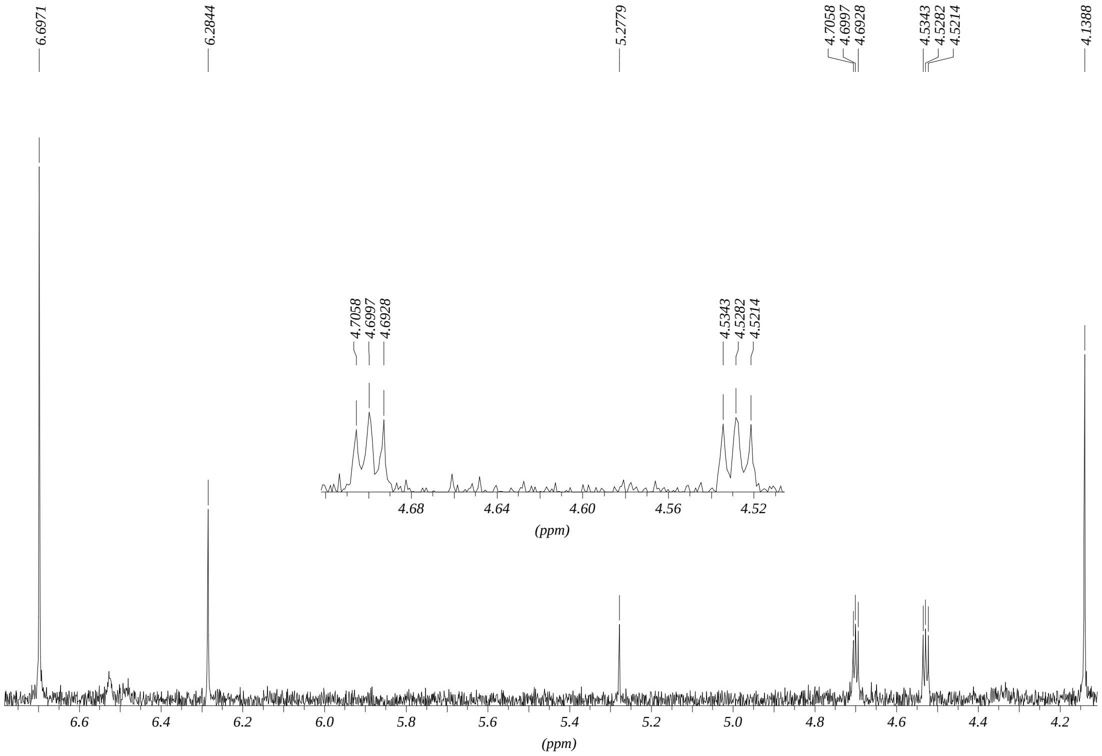

Figure 6.8 ^{1}H NMR spectrum of complex **9** in CDCl$_3$

5. Future work

Many new opportunities exist to expand and study metal-containing carbene complexes. These refer to the following aspects:

(i) Utilize open spaces (steric) and optimize electronic properties by introducing other metal π-coordinated fragments as substituents.

(ii) Apply concept to Schrock carbene complexes, but to avoid steric complications using tetrahedrally coordinated metal substituents.

(iii) Study reactivity patterns of the new trimetallic carbene complexes towards unsaturated C-C and C-X (X = heteroatom) bonds

6. References

1. U.Schubert, E.O.Fischer, *J. Organomet. Chem.* **1981,** *219* C34.
2. M.F.Semmelhack, R.Tamura, *J. Am. Chem. Soc.* **1983,** *105* 4099.
3. R.B.Silverman, R.A.Olofson, *J. Chem. Soc. Chem. Commun.* **1968,** 1313.
4. E.O.Fischer, B.Heckl, K.H.Dötz, J.Müller, H.Werner, *J. Organomet. Chem.* **1969,** *16* 29.
5. E.O.Fischer, D.Plabst, *Chem. Ber.* **1974,** *107* 3326.
6. D.D.Graf, N.C.Day, K.R.Mann, *Inorg. Chem.* **1995,** *34* 1562.
7. D.D.Graf, K.R.Mann, *Inorg. Chem.* **1997,** *36* 141.
8. D.D.Graf, K.R.Mann, *Inorg. Chem.* **1997,** *36* 150.
9. M.Sabat, M.F.Gross, M.G.Finn, *Organometallics* **1992,** *11* 745.

7 Experimental

1. Standard Operational Procedure

All operations were carried out under an inert atmosphere of nitrogen or argon gas using standard Schlenk techniques. Solvents were dried and distilled in an inert atmosphere according to conventional laboratory methods. Most chemicals were used without prior purification, unless stated otherwise. Column chromatography, using Kieselgel 60 (particle size 0.0063-0.200 mm) or neutral aluminium oxide, as stationary phase, was used for all separations. The column was cooled with ice-water (0°C) in the column jacket or performed at room temperature.

2. Characterization Techniques

2.1 Nuclear Magnetic Resonance Spectroscopy

NMR spectra were recorded on a Bruker ARX-300 spectrometer and on a AVANCE 500 spectrometer. ^{1}H NMR spectra were recorded at 300.135 and 500.139 MHz and ^{13}C NMR spectra at 75.469 and 125.75 MHz respectively. The signal of the deuterated solvent was used as reference, e.g. ^{1}H $CDCl_3$ 7.24 ppm and ^{13}C $CDCl_3$ 77.00 ppm.

2.2 Infrared Spectroscopy

IR spectra were recorded on a Perkin-Elmer Spectrum RXI FT-IR spectrophotometer. All spectra were recorded using either dichloromethane or hexane as solvent. Only the vibrational bands in the carbonyl stretching region (ca. 1500-2200 cm^{-1}) were recorded.

2.3 X-ray Crystallography

Data collection and structure determinations were done by Mr. Dave Liles, University of Pretoria, South-Africa. X-ray crystal structure analysis were done from data collected at 20 °C on a Siemens P4 Bruker 1K CCD diffractometer using graphite-monochromated, Mo-Kα radiation. Data were corrected for Lorenz polarization effects and structures were solved by direct methods (SHELXS) and refined by full-matrix least squares techniques.

2.4 UV spectroscopy

All the complexes were referenced to dichloromethane and spectra were measured in the range 200.0 to 800.0 nm in a quartz cell. A genesis spectronic 5 spectrophotometer was used.

3. Preparation of Starting Compounds

The following compounds were prepared according to known literature methods:
Tisammine(tricarbonyl)chromium[1] and triethyl oxonium tetrafluoroborate.[2]

3.1 (η^6-benzo[*b*]thiophene)tricarbonylchromium[3-9]

Trisammine(tricarbonyl)chromium (2.00 g, 10.7 mmol) was dissolved in diethyl ether (~ 95 ml). Freshly distilled boron trifluoride diethyl etherate (3.95 ml, 33 mmol) was added to the solution, followed by 2.82g (21 mmol) of benzo[*b*]thiophene. The reaction mixture was stirred for 12h. Diethyl ether (100 ml) was added and the solution was cooled to 0°C after which 100 ml air-free water was added. The mixture was repeatedly extracted with diethyl ether until the extracts were virtually colourless. The ether extracts were combined and dried over anhydrous sodium sulphate. The solvent was removed under reduced pressure. The product was purified with column chromatography which afforded the starting compounds and the orange product. The crude product was recrystallized from dichloromethane and hexane. The orange crystals were washed with hexane and dried under reduced pressure. Yield: 0.97g (34%)

4. Preparation of Organometallic Compounds

An excess of 10% of butyllithium was used in the syntheses. All complexes were synthesized according to the General Method.

4.1 General Method

The dropwise addition of a 1.6 mol dm^{-3} hexane solution of LiBu (0.7 ml, 1.1 mmol) to a cooled (-50°C) THF solution (12 cm^3) containing the heteroarene (1 mmol) afforded a lithiated thienyl species in high yields after 30 min. Addition of the metalhexacarbonyl (1 mmol) in small portions over 10 min resulted in a gradual change of colour. After stirring for 1 h in the cold, the reaction mixture was warmed to RT and stripped of solvent under reduced pressure. The residue was redissolved in dichloromethane, cooled to -30°C and carefully treated with triethyloxonium tetrafluroborate (**A**) or titanocene dichloride (**B**) (1 mmol), also dissolved in dichloromethane. After stirring for 1 h and allowing the reaction mixture to warm to RT, the dark coloured solution was filtered through kieselgel or neutral aluminium oxide and washed through with dichloromethane. The solution was dried in under reduced pressure. Details of the reaction are given in Table 7.1 and of the products in Table 7.2.

4.2 Synthesis of complexes 1-8

Table 7.1 Amount and substances used to synthesize complexes **1-8**

Complex	Heteroarene	Mass	Metal-carbonyl	Mass	**A/B**	Mass
1	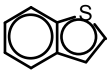	0.14 g	$Cr(CO)_6$	0.22 g	**A**	0.30 g
2	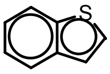	0.14 g	$W(CO)_6$	0.35 g	**A**	0.30 g
3	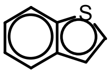	0.14 g	$Cr(CO)_6$	0.22 g	**B**	0.25 g
4	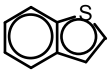	0.14 g	$W(CO)_6$	0.35 g	**B**	0.25 g
5	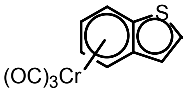	0.27 g	$Cr(CO)_6$	0.22 g	**A**	0.30 g
6	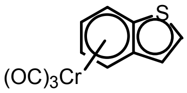	0.27 g	$W(CO)_6$	0.35 g	**A**	0.30 g
7	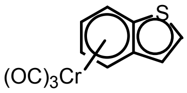	0.27 g	$Cr(CO)_6$	0.22 g	**B**	0.25 g
8	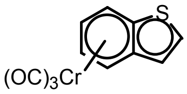	0.27 g	$W(CO)_6$	0.35 g	**B**	0.25 g

A = Triethyl oxonium tetrafluoroborate

B = Titanocene dichloride

Table 7.2

4.3 Synthesis of complex 9

Ferrocene (0.76 g, 1 mmol) was dissolved in hexane. 1.6 mol dm^{-3} hexane solution of LiBu (0.7 ml, 1.1 mmol) and TMEDA (0.15 ml, 1 mmol) was mixed and added to the ferrocene and stirred while increasing the temperature, until the orange adduct precipitated from the hexane solution. The excess liquid was sucked from the precipitate *via* a pipette. The precipitate was cooled to -50°C. Chromium hexacarbonyl (0.22g, 1 mmol) was dissolved in freshly distilled THF and added to the cooled precipitate. After stirring for 1 h in the cold, the reaction mixture was warmed to RT and stripped of solvent under reduced pressure. The residue was washed several times with hexane, redissolved in dichloromethane, cooled to -30°C and carefully treated with titanocene dichloride (0.25g, 1 mmol), also dissolved in dichloromethane. After stirring for 1 h and allowing the reaction mixture to warm to RT, the red-brown coloured solution was filtered through kieselgel and washed through with dichloromethane. The solution was dried *in vacuo* and washed with hexane. The resulting dark brown product afforded two bands on purification with column chromatography (eluent: dichloromethane/hexane 1/1). The first orange band afforded the starting material, ferrocene, yield: 0.05 g (8%). The second red-brown product was identified as **9**, yield: 0.21 g (35%).

4.4 Analytical data of 1-8

Table 7.3 Analytical data of **1-8**

Complex	Molecular formula	Calculated (%)		Found (%)	
		C	H	C	H
1	$C_{16}H_{10}O_6CrS$	50.26	2.62	50.14	2.70
2	$C_{16}H_{10}O_6WS$	37.36	1.95	37.28	2.02
3	$C_{24}H_{15}O_6CrTiSCl$	50.85	2.65	50.73	2.91
4	$C_{24}H_{15}O_6WTiSCl$	41.25	2.15	41.01	2.37
5	$C_{19}H_{10}O_9Cr_2S$	44.02	1.93	43.64	2.07
6	$C_{19}H_{10}O_9CrWS$	35.10	1.54	34.82	1.83
7	$C_{27}H_{15}O_9Cr_2TiSCl$	48.58	2.25	48.35	2.49
8	$C_{27}H_{15}O_9CrWTiSCl$	40.56	1.88	40.14	2.01

5. References

1 E.J.Zaiko, .L.Lipman Jr., G.A.Moser, M.D.Rausch, *J. Organomet. Chem.* **1970,** *23* 185.

2 H.Meerwein, *Org. Synth.* **1966,** *46* 113.

3 S.P.Schmidt, F.Basolo, W.C.Trogler, *Inorg. Synth.* **1985,** *23* 41.

4 S.P.Schmidt, J.Nitschke, W.C.Trogler, *Inorg. Synth.* **1989,** *26* 115.

5 M.Novi, G.Guanti, *J. Heterocycl. Chem* **1975,** *12* 1055.

6 M.Landman, Novel heteroarene complexes of chromium(0), MSc dissertation, University of Pretoria **1997**, p76.

7 M.D.Rausch, D.J.Ciappenelli, *J. Organomet. Chem* **1967,** *10* 127-136.

8 B.McCulloch, D.L.Ward, J.D.Woollins, J.C.H.Brubaker, *Organometallics* **1985,** *4* 1425-1532.

9 R.J.Card, W.S.Trahanovsky, *J. Org. Chem.* **1980,** *45* 2560.